RIVISTA DEL NUOVO CIMENTO Vol. 40, N. 8 2017
DOI 10.1393/ncr/i2017-10138-4

Comets

Cesare Barbieri(*)(**) and Ivano Bertini

University of Padova, Department of Physics and Astronomy, vicolo Osservatorio 3 35122 Padova, Italy

received 28 February 2017

Summary. — The paper reviews properties of comets, from historical sightings and interpretations, to contemporary ground- and space-based knowledge. The importance of comets in understanding the present Solar System and its dynamical, physical and chemical evolution, their relationship with other minor bodies, their possible role for the very early phases of our Earth, will be examined. Emphasis will be on the results of the recently completed European Rosetta mission to comet 67P/Churyumov-Gerasimenko, in particular those by OSIRIS, its imaging system. It is fair to say that Rosetta's results represent a most important step in the development of cometary science, whose full implications start just to surface and will be fully appreciated over several more years.

(*) Emeritus of Astronomy, University of Padova, Italy
(**) E-mail:cesare.barbieri@unipd.it (corresponding author)

1. – Introduction

We present in this paper some notions on comets, namely on those "hairy stars" (from the ancient Greek "$\kappa o \mu \acute{\eta} \tau \eta \varsigma$", the "hairy one") about which many astrologers and philosophers had speculated already millennia ago. We quote for instance the philosopher Lucius Annaeus Seneca (*Quaestiones Naturales* vol. VII, written around year A.D. 65) who pondered about their real nature, why they moved in orbits so different from those of planets, which dimensions they had.

Surely, in every epoch, including our own, comets represent an extraordinary event, in the opinion of many persons capable to foretell good, or more commonly bad, news. The association of comets to great battles, catastrophes, or the birth of a prince, can be found in many cultures, from China to Japan to Mesopotamia to Greece to Rome and so on. This association, although based on superstition, has had the great merit of recording not only the dates of cometary apparitions, but also their motion on the celestial sphere, their colour and aspect, and other circumstances so important for modern science.

Even today, the passage of a great comet raises the interest of literarily billions of watchers, armed with very sophisticated telescopes, digital cameras, software for image processing, internet connection for real time exchange of information, but also simply using their eyes for the sheer pleasure of admiring a beautiful celestial phenomenon.

A great example is comet Halley, so to speak the 'mother of all comets', which will be recalled many times in this review.

Since more than a century, the new observational means provided by large optical telescopes, by radio telescopes, by satellites above the Earth atmosphere and finally by spacecraft navigating in the proximity of the comets have produced an impressive amount of data and stimulated more and more refined theories. An immense amount of literature, which will only be sparsely quoted in this review, where great attention will be given to the results provided by the European Rosetta mission, and in particular by its imaging system OSIRIS.

2. – Comets in history

Probably, the most ancient records of comets date back to Chinese *Histories* of 2300 B.C., and surely they appear in documents of the Shang period around 1100 B.C. We owe to the Jesuit father Antoine Gaubil, who died in Beijing in 1759 (the same year of the re-apparition of comet Halley) the *Catalogue des Cometes vues en Chin.*

Very important are also Chaldean and Babylonian records engraved in tablets dating to the II and III century B.C.

Philosophers started very soon to speculate about their nature. Seneca was just one of the many thinkers of the past to be attracted by comets. In Greece, several different hypotheses were expressed: the Pythagoreans and Democritus of Chios held the conviction of celestial bodies, Anaxagoras and Democritus were in favour of conjunctions of stars and planets, but others thought of atmospheric phenomena. Aristotle in particular, who had the venture to observe the great comet of 371 B.C., wrote in his *Meteorics* (about 350 B.C.) that comets were below the sphere of the Moon and had the same igneous substance composing the Milky Way. Moreover, he associated comets to strong winds and periods of drought. Indeed comets, with their sudden apparition, irregular motion, enormous variations of brightness and shape, did not fit with his vision of a fixed and immutable celestial sphere.

Strange enough, Claudius Ptolemy (second century A.D.) in his *Almagest* entirely ignored comets. Five centuries later, the English monk Venerable Bede observed three comets, one in August 678, which remained visible for three months, rising in the morning, and two in the year 729. The two comets appeared in January around the Sun, striking terror into all who saw them. One comet rose early and preceded the Sun, while the other followed the setting of the Sun at evening, seeming to portend awful calamity to the east and west alike.

The apparition of comets was recorded also in art and literature. Consider for instance Halley's: its passage of 684 was depicted in the *Liber Chronicorum* (Nurnberg, 1493); that of 1066 in Bayeux tapestry and in a manuscript in Viterbo (Italy); that of 1145 in the Eadwine *Salterium*; that of 1301 was depicted by Giotto in the Scrovegni Chapel in Padua. Historical passages of Halley's are listed for instance in refs. [1-5].

3. – Early scientific studies of comets

During the XV century, several observers made careful observations with a genuine scientific interest. Of particular importance was the comet of 1456, which we now know it was Halley's. Paolo Toscanelli, Georg von Puerbach and Johannes Mueller (in Latin, *Regiomontanus*) all left important and for the time accurate observations.

The subsequent passage of Halley's in 1531, convinced G. Fracastoro and Petrus Bienewitz (in Latin *Petrus Apianus*) that the cometary tails point to the anti-sunward direction.

Then, two astronomical events occurred, the Supernova of 1572 and five years later the great comet of 1577, that were of utmost importance to reopen the debate about the nature and distance of celestial objects. Tycho Brahe, then in the island of Hven, made very accurate determinations of the position of the comet, which in conjunction with simultaneous observations made in Prague, 600 km away, demonstrated that the comet was much more distant than the Moon, and probably on a non-circular orbit.

Years later, his former disciple Johannes Kepler made precise observations of Halley's in 1607, and of three comets which appeared in 1618. His measurements showed that the comets were farther than the Moon. On the contrary, Galileo Galilei was not convinced of the extra-terrestrial nature of those comets, and in his *Saggiatore* attributed their nature to atmospheric phenomena.

The debate was soon over thanks to Isaac Newton, who demonstrated in his *Principia* that the comet of 1680 had an elliptical orbit, which brought it to a very small distance from the Sun. By virtue of Newton's method, Edmond Halley was able to determine the

orbits of 23 comets. Fundamentally important was the apparition of the comet of 1682, which Halley noticed to have the same orbital elements of the comets observed in 1456, 1531 and 1607. The comets had to be the very same celestial body, and he predicted its reappearance in 1758-1759.

Actually, Johan Palasch recovered the comet in December 1758, when Halley had been dead for several years. In his honour, the comet was named after him. Being the first comet demonstrated to be periodic, Halley's is known also as 1P.

This passage, recorded for instance in a fresco of the *Specola* in Padua, was also a powerful confirmation that Newton's laws apply to very great distances and are independent of the orbital elements. Indeed, Halley's orbit is different from those of the great planets and of the asteroids of the Main Belt (not yet known to Halley), being described in the opposite (retrograde) sense and having a fairly large inclination to the ecliptic plane. The eccentricity is large, 0.967, the semi-major axis of 17.8 AU, and the period varies between 74 and 76 years, variations mostly due to Jupiter's perturbations.

The following 150 years witnessed the great development of Celestial Mechanics. In addition to the exhaustive treatment of the classical two-body problem, the perturbations caused by planets found in comets a precious ally of the theories. Great names come to mind, Euler, Laplace, Olbers, Gauss and many others.

4. – Orbits of comets

In the absence of perturbations by the planets or of non-gravitational forces, the orbit of a comet, which can be considered a point of negligible mass, is described according to the two-body laws. The generic orbit is a conic curve having its focus in the centre of the coordinates (the Sun, or in a more refined treatment the barycentre of the Solar System). The sign of total energy E determines the value of the eccentricity e:

$$\begin{aligned} E<0:&\quad 0\le e<1 \text{ (the orbit is an ellipse, } e=0 \text{ is a circle)},\\ E=0:&\quad e=1 \text{ (a limiting case, the orbit is a parabola)},\\ E>0:&\quad e>1 \text{ (the orbit is a hyperbole)}. \end{aligned}$$

It is convenient to identify an origin on the conic with the point of minimum distance (perihelion), which in the case of an elliptical orbit is located on the line passing also for the point of maximum distance (aphelion). It is then customary to write the conic curve as

$$r=\frac{q(1+e)}{1+e\cos\nu}\,,$$

where the angle ν is called "true anomaly" and increases in the same sense as the motion of the comet. The energy per unit mass and the modulus of the velocity V are then

$$E=-\frac{GM}{2}-\frac{1}{a}\,,\qquad V^2=GM\left(\frac{2}{r}-\frac{1}{a}\right),$$

valid also for parabolic ($1/a=0$) or hyperbolic ($1/a<0$) orbits. For a parabolic orbit, the value of V at the distance of the Earth from the Sun is approximately 42 km/s

(the escape velocity from the solar system at 1 AU([1])). Therefore a comet free falling from zero velocity at infinity toward the Sun, could impact the Earth with velocity in the range 42 ± 30 km/s, being 30 km/s the orbital velocity of the Earth.

When the comet is gravitationally bound to the Sun ($E < 0$; $0 \leq e < 1$), the line joining perihelion and aphelion is called the *line of apses*. In such case, usually the orbit is written as

$$r = \frac{a(1-e^2)}{1+e\cos\nu} \cdot q = a(1-e) \text{ perihelion distance}, \qquad Q = a(1+e) \text{ aphelion distance},$$

where a is the semi-major axis of the ellipse.

These expressions of Kepler's first and second laws are fair approximations to the true orbit, at least for short arcs of the trajectory, and an extremely useful departing point for further theoretical developments when many bodies or non-gravitational forces are considered. The corrections due to General Relativity are taken into account by the most refined astrometric and navigational programs. While the eccentricities of the great planets have small values, there are comets with very large values of e, practically indistinguishable from 1, namely comets on parabolic orbits, and even comets with $e > 1$, namely escaping from the Solar System.

The period of revolution P on the ellipse, whose area is $A = \pi ab$, is given by Kepler's 3rd law:

$$P = 2\pi \frac{a^{3/2}}{\sqrt{GM}},$$

where rigorously M is the sum of the mass of the Sun and of the particle, but in our case the mass of the comet is essentially zero. Notice that P depends only from the total energy, but not from the eccentricity. The velocity at any point r on the orbit is then

$$V^2 = GM\left[\frac{2}{r} - \frac{1}{a}\right],$$

so that

$$V^2_{\text{perihelion}} = \frac{GM}{a}\frac{1+e}{1-e}, \qquad V_{\text{aphelion}} = V_{\text{perihelion}}\frac{1-e}{1+e}.$$

The complete description of the orbit requires other elements:

- the time T of passage through the perihelion;
- the inclination i of the orbit to the *ecliptic* (the orbital plane of the Earth); the line of intersection of comet and Earth orbital planes is called *line of the nodes*;
- the verse of description of the orbit, which can be *direct*, namely anti-clockwise if seen from above the ecliptic like all planets, or *retrograde* if described in the opposite sense (like Halley's); for a retrograde orbit, the inclination is larger than 90 deg.

([1]) AU = Astronomical Unit, approximately 1.5×10^8 km.

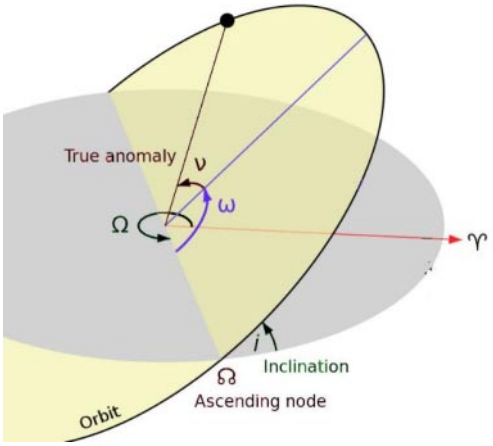

Fig. 1. – The orbit of a comet in space with respect to the ecliptic plane.

The position of the orbit in space is described conveniently by two angles (fig. 1): Ω = the longitude of the ascending node, measured Eastward on the ecliptic from the vernal equinox γ (the point where the Sun crosses the celestial equator around the 21st of March), ω = the argument of the perihelion, namely the angular distance of the perihelion from the ascending node, measured on the orbital plane of the comet, as is the true anomaly ν. Therefore, the six orbital elements are $(q, e, T, i, \Omega, \omega)$.

Table I gives as examples the 4 sets of values for comet Halley in 1910([2]), Encke and 67P/Churyumov-Gerasimenko.

From the elements of table I, the elements of table II are derived.

For new comets, the parameters (e, i) take essentially all possible values, a major proof that they come from a spherical cloud at the borders of the Solar System. Comets of the Jupiter Family (JFCs) have instead their aphelion close to Jupiter's orbit and inclination within approximately ± 12 deg from the ecliptic.

The perturbations of the cometary orbit due to large planets are exceedingly difficult to treat in a rigorous way. See an example in fig. 2, which shows a large perturbation due to planet Jupiter.

This is the sort of perturbation experienced by a JFC like 67P/Churyumov-Gerasimenko, primary scientific target of the Rosetta mission.

There is a useful criterion, known as *Tisserand's invariant*, which can be used to follow the changes of the orbital elements of a comet after a near pass, for instance with Jupiter. Call (a, e, i) the initial elements and (a', e', i') those after the encounter. It can be shown that

$$\frac{1}{2a} + \sqrt{a\,(1-e^2)}\cos i = \frac{1}{2a'} + \sqrt{a'\,(1-e'^2)}\cos i'.$$

In this example, the unit of length is the Sun-Jupiter distance, the unit of mass is Sun's mass and the time scale is such that Jupiter's orbital angular velocity is unity. Asteroids

([2]) For Halley's, the elements at 1910 are given, when the comet was called 1910II, because that year there was another comet, brighter than Halley's and often confused with it.

TABLE I. – *Orbital elements for three comets.*

Element	Halley 1910 II	Encke 1967 XIII	67P/C-G
q (AU)	0.59	0.14	1.24
e	0.967	0.847	0.64
i (deg)	162	12	7.04
T	1910 Apr. 20.2	1967 Sept. 22.1	2015 Aug. 13
Ω (deg)	58	334	50.08
ω (deg)	122	186	13

have typically Tisserand's invariant larger than 3, while for comets it is less than 3, a useful criterion to distinguish among the two families of Minor Bodies. However, the criterion is not a rigorous one, nor does it provide a definite proof that the comet observed after the encounter is the same observed before; nevertheless, if the orbital elements are widely different, it can be concluded that the two sets do not belong to the same comet.

Although not pertaining, strictly speaking, to the orbital elements, the rotational state of the nucleus (obliquity of the rotation axis with respect to its orbital plane, angular velocity, verse of rotation) plays a great role both in the dynamical evolution of the orbit and on the activity (this point will be discussed later on). Regarding the orbital changes, it was soon appreciated that the gravitational force is not the only one acting on a cometary orbit. The passage of Halley's in 1835 prompted W. Bessel and others to consider *non-gravitational forces*. In addition to the radial gravitational force due to the Sun, a non-necessarily radial acceleration had to be present, capable to alter the orbital elements, in particular the period. Based on his visual observations and accurate drawings, Bessel put forward a model, named "fountain of matter" coming out of the nucleus (see fig. 3). At the same time, a Russian astronomer, F. Bredikhin, started the examination of the acceleration of the tails, and introduced a classification, still in use today, on the basis of the ratio between the repulsive anti-solar force and the solar gravitation. This ratio is usually expressed by the parameter $(1 - \mu)$: Type I, the straight bluish gaseous tails, have $(1 - \mu) \approx 11$–18, Type II, the curved, amorphous yellowish dusty tails, have $(1 - \mu) \approx 0.7$–2.2. Bredikhin introduced in addition a Type III tail, shorter and stubby, due to heavier dust particles. At the time, neither Bessel nor Bredikhin could make any physical distinction between material particles, neutral or ionized molecules and atoms.

TABLE II. – *Derived elements for the comets of table I.*

Element	Halley 1910 II	Encke 1967 XIII	67P/C-G
Period P (years)	76.1	3.3	6.45
Semi-major axis a (AU)	17.96	2.22	3.46
Velocity at perihelion V_p (km/s)	54	70	34.2
Velocity at aphelion V_a (km/s)	0.9	6	7.5

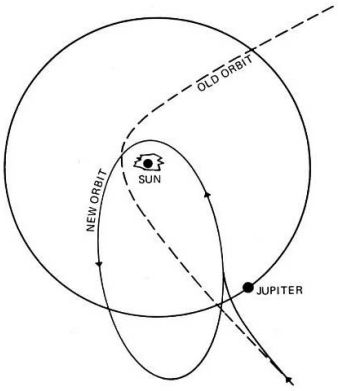

Fig. 2. – Schematics of a very large perturbation by planet Jupiter, which captures the comet in a short-period orbit.

Regarding the presence of solid particles in the comae and tails, already in 1819 D.F.J. Arago was able to prove that the light from the comet was slightly polarized, and therefore at least partly made of solar light scattered by small solid particles. Fifty years later, Father A. Secchi S.J. contributed very much to this subject, showing that the outer coma of comet 1862 III Swift-Tuttle was strongly polarized, while the regions around the nucleus remained unpolarized. We know today that solid particles have a very wide range of sizes, from sub-micron to decimetre and even metre scales, as discussed again in later sections.

Consider now the two nodal points of fig. 1. They are of particular interest for the meteor showers, because it is there that the Earth crosses the stream of debris left by the comet along its orbit. Around 1875, the Italian astronomer G. V. Schiaparelli conclusively proved the association between some meteor showers and orbits of comets. There are numerous examples in point, like comet 3D/Biela's associated with the so-called Andromedids shower. The comet broke up into pieces in 1843 and the associated shower was spectacular in 1872 and 1875; today the shower is almost invisible. Another well-known shower is Perseids, in mid-August, associated with comet Swift-Tuttle. Other noticeable showers are reported in table III. Notice that comet Halley produces two showers, the Eta Aquarids in May and the Orionids in October.

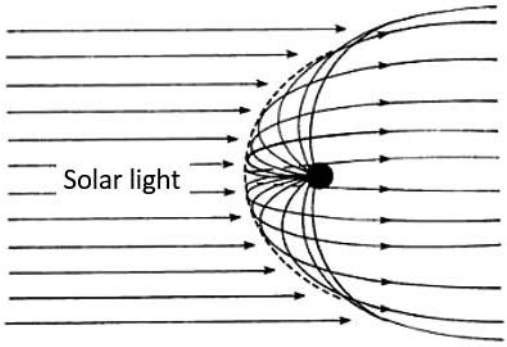

Fig. 3. – Bessel's "fountain model".

TABLE III. – *Some meteor showers and their association to known comets.*

Approximate peak date	Name of shower	associated comet
April 21-22	Lyrids	Thatcher, approximate period 415 years
May 5-6	Eta Aquarids	1P Halley, approximate period 75 years
July 28-29	Delta Aquarids	96P Machholz?? Period about 5 years
August 11-12	Perseids	Swift-Tuttle, period about 133 years
October 7	Draconids	21P/Giacobini-Zinner, period about 6.6 years
October 20-21	Orionids	1P Halley, approximate period 75 years
November 4-13	Taurids (North + South)	Very complex, Encke??
November 16-17	Leonids	Temple-Tuttle, period 33 years
December 13-14	Geminids	shower associated not with a comet but with asteroid 3200 Phaethon, period about 1.4 years.

Schiaparelli's papers confirmed that in addition to gaseous substances, comets contain solid particles that occasionally can reach the ground and can be collected as meteorites. Such long held association between meteorites and debris of asteroids and comets had another proof around mid-1970, when stratospheric aircraft like the U-2s, started collecting microscopic grains of interplanetary dust. The chemical composition of such particles was identical to those of carbonaceous chondrites typical of asteroidal origin, but sometimes their high velocity was indicative of a truly cometary nature. Those grains are usually called "Brownlee grains", from the name of the principal investigator of those pioneering researches.

5. – The contemporary age

In the second part of the XIX century, two great technical and scientific developments took place, namely the introduction of spectroscopy and the invention of the photographic emulsion. By visual observations made in 1864, the Italian astronomer G. Donati observed for the first time three emission bands in comet Tempel. Few years later, Sir W. Huggins associated the bands seen by Donati with emissions from the molecule C_2 (those bands are known as *Swan bands*), and finally in 1881 he obtained the first photographic spectrum of a comet. It was then possible to identify other prominent emissions, due to other transitions of the C_2 molecule, to the molecular radical CN in the violet (388.3 nm), to atomic sodium Na in the yellow (588.6 nm), and so on.

In other words, in addition to the determination of orbits and morphological changes, at the end of the XIX century the way was open to study the chemistry and physics of comets. Very soon, the application of the basic laws of Thermodynamics and the first discoveries in Quantum Mechanics allowed precise determination of chemical composition, density, pressure, temperature of comae and tails. However, the explanation of some basic facts, like the morphological changes or the mechanisms responsible for the excitation and changes of intensity of the emission bands, had to wait for another 40 years or so.

One of the many puzzles brought forward by early spectroscopy was the reason for the different aspect of cometary molecular bands with respect to laboratory spectra. This problem was clearly expressed by K. Schwarzschild at the beginning of the XX century. The explanation came decades later from fundamental papers of P. Swings, who examined in detail the excitation mechanism. In essence, the emission bands are due to a mechanism of fluorescence, namely absorption of the solar UV light by the internal energy levels of the different molecules, followed by immediate re-emission in other wavelengths. However, the solar spectrum in the UV band is not adequately approximated by a black body Planck's law at a temperature around 5900 K, as instead is in the visible band. The many solar absorptions and emissions in the UV spectrum influence the fluorescence mechanism, and so does the variable radial velocity of the comet with respect to Sun. Therefore, the energy levels are not populated by collisions as in equilibrium conditions, but by radiation.

To Swings we owe also a detailed recollection of the history of cometary spectroscopy until 1964, in his "George Darwin Lecture" [6].

Around mid-XX century, three fundamental theories were born, and still dominate the science of comets:

- Jan Hendrik Oort derived his model of a great spherical cloud located some 50000 to 100000 AU from the Sun, containing billions of cometary nuclei.
- Fred Whipple suggested that nuclei were loose aggregate of ices mixed with refractory non-volatile material.
- Ludwig Biermann suggested a corpuscular flow out of the Sun, capable to explain the great accelerations of ions and the morphological changes of the cometary comae and tails. This corpuscular flow, with the associated interplanetary magnetic field, is called today "solar wind".

Some aspects of such theories and their modifications will be described in following sections.

6. – Second half of the XX century, Radio Astronomy and the space era

Around 1960, the newly born space science became a powerful player in the study of comets. The spacecraft Mariner 2 directed to Venus provided the first experimental proof that Biermann was correct. Notice that still today only comets provide information on the solar wind at great distance above or below the ecliptic plane, where almost all spacecraft can fly. Only the ESA-NASA mission Ulysses reached great ecliptic heights, on an orbit bearing some similarity to that of comet Hale Bopp. Thanks to the space era, comets could be observed not only from ground optical and radio telescopes, but also by stratospheric aircraft and balloons, sounding rockets and satellites. The Skylab, a prototype of today's International Space Station, deserves a special mention in this respect, see [7]. Another important spacecraft of those early times was *ICE (International Cometary Explorer)* which went through the tail of comet Giacobini-Zinner in Sept. 1985, and then approached Halley's.

Again starting around 1960, Radio Astronomy flourished all over the world, and in the following decades provided an impressive amount of data (see, *e.g.*, the review paper [8] and references therein). Radio data have important advantages, because the radio spectrum is very rich of molecular bands due to a great variety of molecules.

Those bands are usually due to rotational transitions, simpler to interpret that vibrational or electronic transitions typical of the visual and UV bands; spin temperatures and isotopic ratios can be more accurately determined; furthermore, the measurement of radial velocity is extremely accurate. Comet Kohoutek of 1973 (formally designated C/1973 E1, 1973 XII, and 1973f)([3]), in a way signalled the beginning of such new age for cometary studies. The comet was observed over a very wide range of wavelengths, from UV to Radio. The NASA *Copernicus* satellite allowed the measurement of the Ly-alpha line of hydrogen, already predicted by Biermann and observed on other comets too (see [9], which gives many references to previous studies). Radio telescopes detected the OH radical by its *mased line* around 18 cm [10]. Those observations were the final proof that H and OH both come out of the H_2O molecule by photolysis. Comet Hale-Bopp, observed by several radiotelescopes such as the BIMA and VLA radio telescopes (*e.g.* [11]), provided another example of the usefulness of radio data.

Radar data can be obtained on sufficiently close comets. For instance, radar data on Halley's were provided by the 300 m dish in Arecibo, the 70 m Goldstone antenna detected Hyakutake at a distance of 1.6×10^7 km, measuring not only its distance, diameter of nucleus and coma, radial velocity but also properties and velocities of a coma of cm-sized dust particles. Actually, the echo from the coma was stronger than from the nucleus itself. See, *e.g.*, [12] and references therein. An attempt to observe 67P was made with the Arecibo 300 m dish in 1982 in radar mode (see [13]), when the comet was at 0.4 AU from the Earth. The observations provided only an upper limit to the flux, but even this upper limit gave useful constraints on the nucleus properties. The dielectric permittivity of the subsurface layer had to be constrained in a narrow range of 1.9 to 2.1, the porosity in the range 55 to 65% and the density in the range $\approx$ 600–1000 kg/m^3 for the top $\approx$ 2.5 m layer of the nucleus. Data on 67P provided by Rosetta instruments, in particular by the radar CONSERT quoted later on, broadly confirm such estimates.

Comet Hyakutake provided the first, very surprising detection of X-rays, thanks to the German satellite Rosat [14]. The possibility that comets, interacting with the solar wind, could emit X-rays was quickly confirmed by the Italian-Dutch satellite BeppoSAX observing Hale-Bopp [15]. See also [16, 17], and a review paper on X-ray emissions from Solar System objects (excluding the Sun) in [18]. In essence, X-ray emission is a fundamental property of comets. Such emission is due to the interaction between the solar wind and the comet's neutral atmosphere. Collisions of highly charged solar wind heavy ions (in particular C, O, N, which constitute not more than 0.1% of the solar wind) with cometary neutral species, result in a charge-exchange process where one electron of a molecule or atom of the neutral coma is captured by the heavy ion, with the emission of an X-ray photon. The process is particularly active in the sunward direction of the coma.

For an accurate summary of the pre-1993 knowledge about comets see [19].

In conclusion, by using optical and radio telescopes on ground and Gamma, X, EUV, UV, and far-IR instruments on sounding rockets, spacecraft in extra-terrestrial space, and even navigating near comets, a much more comprehensive chemistry and physics of comets became possible in the last decades. There is an immense literature coming from spacecraft such as IUE, ISO, Herschel, HST, XMM, Chandra, Spitzer, too large to be

([3]) Actually, Kohoutek discovered two comets that year, one extremely faint, the second one, namely 1973 XII, was expected to become spectacular (newspapers dubbed it "the comet of the Century"), but as often happens did not fully meet expectations.

even sparsely quoted (see for instance [20-24]). Nice animations are presented by the web sites of the several space agencies, for instance the one touring two comets, ISON and PanStarrs is provided in [25]. The already quoted review paper [8] on short period comets provides data obtained by the Nançay radio telescope, the IRAM antennas, the Odin satellite, the Herschel space observatory, ALMA, and the MIRO instrument aboard Rosetta. Only few of those results and references will be given in this paper when relevant.

Space brought another fundamental advantage, the possibility to capture atoms, molecules, dust particles flowing out of the nuclei, in other words to study comets through their material content, not only through electromagnetic waves. Instruments such as ROSINA, GIADA, COSIMA, MIDAS on board the Rosetta mission ([26] and references therein) are a vivid illustration of such capabilities, as detailed in several instances throughout this paper. Still lacking today is a sample return mission, often proposed but still not carried out.

A large fraction of the present paper is devoted to two fundamental comets and dedicated European space missions, namely 1P/Halley and the "grand armada" of spacecraft in 1986, and 67P/Churyumov-Gerasimenko and the just concluded Rosetta. Regarding the characteristics of the spacecraft GIOTTO, Rosetta, and the VEGAs and their instrumentation, see appendix A and appendix B.

7. – Solid-state detectors and the spectrophotometry of comets

Space brought another crucial advantage to the study of comets, namely the development of solid state devices, with a linear well calibrated response and very wide spectral range. Soon, such devices became available also to ground telescopes. Starting from the '80s of the last century, the photographic emulsion was replaced by solid state detectors both on cameras and spectrographs. The only sacrifice is the much smaller sensitive area, which can be overcome, *e.g.*, by mosaicking a number of individual chips. Such devices are particularly useful in cometary studies. Reliable estimate of the brightness of a comet has always been a difficult error-prone task, because the comet can be very extended, with faint regions contributing however a sizeable amount of luminosity. Moreover, the comet moves over the stellar field, the comparison sequence changes quickly, and so does the wavelength-dependent extinction due to the terrestrial atmosphere. The observational means are quite crucial in this respect. Before the telescopic era, it was only the unaided eye, then from Galileo in 1609 and onwards until the second half of the XIX Century, telescope plus eye and eventually coloured filters, then the photographic plate in the focal plane of the telescope and much better filters defining accurate photometric systems. Photomultipliers were used too, but they essentially provided a single pixel over the field of view. Finally, solid-state devices appeared, in particular Silicon-based matrices for the UV and visible (CCDs), and matrices of other materials like Hg-Cd-Te for the near-IR.

The linearity of solid-state devices allows to measure the luminosity inside a given isophote over a well-defined interval of wavelengths. In spectrophotometric applications, they facilitate the very delicate operation of subtracting the continuum due to the night sky and the solar light scattered by dust, removing other sources of noise such as moving stars, in order to have a reliable estimate of the absolute intensities of the emission lines and bands. A particularly useful algorithm to process the inner regions of comae was devised by Larson and Sekanina [27] in order to extract information about Halley's. See examples in fig. 4.

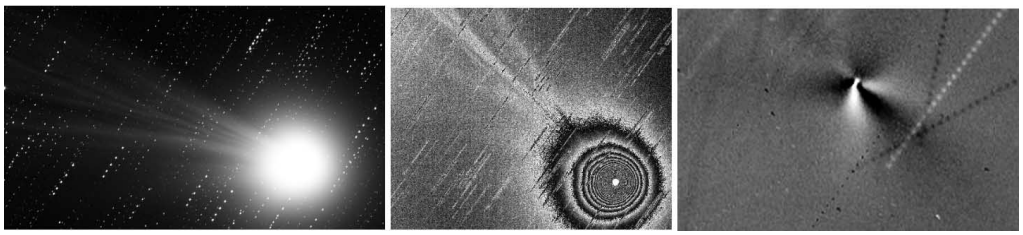

Fig. 4. – Left: comet Lovejoy C/2014 Q2; centre: the isophotes of the nucleus; right: digital images facilitate the removal of noise caused *e.g.* by the dotted moving stellar background, and the application of Larson-Sekanina filter to bring out the structures of the central regions (courtesy P. Ochner, Asiago Observatory).

The two CCDs of OSIRIS on board Rosetta [28] had the following characteristics:

Detector E2V CCD42-40, non-MPP, backside illuminated, Hafnium oxide AR coated.

Array size: $2\,\mathrm{k} \times 2\,\mathrm{k}$ pixels, pixel size $13.5 \times 13.5\,\mu\mathrm{m}^2$, full well $> 120\,000$ electrons/px.

Quantum Efficiency: 250 nm: 50%, 400 nm: 60%, 600 nm: 88%, 800 nm: 65%, 1000 nm: 6%.

Figure 5 shows the accuracy of the photometry of OSIRIS to measure the light curve of 67P (ref. [29]). The further advantage provided by Space, in addition to lack of atmospheric disturbances, is the possibility of uninterrupted observations for time intervals comparable to the period of rotation of the Earth (in the present case around 12 hours), an observational bias for terrestrial telescopes often leading to aliases in the determination of the true period.

The imaging spectrophotometer VIRTIS on board Rosetta [31, 32] utilized a CCD to observe from 0.25 to $1\,\mu$m, and a Hg-Cd-Te infrared focal plane array to observe from $0.95\,\mu$m to $5\,\mu$m.

Another important improvement brought about by solid-state detectors is the precision in expressing the integrated luminosity of the comet as function of the position in its orbit. In order to make a fair comparison between the different circumstances, all

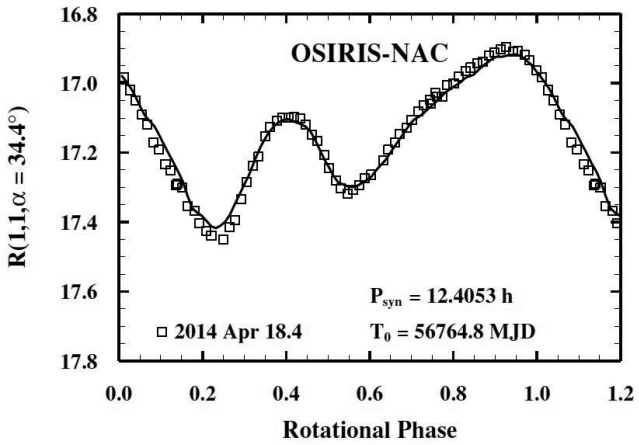

Fig. 5. – Light curve of the 67P nucleus obtained by OSIRIS on April 2014 (reproduced from [30] with permission @ESO).

measurements of luminosities, diameters etc. are reported to unit distance $r = \Delta = 1$ AU, where r is the heliocentric distance and Δ the geocentric one.

For the changes of luminosity J with distance from Earth and Sun, the approximate formula has been widely used:

$$J = J_0 \Delta^{-2} r^{-n},$$

where n is an exponent determined empirically by the light curve. The theoretical value of n would be $n = 2$ if nothing changed on the cometary material, but actually many comets show $n = 4$. Furthermore, such simple law fails to take into account an important observational parameter, namely the phase angle, defined as the Sun-comet-Earth angle, and implies a symmetry around the perihelion which almost never is realized, because of the seasonal illumination of the nucleus. For instance, Halley's was brighter after, Encke's before the perihelion. Regarding comet 67P, measurements from ground robotic telescopes [33] showed an offset in the peak brightness post perihelion, and a strong asymmetry: the comet was brighter at the same distances post-perihelion than pre-perihelion.

From a physical point of view, n depends on the sublimation rate of ices, which is very hard to predict. In many cases, the high luminosity expected from the first observations did not materialize, as it happened for the already quoted Kohoutek's or for comet ISON. In other comets, it worked well, as in the case of Hale-Bopp's. Therefore, the above formula maintains its usefulness as starting point.

It is customary to employ a magnitude scale

$$H = H_0 + 5 \log \Delta + 2.5 n \log r.$$

The parameter H_0 can assume different values, for instance it was estimated 5.9 in West 1976 VI, and 7.6 in Bradfield 1974 III, two bright comets indeed.

Another useful quantity to recall is the wavelength dependent *albedo* of the surface, namely the ratio between reflected and incident radiation. To be more precise, two definitions of albedo are used in the literature:

- the **geometric albedo** over a given spectral band, *e.g.* visual, is the ratio of its actual brightness as seen at zero phase angle to that of an *idealized* flat, fully reflecting, diffusively scattering (Lambertian) disk with the same cross-section;
- the **Bond albedo** is the fraction of power in the total electromagnetic radiation incident on an astronomical body that is scattered back out into space.

In the following, geometrical albedos are meant. Typical values for cometary nuclei are around few percent. However, visual or photographic observations have always been very difficult to calibrate, a problem today largely removed. Space entirely avoids the air-mass and seeing problems, but the correction for illumination due to the phase angle becomes crucial, especially when the spacecraft is so near to the comet that small facets with different inclinations become resolved, as in the case of Rosetta. In such case, different angles have to be taken into consideration for a proper analysis of the data, because each facet will see the Sun under specific geometric circumstances, and scatter light towards the detector again with a specific geometry. The mathematical model usually employed in such analysis is that by Hapke [34].

The excellent detectors on board Rosetta have provided a wealth of accurate, well-calibrated, spectrophotometric information. Among the many papers, we have singled out those by Fornasier *et al.* in [35] and [36], which use data from OSIRIS and VIRTIS. Both instruments agreed on a very dark nucleus, with a global geometric albedo of $\approx 6\%$, namely a surface covered with a crust rich of organic material. The previously defined parameter H_0 in the visual region was determined as $H_0 = 15.74$, with a strong opposition effect (namely a sudden brightening of about 0.4 mag when the phase angle was zero). Excluding this opposition effect, the magnitude of the comet would increase (the brightness would decrease) with the phase angle by about 0.06 mag/deg. The different filters allowed to measure the disk-integrated geometric albedo, varying from 0.03 at 300 nm to 0.08 from 700 to 1000 nm. In addition to global values, the space and time resolution allowed spectrophotometry on single small areas on both hemispheres of the comet, both before and after the perihelion. The spectral slope, *i.e.*, the slope *vs.* wavelength of the ratio of the comet's spectrum to a solar spectrum has been evaluated in the 535–882 nm range, on co-registered and illumination corrected images using the Lommel-Seeliger scattering law, and the shape model from [37] and references therein. It might be recalled that the Lommel-Seeliger scattering law, appropriate to low albedo surfaces, can be expressed as

$$D(i, e) = \frac{2 \cos i}{\cos i + \cos e} ,$$

where i and e are, respectively, the incidence and scattering direction of the solar radiation.

The OSIRIS images in these papers had an effective resolution around 6×6 metres on the surface, and could repeatedly cover the rotating nucleus, allowing to measure the dependence of colours from the phase angle and determine the parameters of the Hapke model. By expressing the reflectance R of each area as

$$R = p \cdot R_{\text{ice}} + (1 - p) \cdot R_{\text{dark terrain}}$$

(where p is the relative surface fraction covered by water ice or frost), three types of terrain, ranging from the relatively bluer water ice-rich mixture to the redder ones, associated mostly with dusty regions, were identified over most of the northern hemisphere. The southern hemisphere showed an absence of wide spread smooth or dust-covered terrains, which resulted in a lack of very red regions compared to the northern hemisphere. Occasional water ices patches (and even CO_2 ice patches, see [38]) could also be identified. The very accurate measurements allowed the determination of important characteristics of the surface, such as the evolution of the dust mantle and exposure time of water ice. These topics will be re-examined in the section about the surface of comet 67P.

8. – Sun and planets grazing and plunging comets

Sun-grazing comets are comets that arrive very close to the surface of the Sun. A most spectacular one was the great comet of 1680: passing 0.42 AU from Earth on 30 November 1680, it swung a very close perihelion of 0.0062 AU on 18 December 1680.

An extreme case is when the comet plunges directly into the photosphere, is quickly burned and deposits in the solar atmosphere material not originally present (these topics will be considered in a later section about the cometary plasmas and solar wind).

At the end of the XIX century, before the discovery of nuclear reactions, the idea was put forward that the continuous infall of comets inside the Sun could provide the fuel needed for the huge energy poured by our star. Such hypothesis was soon discarded, because the needed amount was so high that the fraction of comets intercepted by the Earth would lead to a much higher temperature of our atmosphere than observed.

As a rule, most Sun-grazing or Sun-plunging comets escape detection from ground observations. Therefore, the statistics of the perihelia distribution of the cometary population is severely affected by this selection effect. Satellites equipped with suitable coronagraphs are much more efficient than ground telescopes to discover such comets. Among these spacecraft, the ESA/NASA Solar Heliospheric Observatory (SoHO) maintains a record of more than 2000 (and growing) discoveries, partly due to students and amateur astronomers all over the world.

Many nuclei do not survive the complex of thermal and mechanical stresses taking place around the perihelion, and fragment in two or more pieces, or even disappear. The comet seen to fragment by Aristotle is likely the origin of the so-called *Kreutz family of sun-grazing comets*, Biela's fragmentation gave origin to the Bielids, so did fragment comet West of 1976, or Schwassman-Wackman 3 in 1995, and many others. Three recent examples can be quoted:

– Comet C/2011 N3 (SOHO) was completely destroyed on July 6, 2011, when it swooped 100000 km above the solar surface. NASA's Solar Dynamics Observatory (SDO) recorded the disintegration [39]. As the comet moved through the hot corona, cold gas lifted off the nucleus and within minutes warmed to more than 500000 K, hot enough to shine brightly in SDO's extreme UV telescopes. The gas was rapidly ionized by a charge exchange process, which made it responsive to the Sun's magnetic field. The ionized tail wagged back and forth wildly in the moments before final disintegration. A hypothesis to be tested is the following: some of the cometary ions might mix with the solar wind and be thrown back, eventually reaching the Earth, where they could be identified of cometary origin as an anomaly in the composition of the solar wind (for instance an over-abundance of oxygen).

– Comet C/2011W3 (Lovejoy), most likely a member of the Kreutz family and quite possibly not on its first visit to the inner solar system, seemed to survive its very close passage above the Sun's surface in 2011. However, three days later the nucleus completely sublimated, and ceased to exist at the end of December 2011 (*e.g.*, [40]).

– Comet C/2012 S1 (ISON), an Oort Cloud object with a record small perihelion distance of 2.7 solar radii, shortly disintegrated hours before perihelion, on Nov. 28, 2013. The comet showed a series of remarkable events, recorded by ground telescopes, a sounding rocket and satellites [41-43]. Near-perihelion images of its tail showed an early massive production of gravel at heliocentric distances of up to ~ 100 AU. A week before perihelion, a rapid series of powerful explosions of water vapour with dust at extremely high rates, caused fragmentation of the nucleus into a vast number of sublimating boulders. Few days later, the comet experienced a major, sudden drop in gas emission. The disintegration was complete by about 3.5 hours before perihelion, at a heliocentric distance of 5.2 solar radii, when C/2012 S1 ceased to exist. The orbital motion in this period of time was subjected to progressively increasing outgassing-driven perturbations.

Sungrazer comets act as "test particles" for studying the Sun's atmosphere. A most peculiar and spectacular comet, coming to 0.17 AU from the Sun in 2007, was McNaught's C/2006 P1. The comet was monitored by space-based solar observatories, and ref. [44] provided evidence that an arch-like tail observed by the Heliospheric Imager aboard the NASA *STEREO* spacecraft is the first ever detected tail composed of neutral Fe atoms, possibly coming from evaporation of troilite (FeS).

Planet Jupiter, by virtue of its great mass and diameter, is also very effective in modifying the orbit or even in capturing passing-by comets. A spectacular plunge in its atmosphere was made by comet Shoemaker-Levy (1993e, D/1993 F2) in July 1994. The tide exerted by Jupiter on the loosely held together comet made it fragment on several pieces that one after the other entered its atmosphere. The event was witnessed in great detail by the Hubble Space Telescope (HST). It also provided evidence of a maser-amplified water emission in the radio regime (see again ref. [10]). In 2009/2010, the ESA Herschel and NASA Infrared Facility telescopes helped to solve a long-standing puzzle about the origin of the water vapour detected by ISO in 1995, shortly after the plunging of S-L. An internal deep source of water vapour could be excluded, because the vapour cannot pass through the "cold trap" that separates the stratosphere from the visible cloud deck in the troposphere. It was widely speculated that comet Shoemaker-Levy 9 may have been the origin of this water, but direct proof was missing. Finally, Herschel showed that the higher layers of the Southern Hemisphere of Jupiter, namely the hemisphere where S-L impacted, is richer in water that the northern one, a direct proof that most of the water vapour in the planet's high atmosphere is due to such cometary impact [45].

Another example in point is comet 67P. The comet was captured by Jupiter in 1959, when the distance Jupiter-comet became approximately 0.05 AU. Since then, 67P is a member of the Jupiter Family of Comet (for a discussion of such family see for instance [46]). A dynamical analysis of 67P's orbit, demonstrating its chaotic properties, was carried out by [47] and references therein. The secular orbital evolution of JFCs has been studied by [48], who included in their analysis not only a purely dynamical model, but also erosion of nuclei by ice sublimation. Their conclusion is that standard erosion models are not adequate to explain the known properties of this family, in particular the distribution of inclinations.

Comets can also graze planet Mars, as directly shown by C/2013 A1 (Siding Spring). The comet passed close to Mars (less than 300000 km) in Oct. 2014, and caused a precautionary parking of the several satellites circling the planet on the opposite hemisphere for the duration of its passage. The comet deposited in Mars' atmosphere a noticeable amount of dust and gases [49]. Intense emission from magnesium and iron caused by a meteor stream following comet Siding Spring, was observed with the MAVEN's Imaging Ultraviolet Spectrograph. Ionized magnesium emissions, resulting from resonant scattering of solar ultraviolet light, caused the brightest emission from the planet's atmosphere for many hours. Modelling suggests a substantial fluence of low-density dust particles from 1 to 100 μm in size. The event created a temporary planet-wide ionospheric layer below Mars' main dayside ionosphere.

Surely, comets have impacted the surface of Mars, with important effects on its soil and atmosphere, see for instance in [50]. Evidence for such impacts might be provided by an ESA MarsExpress image of an icy lake located on *Vastitas Borealis*, a broad plain that covers much of Mars' northern latitudes. The crater is 35 kilometres wide and has a maximum depth of approximately 2 kilometres beneath the crater rim. The circular patch of bright material located at the centre of the crater is water ice, which could be the residual of a cometary impact. An image can be seen in [51].

TABLE IV. – *Passage inside 0.1 AU recorded in the telescopic era, plus Halley's in A.D. 374 and 607.*

Distance from Earth (AU)	Date	Designation
0.0151	1770 July 1.7	D/1770 L1 (Lexell)
0.0229	1366 Oct. 26.4	55P/1366 U1 (Tempel-Tuttle)
0.0312	1983 May 11.5	C/1983 H1 (IRAS-Araki-Alcock)
0.0334	837 Apr. 10.5	1P/837 F1 (Halley)
0.0366	1805 Dec. 9.9	3D/1805 V1 (Biela)
0.0390	1743 Feb. 8.9	C/1743 C1
0.0394	1927 June 26.8	7P/Pons-Winnecke
0.0437	1702 Apr. 20.2	C/1702 H1
0.0617	1930 May 31.7	73P/1930 J1 (Schwassmann-Wachmann 3)
0.0628	1983 June 12.8	C/1983 J1 (Sugano-Saigusa-Fujikawa)
0.0682	1760 Jan. 8.2	C/1760 A1 (Great comet)
0.0832	2017 Feb. 11.4	45P/Honda-Mrkos-Pajdusakova
0.0839	1853 Apr. 29.1	C/1853 G1 (Schweizer)
0.0879	1797 Aug. 16.5	C/1797 P1 (Bouvard-Herschel)
0.0884	374 Apr. 1.9	1P/374 E1 (Halley)
0.0898	607 Apr. 19.2	1P/607 H1 (Halley)
0.0934	1763 Sept. 23.7	C/1763 S1 (Messier)
0.0964	1864 Aug. 8.4	C/1864 N1 (Tempel)
0.0982	1862 July 4.6	C/1862 N1 (Schmidt)

9. – Near-Earth comets and the origin of life

It might happen that a comet comes very close to Earth (a circumstance which of course does not mean proximity to perihelion) and allows the observations of effects strongly dependent from the relative distance. For example, C. Cosmovici and S. Ortolani [52] could identify the never observed before molecules HCO and H_2S^+, and possibly the formaldehyde CH_2O, in comet IRAS Araki-Alcock thanks to the extraordinary nearness of the comet, which allowed not only good spatial but also temporal resolution of rapidly evolving phenomena. Table IV gives a non-exhaustive list of close passages as recorded after 1700, namely in telescopic era, plus few very close passages of Halley's.

To appreciate the problem of spatial resolution, it may be remembered that 1 second of arc at 0.1 AU corresponds to about 70 km. With sophisticated image processing, the HST can resolve around 0.1 arcsec, namely 7–10 km on a nucleus at 0.1 AU, a rare occurrence indeed. See for instance in ref. [53] who studied the properties of the nuclei and comae of 10 ecliptic comets from HST multi-orbit observations.

Cometary nuclei and asteroids actually impacted our Earth, especially during the first billion years after the formation of the Solar System. Their influence on the terrestrial climate and even the evolution of life has been debated since long (*e.g.* the books in [54] and [55]). A most important impact crater is Chicxulub in Yucatan. The abundance of iridium in excavations around Gubbio (Italy) by Walter Alvarez and co-workers pointed

to an extra-terrestrial motivation for the massive K/T extinction (including dinosaurs) about 66 million years ago. There are quite recent impacts too. The interested reader can find many papers on the nature of the Tunguska event in 1908 (for instance [56] identified the cosmic body with an asteroid). A more recent example was provided by the Cheliabinsk bolide in February 2013. As is well known, amino acids, nucleic acid bases, sugars and mononucleotides necessary for the formation of life can be synthetized with biogenic atoms such as H, C, O, S, P, bi- and tri-atomic molecules such as H_2, O_2, CN, C_2, CH, NH, OH, H_2O, HCN, HN_3, H_2S, and phosphates. All these basic constituents of living organisms are present in interstellar space, meteorites, asteroids, and also in comets.

The debate about the relative importance of impacts by asteroids *vs.* cometary nuclei is not entirely solved, especially since the discovery of objects intermediate between the two classes. Asteroids and comets could be the end-members of a continuous distribution, which includes several bodies of our Solar System with compositions varying from the very rocky to the very icy, and transition objects in between. Among these transition objects we cite the Near-Earth asteroids with associated meteor streams like Phaeton (Geminids) and 2001YB5, Damocloids having Halley-type or long-period cometary-like orbits (likely extinct comets), and the so-called Main-Belt Comets (MBCs, see [57] and references therein). MBCs play a special role in this context, because they appear to be active objects, although their orbit is completely embedded in the asteroidal Main Belt between the orbits of Mars and Jupiter. For some of them, the activity is just temporary, due to a recent impact that surrounded the two bodies with a cloud of dusty debris, or in other cases due to rotational instability of the body. OSIRIS has brought a most important contribution to the evaluation of the present-day impact rate in the Main Belt, by determining the date of the impact occurred to asteroid P/2010A2 around 2009 (see [58]). Other MBCs instead show a recurrent activity which can only be explained with a genuine cometary behaviour of ice sublimation. Dynamical and thermal models show that MBCs likely formed at their current locations and stored crystalline water ice buried 50–150 m below the surface for billions of years. A recent collision with a small m-sized body would then have excavated totally or partly the isolation surface layers, bringing the ice reservoir close enough to the surface to let the solar radiation subliming the volatile material.

Therefore, the recurrent MBCs can be related to the presence of water in our planet. According to the theory of the "late veneer" scenario, the Earth formed in a region of the solar nebula where the temperature was too high for hydrous mineral phase to be stable and form a wet planet. Consequently, the water present in our planet was delivered from the outer solar system, carried by ice-bringing bodies colliding with the young Earth relatively late in its formation period. At first sight, the most likely candidates as ice bringers are comets, since they contain a large amount of water ice. Yet, with the exception of comet Hartley 2, D/H values in comets are several times larger than Earth's ocean and crust values([4]), suggesting comets are not the main responsible for the presence of water on our planet. Other likely candidates are Main-Belt asteroids, because the D/H in meteorites of asteroidal origin is very close to the one of our planet. MBCs indicate that the abundance of ice in the Main Belt is larger than previously estimated, implying that either icy bodies can form closer to the Sun than was thought, or that significant migration of planetesimals took place very early in the Solar System's history. It is fair to say that nowadays only dust clouds were detected in the vicinity of

([4]) According to the Vienna standard model, the mean ocean water has a D/H ratio of 1.56×10^{-4}. D/H in the bulk Earth is 1.49×10^{-4}, whereas the solar wind has a D/H of $\leq 2 \times 10^{-7}$.

these objects, whilst a direct observational evidence of the presence of water ice is still missing. However, this lack of detection is most probably due to the faintness of the phenomena, which are well below the observational limits of present day telescopes. It appears therefore mandatory to obtain a direct confirmation of the presence of water ice in these objects, together with the full characterization of their physical properties. The only way to prove this is through a dedicated space mission, such the proposed Castalia mission [59], which has the aim to reach and study the first discovered and prototype of MBC 133P/Elst-Pizzarro.

The measurements of D/H in 67P, made with the ROSINA mass spectrometer onboard Rosetta, have brought further doubts about comets as main water bringers to Earth. According to [60], 67P has a fraction D/H in its H_2O ice amounting to $(5.3 \pm 0.7) \times 10^{-4}$, about three times the terrestrial value, and 20 or 30 times higher than in giant planets and the proto-solar nebula. Such measurements preclude the idea that the water reservoir of JFCs is solely composed of Earth ocean-like water.

The Moon, which provides an impressive record of the number and duration of impacts, not modified by terrestrial agents such as weather, brings other important constraints to the question of Earth impacting comets and asteroids, because a sizeable fraction of the bodies directed toward the Earth was intercepted by the Moon. Most of these impacts are attributed to the intense bombardment occurred from 4.1 to 3.8 Gy ago, the so-called Late Heavy Bombardment (LHB). Most of these impacts are of asteroidal origin, so the question arises of where are the missing cometary impacts foreseen by the Nice model ([61], and further modifications). Such question has been discussed by several authors, see ref. [62]. According to this paper, the bombardment of Mercury, Moon and Mars was certainly dominated by asteroidal impacts, nevertheless comets have been more important than commonly assumed. Smaller lunar maria might have been preceded by cometary impacts. Another piece of evidence is the Ar abundance found by ROSINA [63] on comet 67P, consistent with the abundance in the Earth's atmosphere. A second question is the delivery of volatile substances to Earth and Mars by LHB comets, which is far less than their water inventory. The two planets must have obtained most of their water very early in their histories. Quoting again from [63], provided that 67P is representative of the cometary ice reservoir, the contribution of cometary volatiles to the Earth's inventory was minor for water ($\leq 1\%$), carbon ($\leq 1\%$), and nitrogen species (a few % at most). However, cometary contributions to the terrestrial atmosphere may have been significant for the noble gases.

To be sure, the mere value of D/H is only part of the story. Paper [64], which contains a very rich literature, discusses the distribution of water and the variation of D/H on the Moon. Improved analytical techniques have revealed that pyroclastic glass beads in Apollo samples contain measurable amounts of water. The pre-eruption magma could have contained water in concentrations that are similar to the mantle sources of mid-ocean ridge basalts on Earth. Lava flows from vast basaltic plains (the lunar *maria*) also contain appreciable amounts of water, as shown by analyses of apatite in *mare* samples. In contrast, apatite in most non-mare rocks contains much less water than the mare basalts and glass beads. The hydrogen isotopic composition of lunar samples is relatively similar to that of the Earth's interior, but the D/H ratios obtained from lunar samples seem to have a larger range than found in Earth's mantle. Thus, measurements of water concentration and hydrogen isotopic composition suggest that water is heterogeneously distributed in the Moon and varies in isotopic composition. The variability in the Moon's water may reflect heterogeneity in accretion processes, redistribution during differentiation or later additions by volatile-rich impactors.

Water, D/H and noble gases such as Ar are not the only elements to be taken into account in the context of life building chemical blocks, other species such as O_2 and NH will be further discussed in a later section.

10. – Non-gravitational forces

This section discusses some applications of celestial mechanics typical of comets. First, we discuss the trajectory of the nucleus, then the dynamics of dust and gaseous tails and finally of individual grains.

As already pointed out, it became soon evident that the orbits of the nuclei are influenced by causes different from gravitational perturbations induced by the great planets. To be sure, non-gravitational (NG) accelerations are usually very small when compared with gravitation, say 10^{-7} of the solar gravity at 1 AU, nevertheless well discernible in long series of astrometric data as variation of orbital elements, for instance the period. The first hypothesis for such changes was a resisting medium pervading the solar system, but that explanation proved soon to be untenable, because a mechanical resistance would imply a decreasing semi-major axis, and therefore a shorter period, while several comets showed the opposite effect. The cometary activity, with the loss of mass as gases and/or dust, was the true culprit, providing a sort of "rocket effect" whose amount depends not only on the mass-loss rate, but also on the rotational status of the nucleus (direction of the spin vector with respect to orbit, amount and verse of the angular velocity), and its shape.

The intensity of the NG force can be specified with three parameters, A_1 along the Sun-comet direction, A_2 in the transverse direction along the orbital plane, A_3 perpendicular to the orbit and usually negligible (but see later). Although A_2 is much smaller than A_1, its effects are cumulative and can become the most important component, especially in periodic comets. Outgassing, mostly by H_2O, depends on the distance from the Sun, and should be very small beyond few AU. The conventional limit (the so-called water frost line) is around 3 AU, essentially just beyond the orbit of Mars.

Therefore, neglecting A_3, the dynamical equation of a comet can be written as

$$\frac{\partial^2 \mathbf{r}}{\partial t^2} = -\frac{GM}{r^3}\mathbf{r} + \frac{\partial R}{\partial \mathbf{r}} + A_1 g(r,t)\frac{\mathbf{r}}{r} + A_2 g(r,t)\mathbf{T},$$

where R is the perturbing function due to large planets, $\mathbf{T}$ is the unit vector in the orbital plane perpendicular to the radius vector, and $g(r,t)$ represents the sublimation of ices, not necessarily symmetric with respect to the perihelion.

A specific study of the modifications induced to the orbital elements (longitude of the ascending node Ω, inclination i, and argument of perihelion ω) by erosion-driven activity on dwarf comets of the Sun-grazing Kreutz family has been performed by [65]. The effect is a strong non-gravitational acceleration perpendicular to the orbital plane, in exceptional cases being similar to the gravitational acceleration. The mechanism behind such perpendicular acceleration is the erosion-driven transfer of momentum from outgassing to progressively fragmenting debris of the original nucleus of the dwarf sungrazer.

11. – Comae and tails

When a comet approaches the Sun, molecules sublimate from the nucleus due to solar heating, and produce a coma around it (the sublimation of gases has the other

effect of dragging with them a dusty component, which will be discussed later on). When exposed to solar radiation, most molecules break apart, for instance an original ("parent", "mother") molecule of H_2O can be split by a solar photon of energy $h\nu$ in H + OH, and successively by another photon in H + O ("daughters"). In the visible band observable from ground-based or Earth-orbiting telescopes (earthly telescopes), daughters are easier to observe than mothers, because they have strong emission lines and bands in such spectral region. The study of parent molecules is better done at radio frequencies and from spacecraft. The distance from the Sun at which a given molecule appears varies within very ample limits, and is very sensitive to the observational frequency. For example, the radical CN in the violet at 3883 A is seen already at 3 AU, followed by CO and CO_2. Atomic lines, such as Na or [OI] appear much closer to the Sun, say below 0.7 AU. The rotational transitions [2-1] at 330 GHz of CO were discovered on comet 29P/Schwassmann-Wackmann1 already at 6 AU.

The initially neutral gases leave the comet with a velocity around 0.5 km/s, and make an electrically neutral and roughly spherical coma around the nucleus. On images taken from ground telescopes in the visible, the coma seems roundish. However, the centre of luminosity does not really coincide with the nucleus, because neutral gases are predominantly ejected toward the Sun. In the inner coma, the density is sufficiently high to insure a large number of collisions, and therefore thermal equilibrium. In such equilibrium conditions, Boltzmann and Saha formulae provide the distributions of atoms and molecules among the levels of excitation and ionization, according to the very low temperatures of the cometary matter. Applying the equation of state for perfect gases:

$$P = \rho k T,$$

where k is Boltzmann constant ($k = 1.4 \times 10^{-16}$ erg/K), we can calculate the mean velocity V_t and the sound velocity in the medium V_s:

$$V_t = \sqrt{\frac{3kT}{m}}\,, \qquad V_s = \sqrt{\frac{\gamma kT}{m}}\,,$$

for a particle of mass m. The constant γ is the ratio between the specific heat at constant density and that at constant volume; its values are 5/3 for a monoatomic gas, and 7/3 for a diatomic one. In other words, the two velocities have approximately the same value, and both are higher than the escape velocity from the low-gravity nucleus.

The sound velocity expresses the velocity with which perturbations move in a neutral medium. However, the coma cannot remain neutral for arbitrary lengths. It is not difficult to demonstrate that the density must decrease with the square of the distance from the nucleus (notice though that the apparent decrease observable from earthly telescopes goes linearly with the distance, because of the integration along the line of sight). At sufficiently high distances from the nucleus and consequently low densities, there are not enough collisions for unit time to insure neutrality, and both atoms and molecules will be ionized by solar UV, *e.g.* CO + $h\nu$ produces CO^+ plus a free electron. In typical situations, beyond approximately 1000 km ionization will appear, at least for a sizeable fraction of gases. Such ionized component will feel the pressure of the solar wind, and so will move in the anti-solar direction, with disturbances propagating with the Alfvén velocity defined in the next section.

As already remarked, the sublimation of gases has the other effect of dragging with them the dust (the gas-dust hydro-dynamical interactions are a very difficult problem),

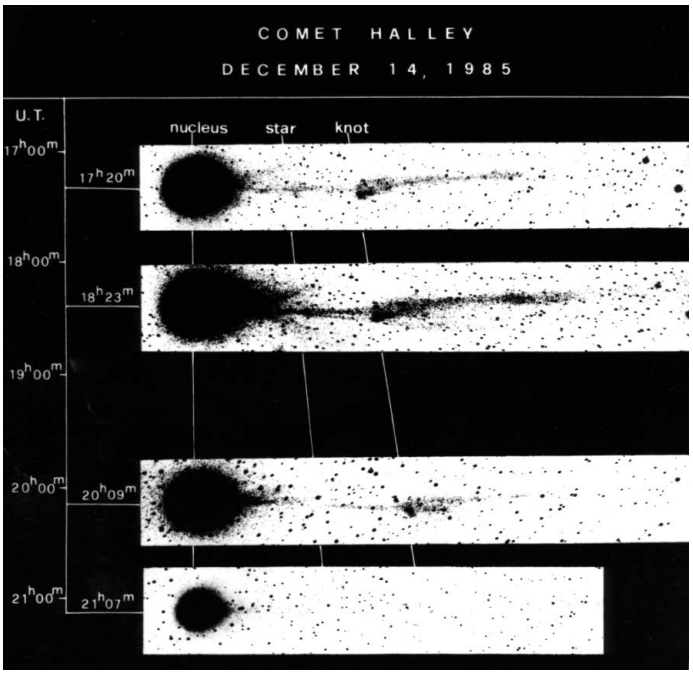

Fig. 6. – Fast phenomena observed in the tail of comet Halley in Dec. 1986 (reproduced by courtesy of the UK Schmidt telescope).

which will fill the neutral coma. Above few nuclear radii, grains are effectively free from the gravitational field of the comet. Their dynamics depends critically on their sizes, as will be discussed in the next section, but essentially the smallest grains will attain velocities similar to that of the gases, which is larger than the escape velocity; therefore, they will fill the coma and subsequently will be pushed to the Type II tail by solar radiation pressure. Assembly of grains too heavy to be ejected may fall back on the surface and contribute to the formation of a rubble mantle. However, large chunks may detach from the nucleus when the comet is very active and near the Sun, replenish the cloud originating the Zodiacal light, and originate the already discussed meteoric showers.

The above considerations explain, although in a very qualitative way, why observations show an inner neutral coma of few thousands km, surrounded by an outer partially ionized coma extending to hundred thousand km, and the two tails of different direction, extension and colour. The ionized, blue tail follows the nucleus pre-perihelion, leads it post-perihelion, but quite often is seen disturbed. Ions feel both density, velocities and magnetic irregularities of the solar wind, so that very complex phenomena can be observed over time scales of few minutes. Figure 6 shows an example for comet Halley.

Needless to say, the reality is very complicated. There are very dusty comets, and gas-only comets. Gases sublimate far from uniformly, and the rotation (and sometimes nutation) will produce spiral shape features arbitrarily oriented with respect to the orbital plane. The dust itself can be a non-negligible source of gases, even far from the nucleus. Finally, ground observations are made from a particular point, and perspective effects

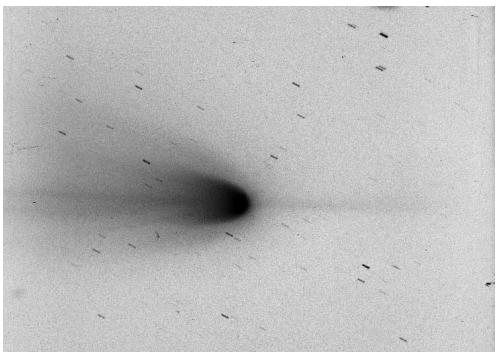

Fig. 7. – The sunward jet of Comet Arend-Roland (1957 III) as seen on a 5-min unfiltered 103a-O plate nr. 2935 taken on 26 April 1957, UT 21h37m at the Asiago Observatory.

can interfere with a proper description of the phenomena (*e.g.* tails apparently directed towards the Sun, like in the famous example of comet Arend-Roland (1957 III)) as in fig. 7. The orbit of this comet has high inclination over the ecliptic, and retrograde motion. The anomalous tail lasted a dozen of days and was at its maximum when the Earth crossed the orbital plane of the comet. The explanation resides in the fact that the comet had two dust tails, the second one made of much larger particles that lagged behind the other tail (see the books [3] and [4]).

As already pointed out, the neutral coma starts to develop well before the conventional boundary of 3 AU. The initial inset is not easily studied in the visible from ground telescopes, if not only because of seeing effects: at 3 AU it is difficult to see a coma with extension less than 4000 km, so IR and radio data are more useful. An interesting case was presented by the very distant comet Bowell, which reached perihelion in 1982 at 3.4 AU on an almost hyperbolic orbit. IR data showed a well-developed coma well before perihelion, composed by water ice particles with dimensions of several microns. Such early inset poses several questions on the source of energy. Several agents have been proposed, such as water ice phase changes, polymerization of surface molecules, fracture of the refractory crust, sublimation of ices from the interior. Reference [66] discusses such problem of energy source, presenting data for two long-period and three dynamically new comets observed at heliocentric distances between 5.8 to 14.0 AU, and which exhibited activity well beyond the water frost line. Experiments on amorphous ice samples show that considerable gas emission occurs when the ice is heated below the temperature of the amorphous-crystalline ice phase transition ($T \sim 137$ K). Thus, annealing of amorphous water ice could be the driver of activity in comets as they first enter the inner Solar System. During annealing, large grains can be ejected at low velocity, and therefore the rate of brightening of the comet should decrease as the heliocentric distance decreases. The distance at which the onset of activity in a dynamically new comet occurs, is a sensitive indicator of the temperature at which the comet had formed, or represents the maximum temperature that it has experienced.

Comet 67P was already active when observed at the beginning of 2014, and actually already before the observations by Rosetta, as shown by ground data [67, 68]. As expected, the activity gradually augmented with the decrease of the distance from the Sun and illumination of the Southern Hemisphere.

Fig. 8. – The two tails of comet Hale-Bopp (image courtesy of the Cortina amateur astronomers, `http://www.cortinastelle.it/aboutus.html`).

11˙1. *Dynamics of dusty tails*. – The term "dust" indicates aggregations of non-volatile elements composed essentially of silicates including magnesium, iron, aluminium and other metals. Another population of grains can be found where Si is substituted by C, the so-called CHON grains found also in the interstellar medium. The dimensions of dusty components vary in an extremely wide range, from sub-micron particles to meter-sized aggregates. The normal observations in the visible tend to favour particles in the range from few tenths to few tens of microns, because they scatter very effectively the solar light, as discussed for instance in ref. [69], and their number is much greater than larger aggregates. While the dusty component of the neutral coma in the visible region has essentially the colour of the solar light, in the far IR it shines by its own thermal radiation.

Regarding the dynamics of Type-II dusty tails, when the comet displays well discernible both dusty and gaseous tails, the two are spatially and morphologically separated. A good example was provided by comet Hale-Bopp, see fig. 8. Type-II tails scatter the sun light, are yellowish in colour, spread out and usually curved along the orbit. On ground telescope images, they show very little or no structure, nor it is always possible to separate them from the dust coma. However, there are cases when the localized emission from the nucleus or its rotation produces jets or spiral structures, which can be detected with appropriate image processing techniques (see again fig. 4). Such localized structures instead, are plainly evident on images taken *in situ*, for instance by the OSIRIS imaging system on board Rosetta, see, *e.g.*, refs. [70] and [71].

A specific characteristic of dusty structures is their possible polarization, first detected two centuries ago, as already mentioned. A recent discussion is provided in [72], who report imaging polarimetry observations of C/2012 S1 (ISON) and 67P using the Hubble Space Telescope. The observations of 67P were timed to be contemporary with the initial rendezvous of Rosetta and the subsequent landing of the probe Philae.

Fig. 9. – Composite of OSIRIS images of 67P showing the trails of dust particles above a heavily saturated cometary surface.

Regarding the dynamics of particles, following the masterly essay on Electricity and Magnetism of C. Maxwell, the Swedish chemist S.A. Arrhenius proposed that cometary matter is accelerated by solar radiation, whose value can be expressed as

$$p = \frac{1}{c}\Phi_{\mathrm{E}},$$

where c is the speed of light, and Φ_{E} is the energy flux, equal to $1.36\,\mathrm{kW/m^2}$ at 1 AU, approximately $9.1\,\mu\mathrm{N/m^2}$. Very soon, this suggestion was taken up by Schwarzschild, who showed that dust grains can get accelerations up to 20 times the solar gravitation, which at 1 AU amounts to about $5.9\,\mathrm{mm/s^2}$.

Let a be the radius of a supposedly spherical dust grain (far from reality, but here we are concerned with orders of magnitude), the radiation flux absorbed by the particle is proportional to a^2, while its mass is proportional to a^3. Therefore, the repulsive force due to radiation pressure is stronger the smaller the particle, and so is the acquired velocity. In other words, the larger grains will never move far from the original orbit, and will gradually fill a torus around it. Such discussion is very incomplete for the smallest grains, because the interactions with light are much more complicated. For very large aggregates of grains, again the situation must be examined in detail, as shown by ref. [73]. Using OSIRIS images, this paper discusses the acceleration of individual, decimetre-sized aggregates in the lower coma of comet 67P, ejected from a confined region on the surface. Those images (see an example in fig. 9) were obtained in January 2016, when the comet was at 2 AU from the Sun outbound from perihelion. Approximately 50 per cent of the aggregates were accelerated away from the nucleus, and 50 per cent towards it, and likewise towards either horizontal direction. The accelerations are up to one order of magnitude stronger than local gravity, and can be attributed to the combined effect of gas drag accelerating all aggregates upwards, and the recoil force from asymmetric outgassing from rotating and/or ice-containing aggregates. At least 10 per cent of the aggregates will escape the gravity field of the nucleus and feed the comet's debris trail, while others may fall back to the surface and contribute to the deposits covering parts of the Northern Hemisphere.

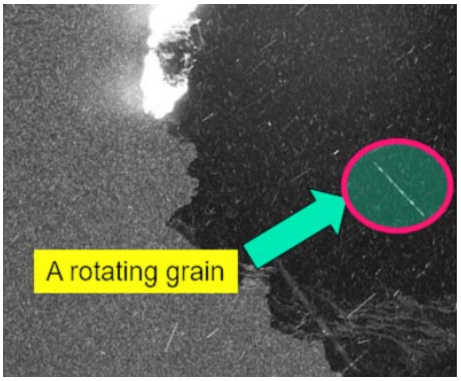

Fig. 10. – A rotating grain from comet 67P as imaged by OSIRIS.

The rocket force plays a crucial role in pushing these aggregates back towards the surface.

Dust grains may rotate, as vividly shown again by images of OSIRIS (see fig. 10), and this rotation provides a lateral acceleration. A detailed discussion of dynamics of non-spherical dust grains under aerodynamic and gravitational forces can be found in [74] and [75]. The authors took into account not only Rosetta data, but also the results of the Stardust mission and analysis of samples of interplanetary dust, which have shown that these particles are highly aspherical. The translational and rotational motion of ellipsoidal particles with various aspect ratios, under the influence of the gravity and of the aerodynamic force and torque, injected in a spherically symmetric expanding gas flow, was numerically integrated in a wide range of physical parameters appropriate to comet 67P.

11˙2. *The parameter* $Af\rho$. – The already quoted comet Bowell 1980b prompted the introduction of the parameter $Af\rho$ as a measure of the solar radiation reflected from the dust coma (see [76]). In the original definition, A is the albedo, f the filling factor and ρ the projected radius of the instrument field of view, so that the quantity $Af\rho$ is expressed in linear units, *e.g.*, km. The filling factor f is just the total cross section of grains within the field of view, $N(\rho)\sigma$, where σ is the cross section of a single grain, divided by the area of the field of view, $\pi\rho^2$. The albedo A is a function of wavelength λ and of scattering angle ϑ, and is defined as the ratio of the total light reflected by the cometary particles to the total light removed from the solar flux by the cometary particles. In other words, the total luminosity from the comet is given by $AN\sigma F_{\rm o}/r^2$, and the product Af can be determined directly from the observations as $Af = (2\Delta r/\rho)^2\ F_{\rm com}/F_{\rm o}$, where Δ and ρ are in km (or cm), r is in AU, $F_{\rm o}$ is the solar flux at 1 AU, and $F_{\rm com}$ is the observed cometary flux. The use of $Af\rho$ for measuring the continuum of a comet was introduced because for most cometary observations, the line of sight column density falls off as $1/\rho$. On the other hand, the projected observational area increases as ρ^2. Thus, the quantity $Af\rho$ is independent of the specific observational circumstances or the instrument settings used, *e.g.* photometric aperture, or slit width and length for spectroscopic observations, and inter-comparison of $Af\rho$ values by different observers can readily be accomplished.

The original definition and its limitations were re-discussed by [77] in preparation for the observations of 67P by the Rosetta instruments, using Mie single-scattering theory and a Direct Simulation Monte Carlo (DSMC) dust outflow model. Their calculations were performed for particle sizes ranging from 0.010 mm to 1.0 cm. A most crucial point

for the correct interpretation of the measured quantity $Af\rho$ is the particle size distribution. A common and simple form of the particle size distribution for particles with radius a is an exponential law given by

$$\frac{\mathrm{d}Q}{\mathrm{d}a} = \left(\frac{\mathrm{d}N}{\mathrm{d}a}\right) = g_0 a^{-\alpha}, \qquad Q(a) \approx a^{1-\alpha},$$

being g_o a normalization constant, and $Q(a)$ the production rate([5]) of particles of size a.

Paper [78] presents the results obtained by COSIMA on board Rosetta, dedicated to the collection and compositional analysis of the dust particles in the coma of 67P. The flux, size distribution, and morphology of the dust particles collected starting at a heliocentric distance of 3.5 AU, were measured with a daily to weekly time resolution. The particles could be classified according to their morphology into two main types: compact particles and porous aggregates. The porous material appears similar to the chondritic interplanetary dust particles collected in Earth's stratosphere, and represents 75% in volume and 50% in number of the large dust particles. Compact particles have typical sizes from a few tens to a few hundreds of microns, while porous aggregates can be as large as a millimetre. The particles were not collected as a continuous flow but appeared in bursts. The average collection rate of dust particles as a function of nucleo-centric distance shows that, at high phase angle, the dust flux follows a $1/\rho^2$ law, which excludes fragmentation of the dust particles along their journey to the spacecraft. At low phase angle, the dust flux is much more dispersed compared to such law, but such dispersion cannot be explained by fragmentation of the particles along their trajectory since their velocity does not support such a phenomenon. The cumulative size distribution of particles larger than 150 μm follows a power law close to $a^{-0.8\pm0.1}$, while the cumulative size distribution of particles between 30 μm and 150 μm has a power index of -1.9 ± 0.3. The excess of dust in the 10–100 μm range in comparison to the 100 μm–1 mm range, together with no evidence for fragmentation in the inner coma, implies that these particles could have been released or fragmented at the nucleus right after lift-off of larger particles. Below 30 μm, particles exhibit a flat size distribution. This knee in the size distribution at small sizes is interpreted by the authors as the consequence of strong binding forces between the sub-constituents. For aggregates smaller than 30 μm, forces stronger than Van der Waals forces would be needed to break them apart.

Detailed measurements were made by GIADA, another dust instrument on Rosetta. As reported by [79], for the first time a dust instrument measured mass, speed, cross-section and the exact detection time/position of individual dust particles simultaneously. GIADA was able to: 1) characterize 67P's dust environment; 2) monitor the dust loss rate and the particle mass distribution at the surface of the sunlit nucleus; 3) monitor the dust mass distribution of 67P as it evolved with time; and 4) in the case of dust detected along closely bound orbits, provide a hint of the region of the nucleus from where the dust originated. Masses in the range 10^{-6} to 10^{-9} kg could be measured, with velocities varying from 1 to 10 m/s (heavier particles had a lower velocity; some outliers with velocity as high as 30 m/s were also detected). Such ejection velocities could be correlated with H_2O production rate, both at local and global level.

([5]) The quantity *production rate* Q is the amount of molecules of a given species produced every second by the comet at a given distance from the Sun. As a rough indication, $Q(H_2O)$ can range from 10^{28} to 10^{31} molecules/s. The sensitivity of the observations can be of few kg/s.

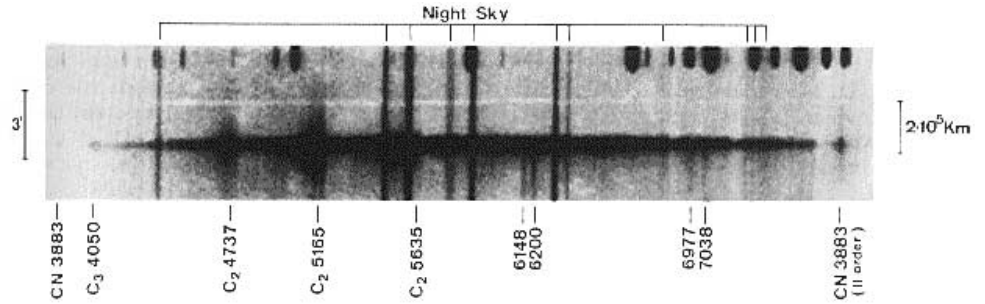

Fig. 11. – The original photographic plate of the discovery of H_2O^+ on comet Kohoutek 1973 (ref. [81]). The ion is seen at $\lambda\lambda$ 6148/6200 and 6977/7038. The emissions are strongly asymmetric, much stronger in the tail than towards the Sun.

More results on dust size distribution and its evolution obtained by Rosetta instruments from 2.2 AU to perihelion are given by [80]. The dust size distribution at sizes > 1 mm observed by OSIRIS is consistent with a differential power index of -4. At sizes < 1 mm, the size distribution observed by GIADA shows a strong time evolution, with a differential power index drifting from -2 beyond 2 AU to -3.7 at perihelion, in agreement with the evolution derived from coma and tail models based on ground-based data. The refractory-to-water mass ratio of the nucleus is close to six during the entire inbound orbit and at perihelion.

11˙3. *Dynamics of Type-I ionized gaseous tails*. – Type-I gaseous tails are thinner, bluish in colour, and pointing approximately to the anti-sunward direction, quite often disturbed, with suddenly varying shape (see Halley's in 1986, fig. 6). However, the much stronger accelerations of molecules in Type-I tails cannot be explained by radiation-pressure, as proven by K. Wurm in 1943, when he derived that the radiation pressure on CN, C_2 and CO^+ could only be 0.7, 1.7 and 47, respectively, far too small than observed. Another mechanism had to be present to explain gaseous tails, as postulated later on by L. Biermann and H. Alfvén.

Ionized tails are also referred to as *plasma* tails. Plasma can be considered as a fourth state of matter, where ions in a low density medium have strong interactions with magnetic (and sometimes even electric) fields. The ion density decreases along the tail, say from 1000 to 10 cm^{-3}. In the visible, the dominant ion is CO^+. Other ions are $CO_2{}^+$, CH^+, OH^+, and H_2O^+, first discovered in Asiago Observatory (ref. [81], see fig. 11).

As already pointed out, Biermann noticed that the ion accelerations were hundreds or even thousands of times stronger than could be accounted for by the radiation pressure. Therefore, he postulated the presence of a stream of ionized particles coming out of the Sun. There was another proof for the existence of such "solar wind", namely the aberration angle of the plasma tail direction, which is not strictly in the anti-solar direction. Biermann interpreted such angle as due to the relative velocity between the comet and the solar wind.

Biermann' theory was soon completed by Alfvén, who added the effects of the solar magnetic field carried away by the stream of ionized particles. The compression of the magnetic field lines was fully able to explain the morphological peculiarities of the ion tail. As is well known, a magnetic field forces an ion to describe a spiral orbit around

the field lines with a Larmor radius r_L given by

$$r_L = \frac{V_p m}{qB},$$

where V_p is the component of the ion velocity perpendicular to the field (say 10 km/s), m its mass, q its electric charge and B the magnetic field in gauss. Given that typically $B \approx 5 \times 10^{-5}$ G, the gyration radius is around 100 m for the electrons, and 25 km for the ions, well consistent with the observations.

Disturbances in the Type-I tails propagate not with the sound speed applicable to neutral species (see previous section) but with the speed of the Alfvén waves given by

$$V_A = \frac{B}{\sqrt{4\pi\rho}},$$

which increases with the decrease of density, from say 10 to 200 km/s.

Plasma tails develop usually when the distance from the Sun is below 2 AU, but there are exceptions, like comet Humason 1961 which had a strong CO^+ already at 5 AU.

Another puzzling observation is that often CO^+ is seen already inside 1000 km from the nucleus, and a molecule of CO can cross such distance in a time much shorter than the ionization life-time. The transformation of the original molecules (the mothers) in the observed ones (the daughters) is a fundamental problem in cometary chemistry, as already pointed out and discussed later on.

There is another important macroscopic phenomenon connected with the interaction between the solar wind and the plasma tail. An important paper describing the plasma around comets is ref. [82]. Here, we assume for simplicity that the solar wind particles reach the comet along straight lines, with typical velocities of 400 km/s, and that the comet has no magnetic field of its own([6]). The cometary ions, which travel say at 10 km/s but are much more massive than solar protons or He nuclei, are soon carried away by the wind, which is then loaded in mass and slowed. At a certain distance from the nucleus, the solar wind velocity passes from a supersonic to a subsonic velocity, with a corresponding discontinuity. The flux propagation becomes turbulent, with the formation of a bow shock and several inner regions. At the cometo-pause, the field lines wrap around the nucleus, and impede the cometary ions to move toward the Sun. The cometary ions are then pushed inside the tail. At the same time, the solar wind ions cannot penetrate such contact surface. The description of all the observed phenomena is extremely complicated, for instance it might happen that the solar magnetic field changes polarity, causing disconnections in the tail. What is definitely clear is that the magnetic field around the nucleus is capable to explain the very strong repulsive force that pushes the cometary ions into the plasma tail. Those magnetic interactions produce also the already quoted X-ray emissions.

Detailed observations were made by the five instruments of the Rosetta Plasma Consortium (RPC), whose main objective was to observe the formation and evolution of plasma interaction regions (see for instance [83]). At the end of July 2015, close to

([6]) The absence of magnetic structures larger than 1 m on comet 67P was shown by the magnetometer aboard Philae during the flight of the lander from the touch-down zone to Abydos on Nov. 12, 2014. See appendix A.

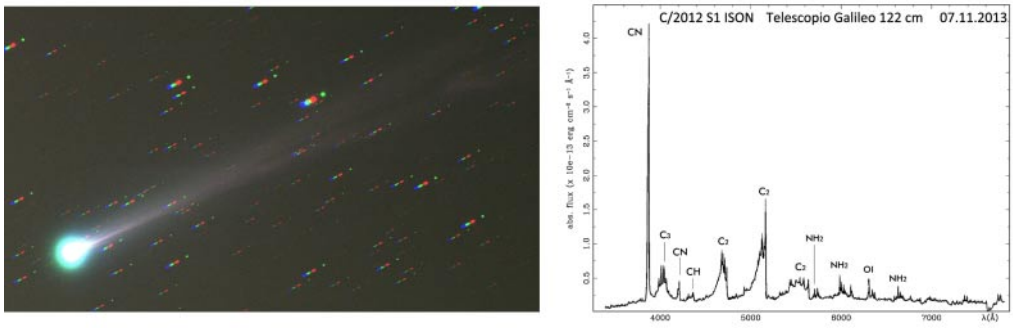

Fig. 12. – Comet ISON C/2012 S1 and its spectrum in the visible region. The underlying solar-type spectrum has a maximum at about 5500 A and represents sunlight reflected and scattered from the cometary dust grains (courtesy P. Ochner and S. Dalle Ave, Asiago Observatory).

perihelion and when Rosetta was about 139 km from the nucleus, ref. [84] reports the detection of a diamagnetic cavity, namely a region that did not contain any magnetic field at all. From mid-September to mid-October 2015, Rosetta was sent to some 1500 km away on the sunward direction to measure the interactions between cometary material and solar plasma. Observations showed that boundaries and regions of solar wind-cometary plasma interaction formed around mid-April 2015 and lasted through early January 2016. At least two regions were observed, separated by an ion-neutral collision-pause boundary. The inner region was located on the nucleus side of the boundary and characterized by low-energy water-group ions, reduced magnetic field pileup and enhanced electron densities. The outer region, located outside of the boundary, was characterized by reduced electron densities, water-group ions accelerated to energies above 100 eV, and enhanced magnetic field pileup compared to the inner region. The boundary shows characteristics similar to observations made on-board the GIOTTO spacecraft in the ion pileup region at 1P/Halley, and is likely related to ion-neutral collisions. Its location is influenced by variability in the neutral density and the solar wind dynamic pressure.

12. – Spectroscopy of comets

Observations from ground or Earth orbiting telescopes have provided a wealth of information about the chemical composition of comets. To the scattered solar light of the dust, neutral and ionized molecules such as C_2, CN, CH, NH_2, H_2O and atoms such as H, O, Ne, Na, Fe add their emission lines and bands (see fig. 12 and fig. 13). As already stated, water ice is the most abundant volatile, followed by CO, CO_2 and by traces of other species. From space, one can observe a huge cloud of H emitting in its Ly-alpha line and a smaller cloud of OH, both coming from the dissociation of water under the solar UV. On Hale-Bopp, the Ly-alpha cloud could be traced for more than 1 AU. Notice that photo-dissociation can occur and persist on the region outside that dominated by collisions, so that H and OH can obtain very high velocities, *e.g.* 20 km/s for H and 7 km/s for OH. OH itself can dissociate, producing a second cloud of H at 7 km/s. At such high velocities, H and OH can travel to great distances before the solar UV ionizes them, and make the respective ions carried away by the solar wind.

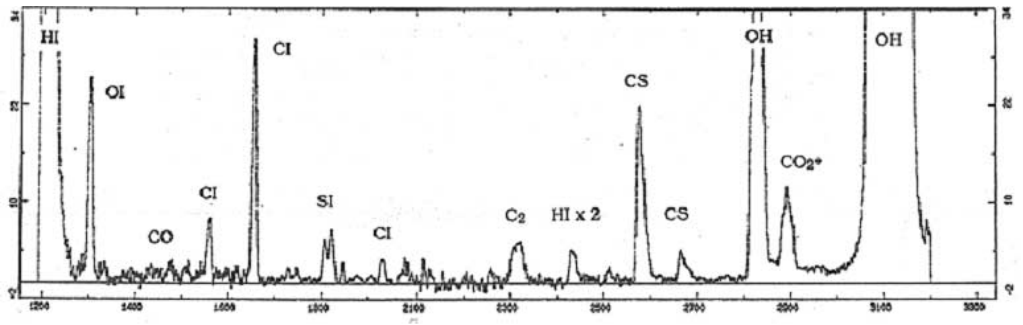

Fig. 13. – Superposition of two UV spectra of comet Bradfield (1979 X) obtained by IUE in Jan. 1980. Ly-alpha and OH transitions are saturated in order to bring out the fainter features (adapted from [21]).

The literature abounds of papers about spectroscopy of comets. Some general references are the book by Huebner [85], and the papers by Mumma and Charnley [86] and Cochran and co-authors [87]. An example of high-resolution spectroscopy of a comet is provided in [88]. Arpigny and collaborators are preparing an *Atlas of cometary spectra*, which will be, so to speak, the successor of the already quoted historic work by P. Swings; a preview can be seen in [89].

Earthly based observations have the already mentioned severe difficulty to determine the true composition of the cometary gases and the chains of reactions affecting them, because of the chemo-physical degeneration quickly performed by the solar UV radiation and the inability to disentangle the different regions producing the different species. Some of these reactions can be easily understood and quantified, *e.g.* OH coming from dissociation of H_2O; others are more complex, *e.g.* CO is not necessarily a product of CO_2. Furthermore, the volatile parts of the surface could be constituted by clathrate-hydrates, in which several different elements (like methane, ammonia, carbon dioxide and so on, but also small solid particles) are trapped inside "cages" of hydrogen bonded, frozen water molecules. Already in the 50s of last century, Delsemme and Swings invoked their presence to explain why gases with different sublimation temperatures where observed to sublimate at the same time and temperature. If such hypothesis was entirely correct, then the production rate of the "guest" would be rigorously fixed to $Q(\text{guest}) = Q(H_2O)/6$ by the properties of the hydrogen bond. However, observations do not always adhere to such expectation, for instance in comet West (1976n) it was $Q(CO) = Q(H_2O)/2.5$.

Table V gives an incomplete list of cometary atoms and molecules detected by spectroscopic means, supplementing those listed by the already quoted ref. [8] and those found by ROSINA by capture of ions (see table VI), which will be discussed in short. More than 20 primary chemical species have been detected in bright comets. Notice that the term 'molecule' is used loosely in cometary chemistry to indicate unsaturated compounds, like OH and CN. Even the name itself can be deceiving; for instance, CN is called "cyanogen" even if the "true" cyanogen is C_2N_2.

The chemical composition is not at all uniform, it varies from comet to comet. For instance, on Hale-Bopp the ratio CO/H_2O was around 0.2, five times greater than on most other comets. Furthermore, the observed chemical composition of the gases do not necessarily reflect that of the entire body, especially for short-period comets. Due to the repeated passages around the Sun, a large fraction of volatiles must be gone, and the crust will be rich of refractory insulating elements.

TABLE V. – *Atoms and molecules in the coma (incomplete).*

Atoms and their Ions		Molecules and their Ions	
H	Hydrogen	OH, OH^+	Hydroxyl
O, O^+	Oxygen	H_2O, HDO, H_2O^+, H_3O^+	Water, heavy water, hydronium ion
C, C^+	Carbon	C_2, C_3	Molecular carbon
N	Nitrogen	CO, CO^+, CO_2, ${CO_2}^+$	Carbon monoxide and dioxide
S	Sulphur	S_2	Molecular sulphur
Fe	Iron	CS	Carbon sulphate
Ni	Nickel	CN, CN^+	Cyanogen radical
K	Potassium	CH, CH^+	Hydrocarbon
Ca, Ca^+	Calcium	NH, NH_2	Nitrogen mono- and bi-hydride
Na	Sodium	HCN	Hydrogen cyanide
V	Vanadium	CH_3CN	Acetonitrile (methyl cianide)
Mn	Manganese	CH_2O, HCO	Formaldehyde, radical
Co	Cobalt	NH_3	Ammonia
		H_2S^+	Hydrogen sulphide ion

Another difficulty to properly understand comae, is presented by dust, because its thermal capacity differs from that of the gases. Moreover, when subliming, a mixture of gases and dust has a different hydro-dynamical behaviour of gas alone, and the dust itself could be a secondary source of gases. This latter property was discovered by [90] by means of a third tail of Na in comet Hale-Bopp.

Sun-grazing comets vividly illustrate the complexity of the observations. Comet Hyakutake, which passed the perihelion on May 1st, 1996 at about 35 million km, namely well inside Mercury's orbit, is a first example. For the whole month of February until early March, when the comet reached $r = 1.5\,\mathrm{AU}$, $Q(H_2O)$ was essentially constant around

TABLE VI. – *Partial inventory of gases found by ROSINA on Rosetta.*

Name	Composition
Water	H_2O
Carbon monoxide	CO
Carbon dioxide	CO_2
Ammonia	NH_3
Methane	CH_4
Methanol	CH_3OH
Formaldehyde	CH_2O
Hydrogen sulphide	H_2S
Hydrogen cyanide	HCN
Sulphur dioxide	SO_2
Carbon disulphide	CS_2
Molecular oxygen	O_2
Molecular nitrogen	N_2
Argon	Ar

4.5×10^{28} molecules/s, and so did the CN production. On the contrary, the production of C_2 increased by 50%, and that of dust by 80%. The ratio CO/H_2O was ≈ 0.2, very similar to Halley's. Around March 19, when $r < 1.5$ AU, the ion tail became well developed, with a length of 15 deg, and jets of dust extended up to 10^4 km from the nucleus. The production rates of H_2O, CN and CO quickly increased. Radio data detected a new molecule, OCS, with $OCS/H_2O = 0.004$, in addition to the already known methanol (CH_3OH), formaldehyde (H_2CO), HCN and CO, whose production rate was very high, around 3×10^{28} molecules/s, and about two orders of magnitude higher than that of formaldehyde. Around March 25, radio data reported the detection of HCN, a molecule typical of the interstellar medium, fairly unstable and which could be detected only thanks to the proximity of the comet to the Earth and to its great activity. Other molecules were detected in the radio region, such as CH_3CN, C_2H_6 (ethane) e CH_4 (methane). The same day, the IUE satellite noticed a very strong increase of water production, say 7 times higher than few days before, although the distance to the Sun had increased by only 0.1 AU. Regarding ammonia (NH_3), the abundance in Hyakutake was around 0.25% that of H_2O, sensibly less than for Halley's. Few days later, the water production was back to the values measured before March 25, suggesting that the comet had lost in that date some small piece. A very complex scenario indeed, where several questions were left unanswered, *e.g.* the source of CO, and could be answered perhaps only by *in situ* observations.

C/2012 S1 (ISON) provided many puzzling and conflicting data. According to [91], long-slit high-dispersion infrared spectroscopy showed that $Q(H_2O)$ increased from $(8.7 \pm 1.5) \times 10^{27}$ molecules/s on October 26 (heliocentric distance = 1.12 AU) to $(3.7 \pm 0.4) \times 10^{29}$ molecules/s on November 20 (distance = 0.43 AU, heliocentric velocity around – 62 km/s), with factor of two short-term variability. Compositional changes were also detected, may be the result of a transition from sampling radiation-processed outer layers in a comet approaching perihelion for the first time, to sampling more pristine natal material, as the outer layers were increasingly eroded and the thermal wave propagated into the nucleus. On November 19 and 20, the spatial distribution for dust appeared asymmetric and enhanced in the anti-solar direction, whereas spatial distributions for volatiles (excepting CN) appeared symmetric with their peaks slightly offset in the sunward direction compared to the dust. On the same date, the spatial distribution for most gaseous species showed no definitive evidence for significant contributions from extended sources, except perhaps for NH_3 and OCS. Moreover, abundances of HCN and C_2H_2 were insufficient to account for abundances of CN and C_2. HCN seemed to be only a minor source of CN, whose spatial distribution in the coma suggests a dominant distributed source correlated with dust and not volatile release. On the contrary, NH_3 appeared to be the primary source of NH_2, with no evidence of a significant dust source of NH_2. Again around Nov. 20, a region of about $10^6 \times 10^6$ km^2 around ISON was observed in the UV by means of a sounding rocket (see again [43]). Images were dominated by C I λ1657 and H I λ1216. The carbon and water production rates were, respectively, $Q(C) \approx 4 \times 10^{28}\,s^{-1}$, $Q(H_2O) \approx 8 \times 10^{29}\,s^{-1}$. The radial profile of C I was consistent with it being a dissociation product of a parent molecule other than CO.

It is clear, from what has been said, that comets are fascinating laboratories, where conditions are very different from those of the terrestrial laboratory. The cometary ambient makes it possible the existence for days and even months of compounds that in the laboratory have only very short life-times. However, the complexity of phenomena makes it imperative to perform space missions able to penetrate the comae for a sufficiently long time. In particular, the instruments on board Rosetta have produced an amazing amount of new data.

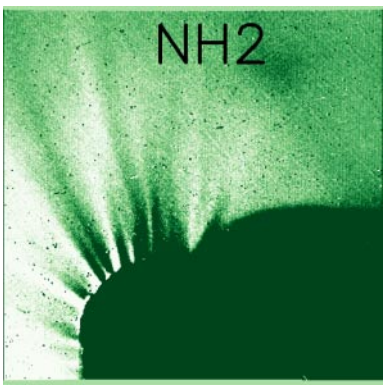

Fig. 14. – An example of an OSIRIS/WAC image in the filter NH_2. The Sun is in the upper direction.

The WAC/OSIRIS was equipped with narrow filters suitable to the study of spectral lines and bands from the several cometary species. Bodewits and collaborators ref. [92] have completed the analysis of images when the comet was between 2.6 and 1.3 AU from the Sun, showing emissions in the filters OH, NH, NH_2, [O I] and CN (fig. 14). A strong plume-like feature observed in the CN and O I filters is present throughout those observations. This plume is not present in OH emission and indicates a local enhancement of the CO_2/H_2O ratio by as much as a factor of three. Another important result is that such lines had a noticeable fading of intensity after March 2015, most likely because the strong increase of activity due to the increasing solar insolation did not allow the solar wind particles to reach the proximity of the cometary soil.

ROSINA has provided a most comprehensive list of gases by *in situ* capture of ions produced by comet 67P. Table VI gives a list of molecules detected in the pre-perihelion months, see ref. [93]. In addition, ROSINA (see ref. [94]) has provided firm evidence for Glycine (NH_2CH_2COOH), the smallest of the 20 amino acids commonly found in proteins, and indeed the smallest possible. Another result by ROSINA has been the discovery of molecular oxygen O_2 with an abundance $O_2/H_2O = (3.80 \pm 0.85)\%$. The loss of O_2 was observed well correlated with that of H_2O. Prompted by such result, the ROSINA team re-examined the data from the GIOTTO mission at comet Halley finding a comparable amount ([95] and references therein). Therefore, O_2 might be a rather common and abundant species, and most likely a "mother", because O_2 can form only at very low temperatures.

Furthermore, ROSINA detected argon (ref. [96]), and variations in the amount of N_2 (the most abundant molecule in the terrestrial atmosphere) and CO as function of time, comet rotation and position of the spacecraft above the nucleus, with an average ratio $N_2/CO = (5.70 \pm 0.66) \times 10^{-3}$, with minimum and maximum values of 1.7×10^{-3} and 1.6×10^{-2}, respectively. Those very low values imply that comets such as 67P cannot be responsible for the Earth's nitrogen.

These findings, and those already quoted about D/H, will certainly add a great deal to the discussion about comets and the origin of life on the Earth.

ALICE allowed the discovery of a new process, showing that free electrons([7]), and not solar photons, are the reason for the rapid dissociation of CO_2 and H_2O [97,98]. The process is a two-step one: free electrons, produced by ionization of H_2O by solar photons, dissociate by impact other neutral H_2O molecules, accounting for the high intensity of H and O spectral lines. Similarly, free electron caused by photo-dissociation of CO_2 dissociate by impact other neutral CO_2 molecules, finally producing the observed strong emissions of C, O and CO. In other words, the main source for the high intensity of the lines of H, O, C and CO is mostly due to transitions from energy levels excited by free electrons in the coma, not by solar photons as previously held. Their relative brightness to HI reflects the variation of CO_2 to H_2O column abundance in the coma. Surprisingly enough, the gaseous outbursts observed by ALICE since April 2015 do not correlate with any of the visible images of outbursts taken with either OSIRIS or the NAVCAM.

Spatially resolved spectra by VIRTIS have produced a wealth of data on the gaseous coma. For instance, [99], determined the H_2O and CO_2 distribution from VIRTIS-M infrared observations taken in April 2015, by means of the vibrational bands of water and carbon dioxide at 2.67 and 4.27 μm, respectively. The maximum H_2O emission was observed within 3 km from the nucleus, mainly concentrated above two active regions, Aten-Babi and Seth-Hapi (see fig. 19). The CO_2 distribution appeared more uniform, with significant emissions coming from both the "head" and southern latitude regions. In the equatorial region, the column densities of both species decreased with altitude, CO_2 decreasing more rapidly than H_2O. The calculated CO_2/H_2O column density ratios above Aten-Babi and Seth-Hapi are $(2.4 \pm 06)\%$ and $(3.0 \pm 0.7)\%$, respectively. A value equal to $(3.9 \pm 1 : 0)\%$ was observed at equatorial latitudes in the region encompassing Imothep. Therefore, the Hapi region showed a high water vapour outgassing, occurring at the same place where the diurnal cycle of condensed water ice was reported [100].

Other important results about the gaseous coma were provided by NASA MIRO. Regarding water losses, while in June 2014 (see [101]) it amounted to a mere 300 millilitre/s (say $Q \approx 1 \times 10^{25}$ molecules/s), around the perihelion it augmented by about 500 times. A surprising initial result was the absence of CO, which should have been a most abundant species, strongly interacting with radio waves and therefore expected to be seen soon after water was detected. Instead, while water was seen early in the summer of 2014, it was only near perihelion that MIRO saw CO. ROSINA had measured CO around the comet well before that, but only in certain areas, not everywhere. Rosetta spent most of its observational time around the Northern Hemisphere, while the CO was mostly coming from the Southern one. Clearly, only *in situ* instruments could have detected such spatial variation of the source locations.

It was already said that comets are loose aggregates of volatile ices mixed with solid particles, gradually accreted starting from primordial constituents (the planetesimals) and usually not further processed, if not on their surfaces, by space weathering and cosmic rays spallation effects. Their composition, including isotopes and isomers, must therefore reflect that of the original solar system and interstellar clouds. Very important is the determination of the noble gases, in particular He, a fraction of which must come from the initial cosmological Big Bang. The abundance of D/H, Ar, O_2, N_2 by ROSINA

([7]) The free electron density was measured by the Langmuir Probe and Mutual Impedance Probe (LP/MIP) of the instrument RPC quoted in table VIII.

has been already discussed. The measurements of ortho- *vs.* para-water([8]) and other nuclear spin ratios (*e.g.* in ammonia and methane), of isotopic ratios (D/H in water and HCN; $^{14}N/^{15}N$ in CN and HCN) mostly by radio data, have provided critical insights on factors affecting the formation of primary species. The identification of an abundant product species (HNC) has given clear evidence of chemical production in the inner coma. Available data lead to estimated formation temperatures between 25 and 50 K. Such low temperatures, typical of the outer Solar System, combined with the very low gravity, mass and ensuing scarcity of radioactive elements, did not provide enough energy to activate the processes of sublimation, metamorphism, fractionation etc., which occurred in the large planets and inner regions. Such are the basic reasons for believing that comets reflect the origins of the solar system some 4.6 billion years ago.

In conclusion, although the physical and chemical properties of comets are a truly complicated matter, surely in need of further data by the incoming large telescopes such as ALMA and JWST, their spectroscopic observations have already provided crucial information about more distant components of the Universe, such as the interstellar clouds and the effects of cosmic rays.

13. – The nucleus

The importance of space missions to determine the nuclear shape and surface characteristics has been underlined several times. Until the data provided by the GIOTTO and VEGAs missions in 1986, no clear consensus about the shapes, dimensions and other characteristics of cometary nuclei was possible. Although GIOTTO could see only one face of the comet, and the VEGAs had limited resolution and dynamic range, the sequence of images allowed to derive several crucial data on Halley's nucleus:

- dimensions of about $15 \times 7 \times 7\,\mathrm{km}^3$,
- very low albedo, around 5%,
- activity limited to few fractures,
- maximum rugosity around 1 km.

Those images changed the perception of cometary nuclei to a new paradigm [102]:

- the dominant component of cometary nuclei is not (water) ice but dust;
- the physical properties of the nucleus are determined by the non-volatile (dust) component;
- the activity comes from limited areas of sublimation (say 10% of the surface);
- cometary nuclei are porous, of low density and tensile strength;
- cometary nuclei are built from sub nuclei (probably hierarchically).

Halley comet looks more an icy dirt ball rather than a dirty snowball, as postulated by the then prevailing model by Fred Whipple.

([8]) In an ortho-molecule of water, the two H atoms rotate in the same sense, in the para-molecule in the opposite one, and the ratio (on Earth is around 2.5) is sensitive to the rotational temperature of the medium the cometary water formed.

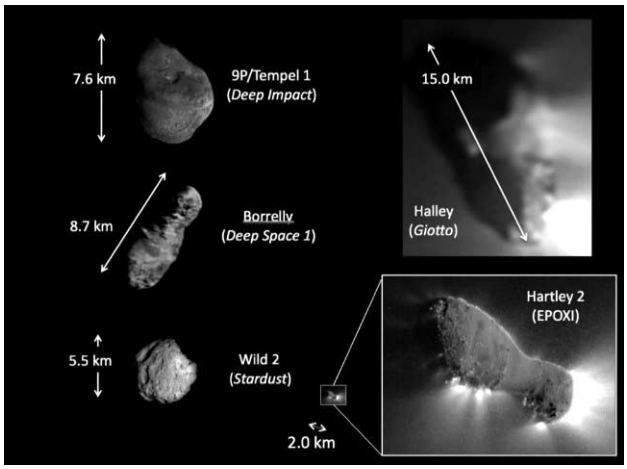

Fig. 15. – Cometary nuclei imaged by space missions before Rosetta.

The spacecraft of the "grand armada" to comet Halley in 1985/86 were astounding scientific and technical achievements, followed by other all-NASA cometary missions before the ESA Rosetta:

– Deep Space 1, 2001, to comet 19P/Borrelly,

– Stardust, 2004, to comet 81P/Wild 2,

– Deep Impact, 2005, to comet 9P/Tempel 1 (with scientific contributions by Rosetta),

– EPOXY, 2010, to comet 103P/Hartley 2,

– Stardust-NExT, 2011, return to comet 9P/Tempel 1.

For a quick link to such missions see [103].

Deep Impact and its target, comet Tempel 1, provided Rosetta the first occasion to exercise its excellent capabilities to produce cometary science. Terrestrial observers, the Deep Impact spacecraft and Rosetta were at the vertices of an 80 to 100 million km sides triangle that defined one of the rare instances when a celestial body can be seen from very different vantage points. For the results obtained by OSIRIS on comet Tempel 1, in particular for the amount of water released after the impact, see for instance [104].

Figure 15 gives a set of images of cometary nuclei obtained by all space missions before Rosetta.

Comet 67P provides the best example to date of a cometary nucleus repeatedly observed for many months both before and after the perihelion, see [105] and the many other references quoted in this review. Figure 16 shows the shape of 67P in context with the previous images. Figure 17 shows the mathematical shape of Halley's adapted from [106], fig. 18 gives more details on 67P shape and dimensions and its mathematical reconstruction (adapted from [107]), while fig. 19 provides a map of the different morphological regions identified on the nucleus of 67P and the given Egyptian names (adapted from [108]).

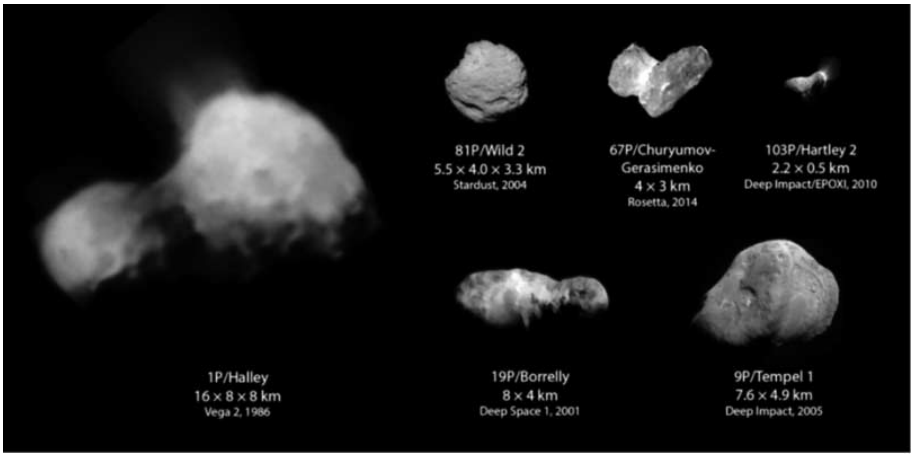

Fig. 16. – 67P in context with previous images, on the left panel Halley's nucleus as seen by the VEGA missions.

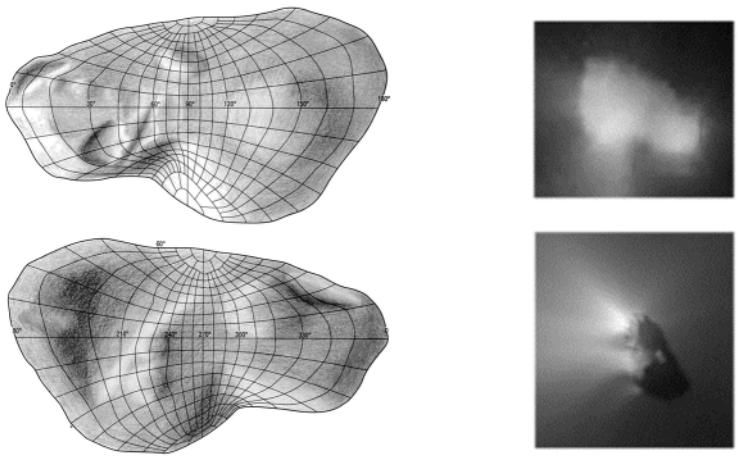

Fig. 17. – Shape model of Halley's nucleus combining images from VEGA (upper right panel) and GIOTTO (lower right panel) (adapted from [106]).

13˙1. *Models of cometary nuclei*. – All pre-space era models agreed on a description of nuclei having dimensions from hundreds of meters to dozens of km, and constituted by a mixture of ices and dust. The hypothesis of an icy conglomerate with the inclusion of dust (*a ball of dirty ice*) was exposed by Fred Whipple in 1950, at variance with the other model of a sand bank, with gases adsorbed on the sand particles. The main difficulty of such sand bank model was that adsorption fails by several orders of magnitude to account for the observed amount of released gases and long life-time of a nucleus, in particular for periodic comets. The most abundant of ices is water in its phases, amorphous ($T < 136\,\mathrm{K}$), crystalline with cubic structure ($136 < T < 173\,\mathrm{K}$), crystalline with hexagonal structure ($T > 173\,\mathrm{K}$) similar to what is found in terrestrial glaciers. When $T > 173\,\mathrm{K}$, water ice starts to sublimate. In hypothetical equilibrium conditions,

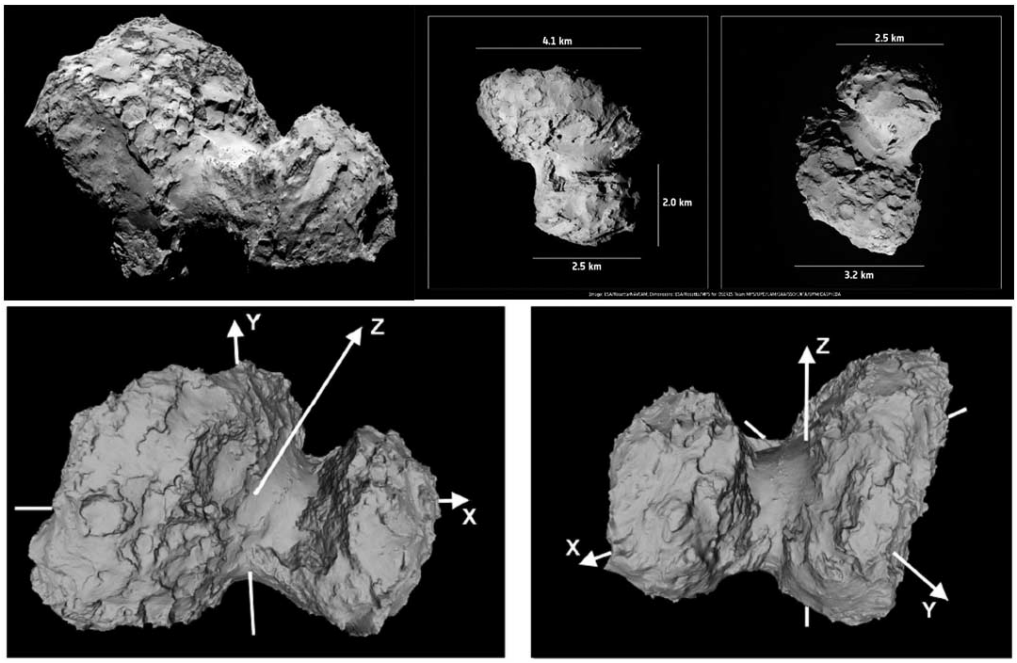

Fig. 18. – Overall shape and dimensions of 67P. Top row: examples of pre-perihelion OSIRIS images. Bottom row: mathematical reconstruction of 67P shape (adapted from [107] with permission @ESO).

the regime $T < 136\,\mathrm{K}$ holds beyond 4.5 AU, while the line $T > 173\,\mathrm{K}$ is crossed at 2.8 AU (Mars orbit). All other ices, like CO, CO_2, CH_4, start to sublimate much earlier than water. The sublimation of gases in the conventional view is the main responsible for the formation of the coma, even of the dusty one, because escaping gaseous molecules carry with them the dust grains. Actually, there is ample evidence that sublimation starts much earlier than the conventional limit, because for instance comet Hale-Bopp had a well-developed coma already beyond 7 AUs, according to some evidence already around 14 AU. When activity ceases? Observations at great distances are difficult, but for instance Halley's produced another surprise in the outer leg, a sudden increase of luminosity at 14 AU [109], most likely driven by CO sublimation. According to [110], Hale-Bopp was still active at about 28 AU!

However, as shown by GIOTTO and VEGAs on Halley's, Whipple model was not fully tenable, and more refined hypotheses were needed. A review paper by M. A'Hearn [111] summarizes the different pre-Rosetta models of cometary nuclei, from Whipple's original dirty snowball model, to Donn's fractal aggregate model, to Weissman's primordial rubble pile model, to the icy glue model of Gombosi & Houpis, and finally the TALPS model of Belton. Such "talps" or "layered pile" model, in which the interior consists of a core overlain by a pile of randomly stacked primordial layers, was prompted by the layering observed on the surface of Comet 9P/Tempel 1 from the Deep Impact spacecraft. Such structure seems ubiquitous on Jupiter family cometary nuclei such as 67P, and appears as an essential element of their internal structure.

As a general feature of all models, the nucleus seems to be formed by a number of small sub-units held together by a small gravity and some cohesive force; those sub-units,

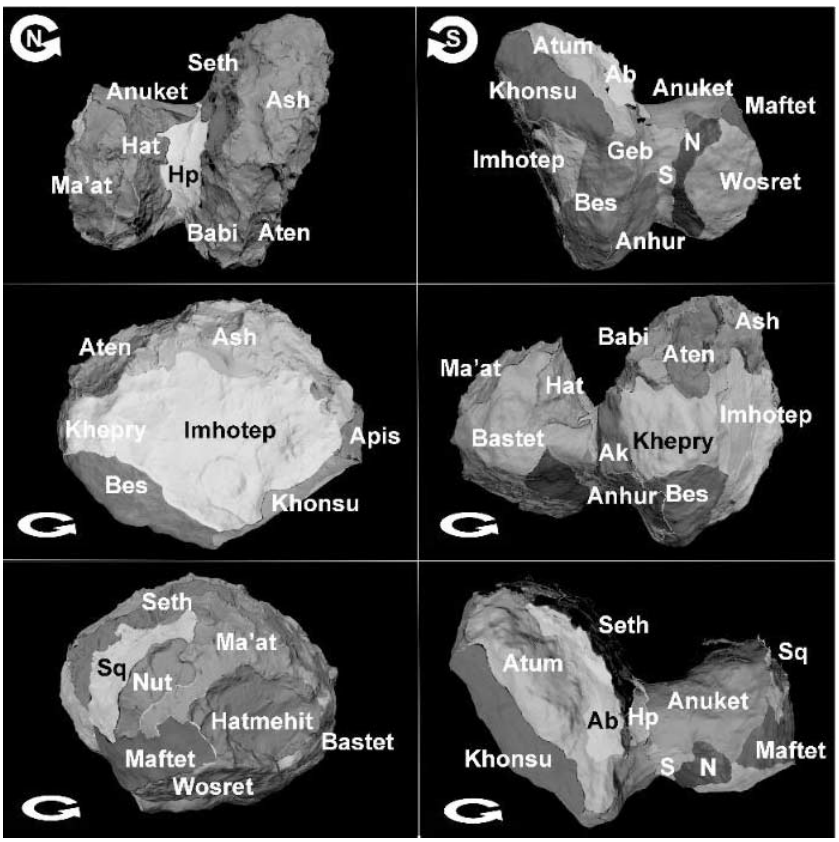

Fig. 19. – The morphological regions on the two hemispheres of 67P. Rosetta ended its life landing in the Ma'at region on Sept. 30, 2016. The rotation verse is indicated (adapted from [108] with permission @ESO).

usually called cometesimals, can be the oldest remains of the original solar nebula. Following the sublimations of gases and release of dust, some parts of the surface are covered by a so-called "rubble mantle" of pebbles and rocks too heavy to be lifted by the gases.

Rosetta has provided a wealth of information on the nucleus of 67P. The images of OSIRIS are of paramount importance not only for surface and activity, but also for understanding the properties of the constituent material and internal structure. For instance, ref. [112] presents a discussion of the gravitational slopes, tensile, shear, and compressive strengths for regions representative of the different morphologies observed on the surface. A general pattern can be identified in terms of the relation between gravitational slopes and terrain morphology:

– low-slope terrains (0–20°) are covered by a fine material and contain a few large (> 10 m) and isolated boulders;

– intermediate-slope terrains (20–45°) are mainly fallen consolidated materials and debris fields, with numerous intermediate-size boulders from < 1 m to 10 m

– high-slope terrains (45–90°) are cliffs that expose a consolidated material and do not show boulders or fine materials.

The best range for the tensile strength of overhangs is 3–15 Pa (upper limit 150 Pa), 4–30 Pa for the shear strength of fine surface materials and boulders, and 30–150 Pa for the compressive strength of overhangs (upper limit 1500 Pa). Quite interesting, the strength-to-gravity ratio is similar for 67P and weak rocks on Earth. As a result of the low compressive strength, the interior of the nucleus may have been compressed sufficiently to initiate diagenesis, which could have contributed to the formation of layers. The value for the tensile strength is comparable to that of dust aggregates formed by gravitational instability, and tends to favor a formation of comets by the accretion of pebbles at low velocities.

The interior of 67P could be seen by images of the walls of several pits down to a depth of several hundred metres along the freshly exposed pit walls. According to [113], pits formation can occur via sinkholes, or else be subsequent to outbursts, the dominant process depending on the status of the subsurface porosity. High porosity should allow the formation of large voids in the subsurface due to the continuous escape of volatiles (a sinkhole), whilst a sealed dust mantle would favour episodic and disruptive outgassing as result of increasing gas pressure in the pores. According to [114], the inner walls of such pits, believed to be sinkholes with material falling into voids in the interior, show evidence of "goose bump" terrain, which appears to be composed of 1–4 meter diameter boulders stacked one on top of another.

The geological analysis of the two lobes of 67P has led to the identification of layers (strata) which can be traced through the interior from one side to the other of the two lobes (see [115] and [116]). Coupled to the accurate knowledge of the point-by-point gravity field, two independent sets of planes enveloping separately the two lobes have been identified. Such reconstruction of the interior of 67P substantiates the first impression of a double nucleus (bi-lobate) comet, where two originally separated sub-units merged together after a low velocity series of impacts in a truly primordial ambient.

CONSERT, one of the instruments on Philae lander on Rosetta, provided other data on the internal structure of 67P, in addition to those given by radio science and navigation. See ref. [117]. From the propagation time and form of the signals, the upper part of the "head" of 67P seems fairly homogeneous on a spatial scale of tens of meters. The average permittivity is about 1.27, suggesting that this region has a volumetric dust/ice ratio of 0.4 to 2.6 and a porosity of 75 to 85%. The dust component may be comparable to that of carbonaceous chondrites.

In closing this section, it can be recalled that some theories postulate that the largest nuclei have an inner denser core heated by the radioactive decay of elements like K, Th, U and mostly ^{26}Al for smaller nuclei. Such nuclei are differentiated from the outer layers, and might have a density greater than 2.

13˙2. *Masses and mass-losses.* – Whatever the model, the nuclei have small masses. Assuming for simplicity a density $\rho = 1$, and radii varying between 100 m and 100 km (a very large nucleus indeed) masses are in the range from 10^{12} to 10^{21} g, namely between 10^{-15} and 10^{-6} Earth masses. Notice that the Earth water in the oceans is around 10^{-4} of the total mass, so that hundreds or thousands of large comets could account for all the water of the oceans, but as discussed in previous sections comets seem not to be the main contributor to earthly water.

The escape velocity and the gravity at the surface of a non-rotating nucleus having radius $R = 1$ km and $\rho = 1$ can be easily calculated:

$$v_f = v_0\sqrt{\frac{M}{R}} \approx 100\,\mathrm{m/s}, \qquad g = g_0\frac{M}{R^2} \approx 0.5\,\mathrm{mm/s^2}$$

(recall that the solar gravity at 1 AU is $= 5.9\,\mathrm{mm/s^2}$). Masses can be determined very precisely by the accelerations of a spacecraft in proximity of the nucleus. Combining GIOTTO and VEGAs data, the value $(1\text{–}3) \times 10^{17}\,\mathrm{g}$ for Halley's was obtained.

Rosetta was the most effective mission in such respect: by orbiting the comet at small distances for many months, the value $1 \times 10^{13}\,\mathrm{g}$ was ascertained, with an error less than one-tenth of a percent. In conjunction with the precise volume measured from the OSIRIS images, the very accurate value of average density $\rho = 0.53 \pm 0.02$ has been derived. The gravity turns out to be very low, approximately 10^{-5} that on the Earth surface. See ref. [118].

The determination of the mass-loss is usually easier than that of the mass itself. The sublimation around the perihelion of a typical comet amounts to tens of tons every second, essentially by dust loss because the gas to dust ratio by mass is typically 1/6 or even lower. The actual numbers vary of course within an ample range, depending on the comet and its orbit, but such an order of magnitude implies that a comet can survive for hundreds of passages, a long time indeed but much less than the age of the solar system. We quote in this respect the data derived from Rosetta on comet 67P which, as already stated, has a gas to dust mass ratio 1/6 (a dusty comet): mass loss at peak activity was 10^5 tons/day (10^{-6} of total mass), corresponding to an average overall peeling of less than 1 meter per perihelion passage. See for instance ref. [119].

Notice though that not all the dust released from the surface is lost. Reference [120] presents evidence for motion of material from one site on the nucleus to another, an "airfall" process by which large grains are decoupled very soon from gas and do not reach escape velocities, therefore falling after a ballistic flight in other areas of the comet. Such mechanism must have been effective in transferring dust from the Southern to the Northern Hemisphere.

13˙3. *Rotation, activity, stability.* – Rotation is another nuclear parameter that can be studied only with difficulty from ground. Nuclear activity depends in a critical way on its rotational status, even if the body had a spherical shape and activity was uniformly distributed, because different areas come into the illuminated hemisphere at different times and for different periods. In reality, the shape of a nucleus is usually complicated and activity restricted to few zones, nor the rotation necessarily takes place around a symmetry axis of the figure. Furthermore, a strong activity could excite nutation of the rotation axis. For a general discussion of the rotational states of comets and asteroids see [121] and references therein. *In situ* observations by spacecraft provide much better data than ground telescopes. However, for Halley's the situation was not entirely clear due to the very short time of the VEGAs and GIOTTO fly-by's.

Reference [122] determined a model for the spin state of Comet Halley's nucleus that simultaneously satisfied imaging data from the VEGA and GIOTTO encounters, and a wide range of ground-based data including observations of CN-jets, CN-shells, C_2 production rates, and photometric variability. The model is that of an excited, axially symmetric, rotating prolate spheroid. The long-axis of the nucleus is inclined to the total angular momentum vector, M, by 66°, and rotates around M with a period P_φ of 3.69 days. The component of spin around the long axis has a period P_Ψ of 7.1 days which compounds with P_φ to produce a total spin period, $P_\mathrm{T} = 2.84$ days. The total spin vector, S, is inclined to M by 21° and freely precesses around the angular momentum vector with a period of 3.69 days. The model has a ratio of maximum to minimum moments of inertia of 2.28, which implies an approximately constant density distribution throughout its interior. When compared to the sense of orbital motion, thespin is direct.

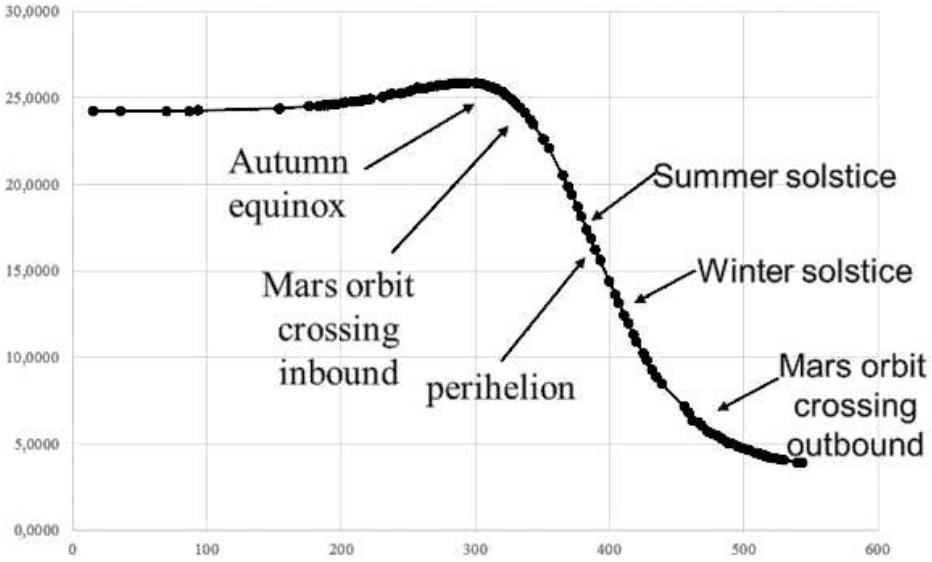

Fig. 20. – After a slight increase of less than 1 minute at the time of the autumn equinox, a regular decrease of the rotational period of 67P into a steady state towards $12^{\mathrm{h}}03^{\mathrm{m}}$ was measured by Rosetta. Abscissa: days since Aug. 6, 2014. Ordinate: period (minutes minus 12^{h}).

Again, Rosetta has provided the best data ever. The long duration of its cruise near the comet has determined with great precision the pole of the rotation axis, and measured a fairly regular decrease of the period from $12^{\mathrm{h}}24^{\mathrm{m}}$ in early 2014 to $12^{\mathrm{h}}03^{\mathrm{m}}$ at the end of the mission (see fig. 20).

According to [123], OSIRIS data show evidence of the nucleus rotating in complex mode. First, the orientation of the spin axis is not fixed in an inertial reference frame, suggesting a precessional motion around the angular momentum vector with a periodicity of approximately $(257 \pm 12)^{\mathrm{h}}$. Second, periodograms of the right ascension and declination (RA/Dec) coordinates of the body-frame Z-axis show a very significant periodicity at $(276 \pm 12)^{\mathrm{h}}$, different from the rotational period of 12.40^{h} determined from light-curves analysis (fig. 5). Spin axis orientation in space and associated periodicities were analysed and compared with solutions of Euler equations under the assumption of a solid-rigid body rotating in torque-free conditions. Under those assumptions, the most likely interpretation is that 67P is spinning with a period around 13^{h} around the axis having the largest inertia moment and, at the same time is precessing around the angular momentum vector with a period around 6.35^{h}. While the rotating period of such body would be around 12.4^{h}, the RA/Dec coordinates of the spin axis would have a periodicity around 270^{h}, as a result of the combination of the two aforementioned motions. The most direct and simple interpretation of the complex rotation of 67P requires a ratio of inertia moments significantly larger than that of a homogeneous body.

The rotational speed of 69P makes the centrifugal force not at all negligible, in some peripheral regions it reaches 40% of the gravity. How long can a comet survive the rotational increase before splitting? This is a very difficult question to answer. OSIRIS images of 67P have revealed many fractures on its body, an example is shown in fig. 21.

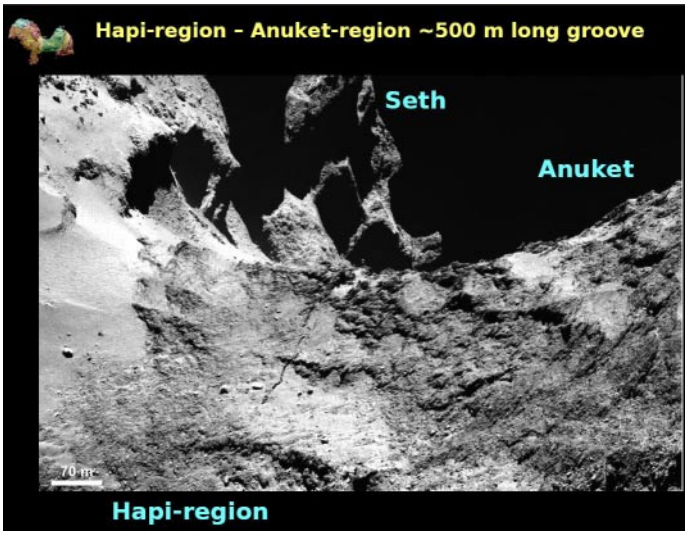

Fig. 21. – The 500 m long fracture seen in the neck of 67P by OSIRIS/NAC.

Is it a precursor of future rotational splitting, or a relict of sticking of the two lobes, or sign of thermomechanical stresses? Thus, such images provide new data to the several theories.

We quote in this respect paper [124], which contains also many references to previous literature. The authors estimate the regions of stability, fragmentation, and destruction for cometary bodies *vs.* rotational breakup in the radius-rotational period plane. By testing different plausible physical models of the cometary nucleus equation of state, they show that such plane can be divided into three regions, allowed, damaged, and forbidden. All well observed comets lie in the allowed region, except for Hale-Bopp which resides in the damaged region, where the body is fractured and only held together gravitationally; as already recalled this comet has a very large nucleus. The extremely high activity demonstrated by comet Hale-Bopp during the 1997 apparition may have been due to its highly fractured state. Comet Hyakutake, observed to emit fragments at perigee in 1996, may be near the boundary of the damaged region. Comet C/1999 S4 (LINEAR) was solidly in the rotationally allowed region, making its disintegration in July 2000 due to sole centrifugal forces very unlikely. Extrapolating such results to 67P, one can estimate that the comet can survive disruption due to centrifugal forces until its period approaches 5^{h}, a long distance away in the future.

Rotational status and activity are closely connects topics. During its two years mission around comet 67P, all instruments on Rosetta had the unique opportunity to follow a comet in the most active part of its orbit. Many studies have presented the typical features associated to the activity of the nucleus, such as localized dust and gas jets (see for instance the already quoted refs. [70] and [71], and [125]).

During the three months surrounding the comet's perihelion passage in August 2015, OSIRIS detected and characterized more than 30 outbursts, approximately one every 2.5 nucleus rotation. The dust plume morphologies associated to these events can be classifies in three main types: a narrow jet, a broad fan, and more complex plumes featuring both previous types together. The great advantage of OSIRIS has been its capability to draw

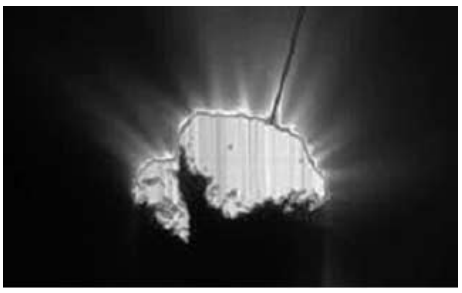

Fig. 22. – An example of global activity shown by an OSIRIS image. The Sun is at 2 o'clock.

a map of the outbursts source locations, and discuss the associated topography. The spatial distribution of sources on the nucleus correlates well with morphological region boundaries, especially in areas marked by steep scarps or cliffs. Outbursts occur either in the early morning or shortly after the local noon, indicating two potential processes:

– morning outbursts may be triggered by thermal stresses linked to the rapid change of temperature,

– afternoon events are most likely related to the diurnal or seasonal heat wave reaching volatiles buried under the first surface layer.

A further mechanism may be at work, in which most of the dust is released upon the collapse of a cliff [126].

In addition to localized features on the surface, the images of OSIRIS and NAVCAM have documented the release of dust and gases from the entire body of the comet (see [127]). Figure 22, shows an example of such activity in an image of OSIRIS taken at the end of May 2015. The grains may have contained also sublimating icy water, as already suggested by [128].

GIADA data obtained during a period which included 67P's perihelion passage, have been discussed by ref. [129]. To better understand cometary activity and more specifically the presence of dust structures, the authors mapped the spatial distribution of dust density in the coma. In this manner, the evolution of high-density regions of coma dust and their connections with nucleus illumination conditions, namely with seasons, could be tracked. The link between dust particle speeds and their masses with respect to heliocentric distance, *i.e.* the level of cometary activity, was determined. Global and local correlations of the dust particles' speed distribution with respect to the H_2O production rate was derived.

The activity was full of surprises, in the Imhotep region a mini-outburst was detected although the area was still in full darkness. According to ref. [130], the outburst lasted for less than one hour, and the average dust production rate during the initial four minutes was of the order of 1 kg/s, surely another tribute to the fantastic sensitivity of OSIRIS.

Another interesting consequence of activity was the production of noticeable changes in localized areas of the surface of the comet, as in the already quoted Imhotep region (see fig. 23, adapted from [131], see also [132]).

Figure 24 shows the spectacular jet of July 29, 2015, two weeks before perihelion, during which decimetre-sized boulders were seen flying away from the comet. The amount of dust released during such outburst augmented by four times, arriving to about one

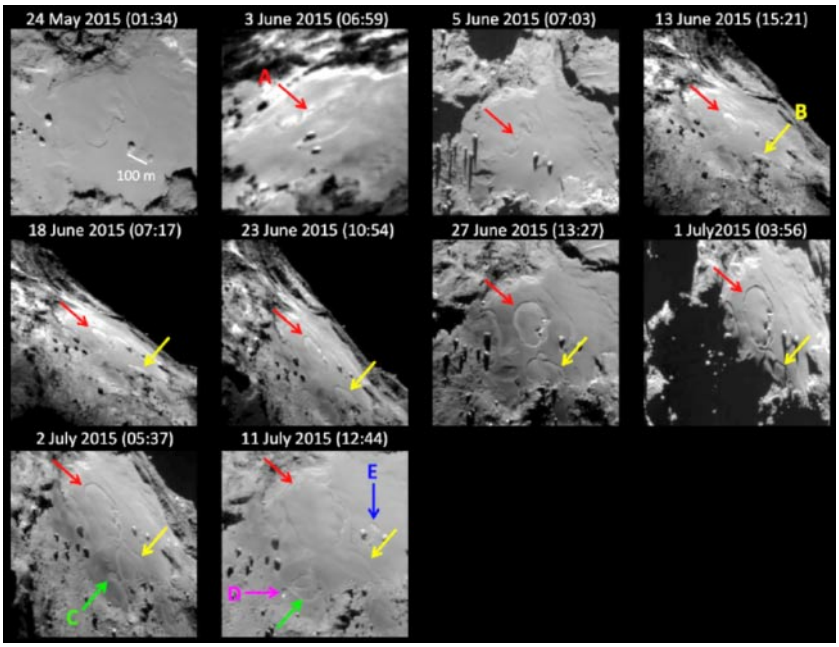

Fig. 23. – Changes in the Imhotep region from May to early July, 2015 documented buy OSIRIS images (adapted from [131] with permission @ESO).

ton/s. The ejection velocity augmented from few to 20 km/s. ROSINA detected a sudden change of composition of the gases: while the H_2O remained essentially constant at about 300 kg/s, CO_2 doubled, methane increased four-fold, H_2S by 7 times, and so on.

Other spectacular outbursts were observed by OSIRIS the day before and twelve days after the perihelion (see fig. 25).

At the beginning of November 2015, comet and Rosetta crossed again the orbit of Mars, this time outbound to enter the asteroidal Main Belt. The comet remained active even during such period of great distance from the Sun, see fig. 26.

Fig. 24. – The spectacular pre-perihelion jet of July 29, 2015 in an OSIRIS frame.

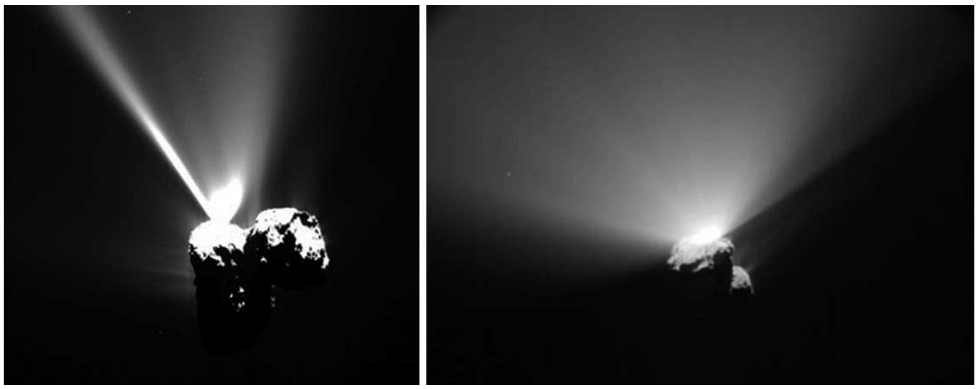

Fig. 25. – OSIRIS images showing on the left a sudden short-lived jet observed on Aug. 12, 2015, and on the right a wide fan observed on August 25, 2015.

Due to the combination of still ongoing cometary activity and satisfactory status of instruments and spacecraft, ESA decided to extend the life time of the mission from the programmed Dec. 31, 2015 to Sept. 30, 2016. A wise decision, very soon rewarded by the comet. The event of Feb. 19, 2016 (see fig. 27) is particularly important. Rosetta was about 30 km above the surface, and nine instrument could operate and provide data [133]. Dust related phenomena (dust counts or brightness due to illuminated dust) showed the strongest enhancements (factors > 10) during such outburst. The neutral gas density increased by 50 per cent, and the brightness of the coma near the nucleus by factors > 100. Actually, the spacecraft itself provided useful information, because its electric potential dropped from -16 to -20 V due to a 3-fold increase of free electrons around it, and the star-trackers detected fast particles ($\sim 25\,\mathrm{ms}^{-1}$). In a way, as in other occasions Rosetta behaved both as a small satellite to the comet and as a scientific instrument.

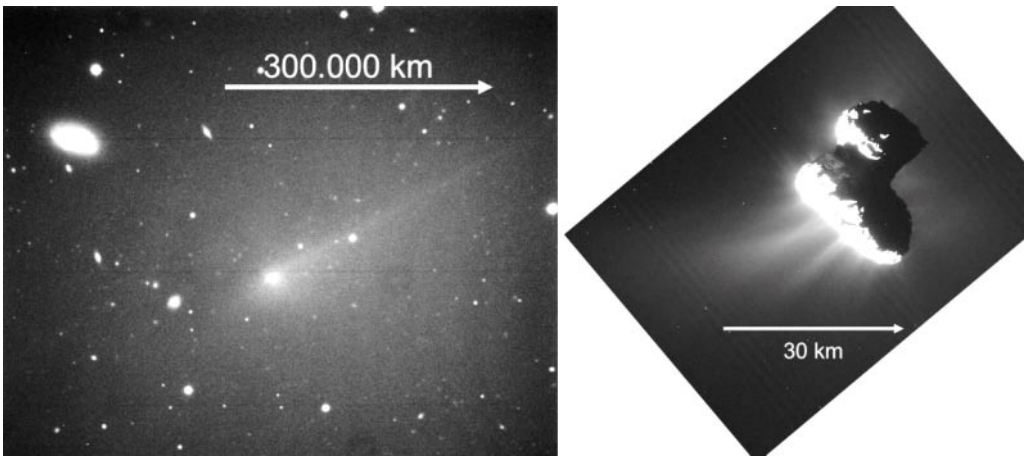

Fig. 26. – Left, an image obtained from the ground (Asiago Copernicus telescope) on Jan. 21, 2016. Right: image obtained the same day by the OSIRIS/WAC. On both images, the Sun is in the lower left direction.

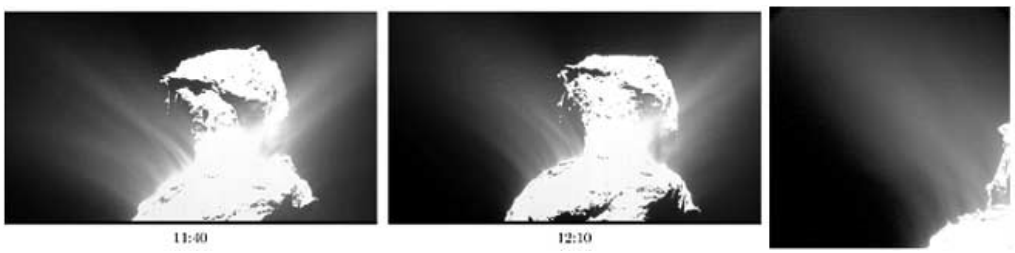

Fig. 27. – Left: two WAC images, right: NAVCAM image of the activity observed in Feb. 19, 2016 (adapted from [133], NAVCAM image: Copyright ESA/Rosetta/NavCam).

The activity of the comet continued to the very end of the observations, both at global and local level, as documented by fig. 28 and fig. 29.

The influence of activity on 67P rotation has been discussed in [134], a paper which provides an account of previous literature on such connexion. The availability of a detailed shape models allowed to calculate the effect of sublimation over about 108000 facets covering the surface to the nucleus. The authors assumed that sublimation is driven by solar energy input (direct, reflected, and re-emitted), and that, owing to the low thermal inertia of the cometary material [135], local thermal equilibrium is reached very rapidly with respect to the typical time of changes in illumination. Under those assumptions, the equilibrium temperature of the surface or of a sublimating subsurface layer depends only on the instantaneous solar energy input and not on the insolation history. The net torque due to sublimation can be written as

$$T = -\sum_i \frac{\mathrm{d}m_i}{\mathrm{d}t} \mathbf{r}_i \times \mathbf{v}_i,$$

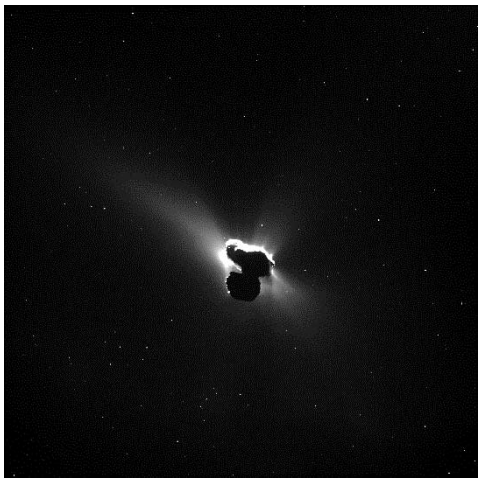

Fig. 28. – Global activity from the entire nucleus, imaged by NAVCAM when on the night side of the comet. Rosetta was 329 km from the nucleus (Copyright ESA/Rosetta/NavCam).

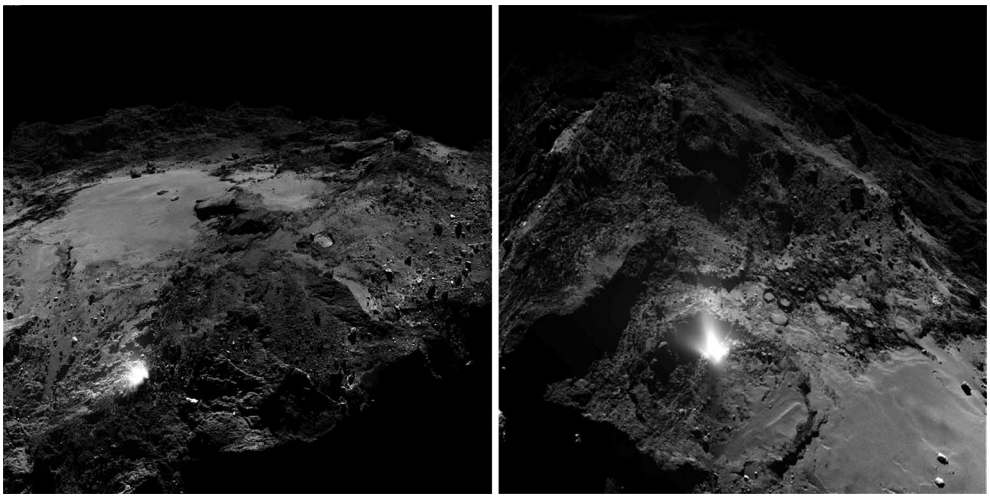

Fig. 29. – Two jets observed by OSIRIS, respectively, in May and July 2016, showing with great clarity where from the jets exited.

where $\mathbf{v}_i$ is a vector describing the gas ejection velocity, with orientation parallel to the facet's normal; $\mathbf{r}_i$ is the vector from the centre of mass to the centre of the facet; and the index i runs overall facets. The term $\mathrm{d}m_i/\mathrm{d}t$ is the mass sublimation rate, whereas $-\mathbf{v}_i\ \mathrm{d}m_i/\mathrm{d}t$ is the reaction force for facet i. The calculations reproduce indeed with fair agreement the major features and times of fig. 20.

What happens on the nucleus following the loss of gases and dust? Most likely, the many grains, boulders and large masses accumulate on the surface gradually form a thick, very dark, C-rich inactive crust that impedes the transfer of solar heat to the inner parts of the comet. Indeed, there is evidence that activity of 67P during the Rosetta mission was about 30% less than during the previous orbit.

13˙4. *Temperature*. – Let us add some qualitative, order of magnitude, considerations about the nuclei temperature by writing a simple equation valid for a hypothetical equilibrium of the nucleus in the solar radiation. Be the comet at r AU from the Sun. A generic elementary surface on the nucleus is illuminated by the Sun at Zenith distance ϑ (the point at $\vartheta = 0$ is said *sub-solar*), its surface albedo in the visible (the wavelength region where it reflects the solar light) be A_V, and A_{IR} the albedo in the infrared region where it radiates thermally. Be T its temperature, $Z(T)$ the sublimation rate and $L(T)$ the latent heat of sublimation. The equation of balance is then

$$F_0(1 - A_V)\frac{\cos\vartheta}{r^2} = (1 - A_{IR})\sigma T^4 + Z(T)L(T),$$

F_0 is the solar constant $= 2.0\,\mathrm{cal/cm^2min}$ (or else $0.137\,\mathrm{Watt/cm^2}$; the solar spectrum can be assumed here as a black body at 5900 K), and σ the Stefan-Boltzmann constant. Let us put for a drastic first approximation $A_V = A_{IR} = 0$. For water ice $L(T) = 11.500\,\mathrm{cal/mole}$ at any temperature of cometary interest (for a comparison, for methane ice $2.200\,\mathrm{cal/mole}$ are sufficient). The observations provide the overall quantity $Q = 4\pi R^2 Z(T)$ of molecules per second (the production rate of molecules of that species). In

TABLE VII. – *Indicative sublimation distance of common cometary species.*

Molecule	Typical production rate *vs.* H_2O	$T_{\rm subl}$ (K)	$r_{\rm equil}$ (AU)
CO	10	35	70
H_2CO	1	65	20
CO_2	5	80	15
CH_3OH	2	100	8
H_2O	100	160	3

an ideal condition of thermal equilibrium, the nucleus would assume the temperature

$$T = 289/\sqrt{r}\,\mathrm{K} \quad (r \text{ in AU}),$$

namely +16 °C at the Earth, −178 °C at Saturn (the above quoted regime for amorphous water), and so on. The maximum of emissivity would then be, according to Wien's law:

$$\lambda_{\max} T = 0.29\,\mathrm{cm},$$

at Jupiter' distance $\lambda_{\max} = 23$ microns, namely in the IR better observable by satellite. More realistically, only the smallest grains will approach such temperature, the rest of the nucleus will remain at much lower temperatures. The indicative sublimation temperature of the most common substances are exposed in table VII.

Therefore, at great distances sublimation is essentially nihil, most of the absorbed energy is reradiated in the far IR, and only a small fraction will go in augmenting the temperature of the outermost layers. When the distance becomes less than 3 AUs, by virtue of water ice sublimation the temperature of the nucleus cannot augment any longer. In a way, the sublimation acts as a thermostat. The surface heat balance can be rewritten as

$$0 = \frac{F_0(1-A_0)}{r^2} - \varepsilon\sigma T^4 + LZ(t) + \kappa\frac{\mathrm{d}T}{\mathrm{d}z}\,,$$

$$\delta = \frac{\kappa}{\rho c} \quad \text{thermal diffusivity,} \qquad \Gamma = \sqrt{\kappa\rho c} \quad \text{thermal inertia,}$$

$$x = \sqrt{\frac{2\delta}{\varpi}} = \sqrt{\frac{\tau\delta}{\pi}} \quad \text{scale length for a heath wave to drop by 1/e, } \tau \text{ duration of heating.}$$

For the Moon, x is typically 5 cm, for Mars 10 to 20 cm. Using values appropriate to cometary nuclei (*e.g.* a thermal inertia of $50\,\mathrm{Wm^{-2}\,s^{-1/2}\,K^{-1}}$, as measured by the Deep Impact mission and MIRO on Rosetta) one can derive the following values:

$$\tau_{\rm diurnal} \approx 10^5\,\mathrm{s} \Longrightarrow x_{\rm diurnal} \approx 1.5\,\mathrm{cm},$$
$$\tau_{\rm orbital} \approx 10^8\,\mathrm{s} \Longrightarrow x_{\rm orb} \approx 44 x_{\rm diurnal} \approx 70\,\mathrm{cm}.$$

In conclusion, within the limits of such elementary discussion, the orbital skin depth is around 70 cm, namely equal or even smaller than the thickness of the surface layer

removed by sublimation. In other words, when activity peaks around perihelion, the surface of an active area recedes faster than the heat wave penetrates.

The instruments on Rosetta, in particular VIRTIS and MIRO, have provided an impressive amount of data on nuclear temperatures.

The spectrophotometer VIRTIS observing in different channels from 0.25 to 5 μm confirmed that the nucleus is typically very dark, with an average reflectivity around 5%. Thus, the surface must be covered by organics rich of C, H and O, which produce a wide absorption band between 2.9 and 3.6 μm. With the diurnal insolation, the temperature of the ground varied from 180 to 220 K in the warmer regions. At night, the temperatures decreased to about 170 K, which is the limit of VIRTIS sensitivity for accurate measurements.

MIRO's continuum channels detected the nucleus since 19 July 2014, and spatially resolved it since early August, with a maximum spatial resolution of about 20 meters in the sub-millimetre channel (562 GHz) and 70 metres in the millimetre channel (190 GHz). MIRO clearly saw diurnal, seasonal, and vertical temperature variations [135, 136], indicative depths being 1 cm beneath the surface in the 0.5 mm channel, and 4 cm in the 1.6 mm one. Measured antenna temperatures varied between 100 and 160 K, with the deeper layers being typically cooler by an indicative amount of 10 K. Temperatures in the Northern Hemisphere were consistently higher than those in the Southern one. Those initial results indicated a very low thermal inertia surface (5 to 40 $\mathrm{J\,K^{-1}\,m^{-2}\,s^{-0.5}}$), as expected for a porous, dusty layer. This extremely low inertia (solid rock or ice would have values ~ 2000) means that vertical temperature gradients are also large, with daytime physical temperatures dropping by $\sim$ 50 K between the surface and 1 cm below. Generally, the lowest thermal inertia values were measured in the equatorial and northern latitudes. The brightness temperatures at high northern latitudes are consistent with sublimation of ice playing an important role in setting the temperatures of these regions where, based on observations of gas and dust production, ice is known to be sublimating. As already stated, the high obliquity ($\sim 50°$) of comet 67P is responsible for a long-lasting winter polar night in the southern regions of the nucleus. Observations of such southern regions were done with MIRO during the period August–October 2014 [137]. Before these observations, the southern polar regions had been in darkness for approximately five years, and started to receive sunlight only in May 2015. Subsurface temperatures in the range 25–50 K were measured, providing a thermal inertia within the range 10–60 $\mathrm{J\,m^{-2}\,K^{-1}\,s^{-0.5}}$, slightly higher than the value of the northern regions. MIRO collected temperature measurements below the surface until the very end of the mission. The antenna beam was only few tens of cm wide during such final phases, and the oscillations of the spacecraft made it wander over the surface. Temperatures varying between about 80 and 160 K were measured.

13˙5. *The surface of 67P*. – One of the many unique characteristics of the Rosetta mission was the long cruise, which allowed a repeated examination of the entire surface of the comet, at varying distances and resolution, both before, during and after the perihelion. The Southern Hemisphere shows a remarkable dichotomy with its northern counterpart, mainly because of the absence of wide-scale smooth terrains, dust coatings and large depressions. An assessment of the overall morphology of comet 67P suggests that the comet's two lobes show surface heterogeneities manifested in different physical/mechanical characteristics, possibly extending to local (*i.e.*, within a single region) scales. See for instance ref. [138] and the papers previously discussed in relation to the measurements of albedo, nuclei models and geomorphology of the terrains. A series

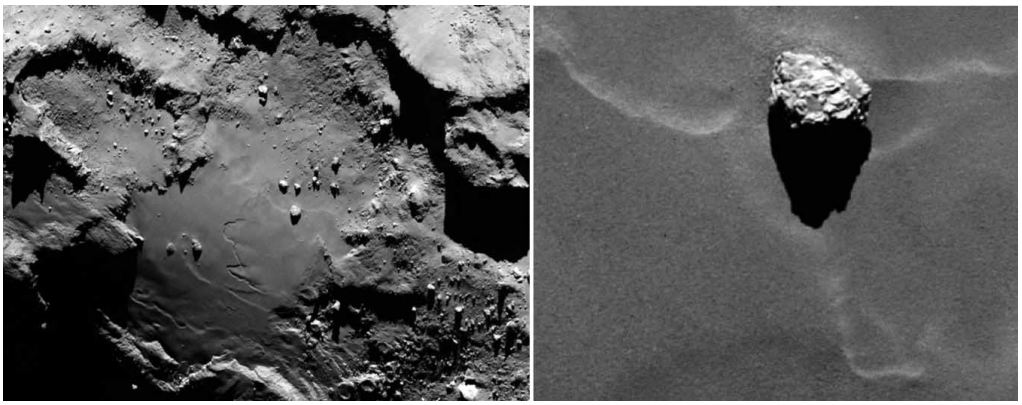

Fig. 30. – Left: the series of boulders named after the pyramids of Giza. Right: the largest of these rocks, named after Cheops, is resolved in smaller sub-unit. Notice the bed of regolith.

of papers deals with the many boulders present in several areas of both hemispheres, *e.g.* [139] and [140]. These boulders (an example is shown in fig. 30) constitute one of the most attractive and puzzling features of the surface.

Extremely interesting are studies of distribution and behaviour of water ice, as a further example of the excellent collaboration among the scientific teams on Rosetta. There is a paucity of areas with exposed water ice (see the already quoted refs. [36] and [141]), sufficient though to constrain the mechanisms of sublimation and re-condensation in a daily cycle identified in [100]. See for instance in fig. 31 the frost detected by OSIRIS and studied by VIRTIS in two different areas.

Moving toward the perihelion, such icy regions disappeared, as shown by images covering the Anhur region. The life time of exposed water ice patches was of only few days, much shorter than the typical orbital exposure time to solar illumination. The

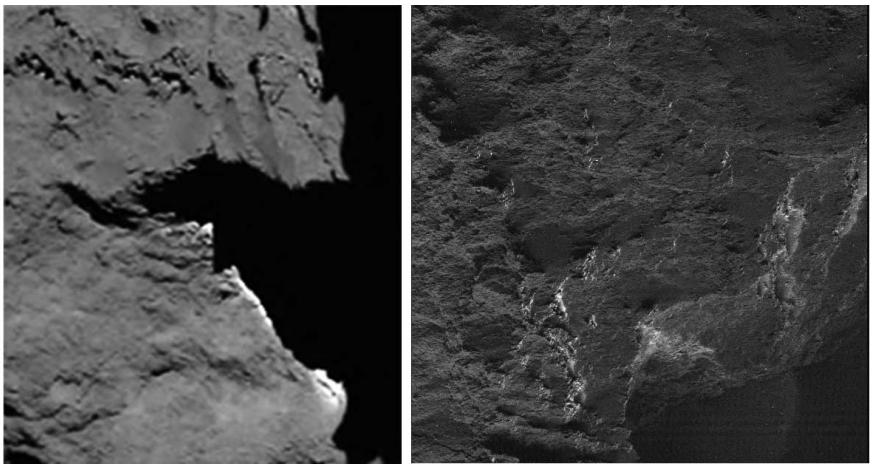

Fig. 31. – The whitish stripes are frost forming and dissolving in the diurnal cycle of water, in a time span of few minutes (adapted from fig. 3 in [36]).

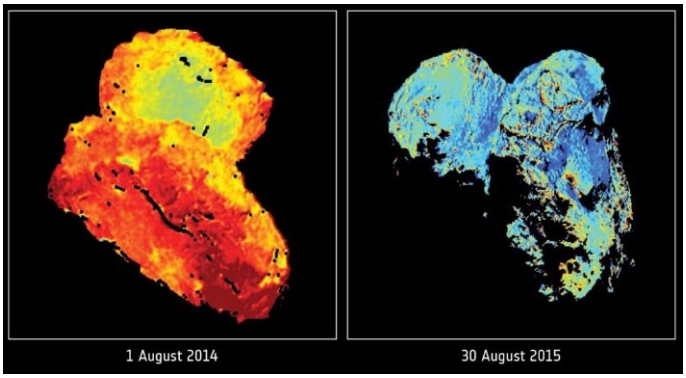

Fig. 32. – These stretched OSIRIS images show an overall change of the colour of the nucleus from early August 2014, when the distance to the Sun was 3.6 AU, to end of August 2015, when that distance was 1.3 AU. The increased activity freed part of the surface from the dust layer, exposing more water icy regions (adapted from fig. 1 in [36]).

estimated ice loss rate ranged from 0.14 to 2.5 $\mathrm{kg\,day^{-1}\,m^{-2}}$, and the solid-ice thickness between 15 and 300 mm for the ice patches. The uncertainty of these figures arises from different models of ice to dust mixture and porosity of the material.

Another stunning result was the possibility to estimate the life time of the frost line at the border of shadowed regions, according to the speed of the shadow cast by the many irregularities on the surface while the comet was rotating. Surface frost, formed when water vapor released from the subsurface re-condenses after sunset, rapidly sublimates (in few minutes) when exposed to the Sun.

The same Anhur region allowed VIRTIS to make another discovery of the greatest importance, namely the presence of patches of solid CO_2, the first time in a comet (see again ref. [38]). This exposed ice was observed a short time after Anhur exited local winter. Following the increased illumination, the CO_2 ice completely disappeared over about 3 weeks. The explanation is that the increased activity removed the surface layers hiding the CO_2, whose presence on the surface seems to have an orbital cycle, not a diurnal one like water.

The merging of VIRTIS and OSIRIS data has shown a small but measurable global variation of surface colours, see fig. 32 (adapted from ref. [36]).

CIVA cameras on board Philae obtained microphotographs of the terrain immediately adjacent to the legs in the patch where the lander ended after rebounding from Agilkia (fig. 33). The rough landscape, dominated by consolidated materials, was examined in detail by [142], with a quantitative analysis of microscopic structures (fractures and pebbles) aided by a comparison with the larger area images provided by OSIRIS. Fractures and cracks are rather ubiquitous at various spatial scales, with network and size (from sub-cm to 10 cm) well correlated to the texture of the landscape. The observed fractures are best explained by insolation leading to thermal fatigue and/or to loss of volatile materials. This surficial fragmentation (up to > 10 cm length) could generate macroscopic erosion that is also visible at larger scale from OSIRIS images (see refs. [143, 144]).

During the final descent to Ma'at, the last days of September 2016, OSIRIS WAC was able to take good images of the surface until the very last moment, because the optics of OSIRIS/WAC without filters had the capability to remain in focus from about 50 m

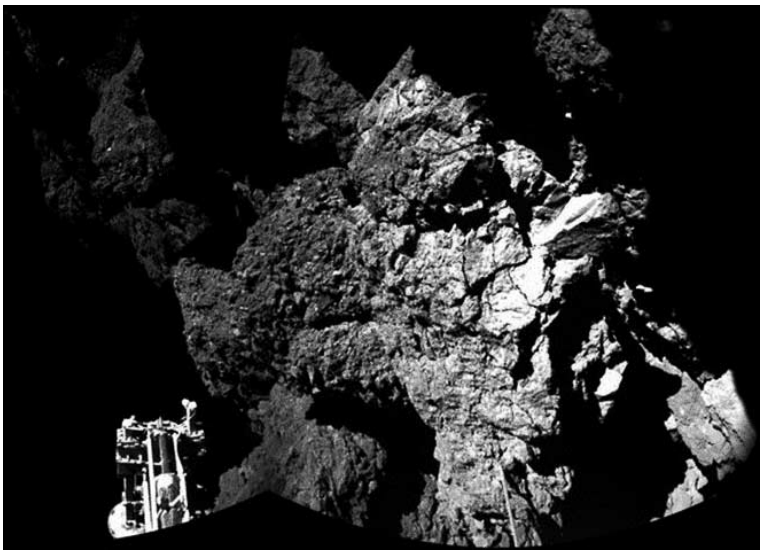

Fig. 33. – Image of the cometary surface adjacent to the leg visible on the lower left (Copyright ESA/Rosetta/Philae/CIVA).

to about 10 m above the surface. However, the capability of data transmission severely limited the field of view which could be sent to ground, so that the final images cover a very limited area. The last image is shown in fig. 34, pebbles and speckles as small as 0.5 cm can be appreciated.

14. – The origin of comets

14˙1. *Early thoughts*. – This section is a recollection of ideas put forward by several authors in the course of the XX century. In 1932, E.J. Öpik examined the stability of

Fig. 34. – The last image transmitted by OSIRIS/WAC.

long-period cometary orbits against perturbations of the nearer stars, concluding that comets could remain gravitationally bound to the Sun up to large distances. Stellar perturbations could be responsible for a huge cloud of comets at the border of the Solar System.

In 1948, Raymond A. Lyttleton re-examined an idea proposed by the Richard A. Proctor in the second part of the XIX century, that comets were the result of the passage of the Solar System across a giant interstellar nebula. The interstellar dust particles captured by the Sun in elliptic orbits, after a very short time would form small aggregates, the seeds of comets. However, Lyttleton model had several difficulties, as pointed out by A. J. van Woerkom who could demonstrate that the perturbing action by Jupiter would expel the great part of those comets back to the interstellar space, and capture the others in short period orbits. In other words, the reservoir of long period comets must be in a remote place far from the perturbations by the large planets, a sort of cloud surrounding the solar system, as already suggested by Öpik.

Finally in 1950, Jan H. Oort proposed the existence of a spherical cloud containing some 10^{11} comets and distant from 50000 and 150000 AU. Notice that 100000 AU correspond to approximately 0.5 parsec, and that the nearest star is at 1.3 pc. Therefore, at those large distances from the Sun, stellar perturbations cannot be neglected, acting in particular to redistribute a possibly flat initial distribution of orbits into a more spherical one, and to throw a small fraction of the comets to the inner regions. Here, the perturbations by the giant planets would scatter a fraction of them back in the cloud, another to the outside of the solar system and a third one into short period comets. Oort's cloud model was refined by many successive authors. For instance, Marsden estimated a semi-major axis of the cloud at about 4×10^4 AU and raised the population toward 10^{12} objects. The total mass of the cloud could then be around 100 Earth masses. Notice that a comet in the cloud cannot be observed even with the largest telescopes, for instance Halley's at 10000 AU would appear of the 60th visual magnitude.

Oort's model has at least two week points, namely that the observed number and orbital inclinations of short period comets cannot be explained, and that perturbations by the massive galactic disk and interstellar clouds are as important as those of the nearer stars. Fernandez and Ip demonstrated that the efficiency of the capture by large planets is too low, while Duncan and collaborators remarked that there was an excess of short period comets with low inclinations. Therefore, the large fraction of short period comets could not have originated in the Oort's cloud. The effect of the Milky Way massive disk was examined by authors such as Harrington and Bailey, while Biermann e Lüst studied the interaction of the Oort's cloud with massive interstellar clouds. Times were therefore ripe to introduce a second source of comets, a flat disk from 40 to 500 AU. Such disk took the name of Edgeworth-Kuiper Belt (EKB), although only the second name sometimes is quoted. By taking into account the perturbations produced by the giant planets, the galactic disk, nearby stars and interstellar clouds, it was concluded that the Milky Way is the main responsible for the dynamical evolution of Oort's cloud and migration of comets from the inner to the peripheral regions. Passing-by stars and interstellar clouds are instead more effective in the redistribution of the orbital inclinations toward a spherical configuration. The EKB, the inner and the outer Oort cloud could constitute a continuum extending to the limit of the Solar System, and it might well be then that the original comets are those of the EKB, which also replenished the Oort cloud.

Several ideas were put forward about another question, how did comets originate? It was quickly excluded that the majority formed in the interstellar clouds, a likely possibility for a small number but clearly inconsistent with the distribution of the great

majority of orbits. Therefore, their origin must reside in the series of the initial events that led to the present configuration of the solar system.

Cameron pioneered the idea that an inner protoplanetary nebula was surrounded by smaller nebulae in almost circular motion at few hundred AU, with density sufficient to form comets but not large planets. His model considered that the initial Sun had a larger mass and went through a T-Tauri phase with a consequent loss of mass. Such decrease of the solar mass would have freed the most distant comets from its gravitational attraction, and produce a migration of inner objects toward the Oort cloud. Therefore, there is no need of planetary perturbations to populate the cloud, and comets could have been born essentially all between Uranus and Neptune. The formation of the large planets would then have been responsible for the redistribution of the orbital inclinations and eccentricities.

14˙2. *New theories of the evolution of the Solar System and the role of comets.* – These early thoughts have been very useful to shape our understanding of the origin of the comets, but recent observational data, such as the large number of TNOs and the scattered disk population [145], theoretical models such as the so-called Nice model of Solar System evolution [61, 146], and space missions, in particular Rosetta, have added new ideas.

About the origin of 67P and its bi-lobated shape, two papers (and the references quoted in them) can be recalled: the first by Morbidelli and Rickmann [147], and the second by Davidsson and the OSIRIS team [148], which delineate two different scenarios.

The first paper starts from the consideration that the measured low bulk densities and the low tensile strength of the surface layers are consistent with low-velocity accretion, in line with expectation for planetesimals formed at large distance from the Sun. Many comets have shown evidence for significant contributions of the super-volatile CO molecule to their outgassing activity, another indication of a chemically pristine nature of their material and reinforcing the idea of a very gentle accretion process. However, the evaluation of the collisional evolution in the population of icy planetesimals leads to two different identifications of the source of JFCs, one in the EKB, the other in the scattered disk, less collisionally evolved than EKB. Nor that a source inside the Oort cloud could be excluded. The Nice model for the early evolution of the Solar System has changed the picture of the origin and evolution of comets in important ways. One central concept is the trans-planetary disk of icy planetesimals formed during the infant stages of the solar system beyond the original orbits of all giant planets, which were originally closer to the Sun. This disk extended out to about 30 AU and had a total mass of 20–50 Earth masses. The planets' subsequent migration toward their current orbits eventually dispersed the disk at the time of the LHB (namely at about 450 My) and produced both the scattered disk and the Oort cloud. Thus, this disk may have been the repository for all the comets observed today, compatible with the lack for any clear-cut differences in molecular composition or D/H ratios between JFCs and comets of Oort cloud provenance, that is, long-period comets and Halley-type comets. The disk was significantly excited before its full dispersion. About 1000 Pluto-sized objects probably existed in the primordial disk. These bodies would have induced a significant excitation in the disk, causing a velocity dispersion of the order of 0.5–1 km/s. If the disk remained in this state for hundreds of millions of years, the collisional evolution of comet-sized objects has probably been severe.

The second paper starts from very similar initial considerations. Comet nuclei have low density, high porosity, weak strength, are rich in volatiles, may contain amorphous

water, water ice and do not display convincing evidence of metamorphism and aqueous alteration. But at variance with [147], paper [148] concludes that the detailed analysis of data collected by OSIRIS cameras show that comets are the ancient leftovers of early Solar System formation, and not younger fragments resulting from subsequent collisions between other, larger bodies. The unusually high porosity of the interior of the nucleus provides the first indication that this growth cannot have been via violent collisions, as these would have compacted the fragile material. The head and body of 67P were originally separate objects, but the collision that merged them must have been at low speed in order not to destroy both of them. The fact that both parts have similar layering also tells us that they must have undergone similar evolutionary histories and that survival rates against catastrophic collision must have been high for a significant period of time. The evolutionary path can be described as follows:

– The first 3 Myr: The initial solar nebula contained a disk at 15–30 AU of about 15 Earth Masses (EM) in solid chunks. The formation of large TNOs (diameters from 50 to 400 km) consumes almost all these pebbles until 2 EM remain, and at this point large TNOs cannot form any longer. The remaining pebbles merge to comet lobes through hierarchical agglomeration growth. Meter-sized bodies merge at very low velocities, less than 1 m/s, so that cometesimals are extremely porous and weak. Most cometesimals do not reach 6 km diameter, so that thermal processing is kept to a minimum.

– The first 25 Myr: TNOs grow by consuming each other, and their viscous stirring elevates cometesimals relative velocities to 30–40 m/s. These enhanced velocities produce layered cometesimals, with more compact outer parts on top of a less dense and more porous core. Collisions among those cometesimals form numerous bilobate structures. Although these cometary nuclei can reach diameters of several tens of km, their growth is slow enough that radionucleid heat generation can be dissipated, and comets remain extremely cold.

– The next 375 Myr: TNOs keep colliding with each other but in a constructive way, so they reach dimensions such as Triton (2600 km), Pluto and Eris (2300 km) in the next 375 Myr. Uranus and Neptune enter the primordial disk (Nice model) and relocate comets to the EKB, scattered disk and Oort Cloud. In conclusions, cometary nuclei incorporate very primitive material, say 3 Myr old.

Those two papers have stimulated plenty of additional discussion. The bi-lobate shape of 67P has attracted great attention (*e.g.*, [149]). Similar structures have been found in other minor bodies having dimensions of few to a dozen km, from asteroid Toutatis to Kerberos, moon of Pluto. Although of poor resolution, the images of VEGA 2 seem to indicate a complex possibly double structure also for Halley's, as shown in fig. 2. Such similarities may hint to a common mechanism of formation. References [150] and [151] have examined both questions, structure and origin. Their results suggest that the formation of such bilobate structures is a natural outcome of the low energy, sub-catastrophic collisions which have the potential to alter the shape of a small body significantly, without leading to major heating or compaction. Therefore, the observed bilobate structure of 67P may not be primordial, but might have originated in a rather recent event, possibly within the last 1 Gy. This may be the case for any kilometre-sized two-component cometary nuclei.

The question of origin of 67P has been discussed also by [152] and [153] on the light of chemical evidence. According to the first paper, the observed outgassing pattern indicates that the nucleus of 67P contains crystalline ice, clathrates, and other ices, and is not consistent with gas release from an amorphous ice phase with trapped volatile gases. If the building blocks of 67P were formed from crystalline ices and clathrates, then 67P would have agglomerated from ices that were condensed and altered in the protosolar nebula closer to the Sun, instead of more pristine ices originating from the interstellar medium or the outskirts of the disc, where amorphous ice may dominate. Reference [153] examines the stability of the S_2 dimer, ubiquitous in all comets. Because S_2 has a short lifetime in the vapor phase, its formation in grains via irradiation must occur only in low-density environments such as the interstellar medium or the upper layers of the proto-solar nebula. In the first case, comets would have agglomerated from icy grains that remained pristine when entering the proto-solar nebula. In the second case, comets would have agglomerated from icy grains condensed in the proto-solar nebula and that would have been efficiently irradiated during their turbulent transport towards the upper layers of the disk. Both scenarios are found consistent with the presence of molecular oxygen.

Surely, the discussion is not over, and the recent hypothesis of the existence of a Planet IX with 10–20 EM well beyond the orbit of Pluto may reopen this entire question. The growing evidence of comets in extra-solar planetary systems might as well bring fresh ideas.

15. – Some conclusions and open questions from 67P

During its two years mission around comet 67P, all instruments on Rosetta had the unique opportunity to follow closely a comet in the most active part of its orbit. All subsystems and scientific instruments have worked to the very end of the mission, which lasted nine months beyond the originally planned life-time. In particular, OSIRIS has acquired more than 80000 images which have been calibrated and made public, a data base of exceptional value which will require some more years for its examination. However, already now it is possible to identify several sound facts useful for a better understanding of the cometary physics, but also some still unanswered questions (see for instance [154]). Here is a selection of those facts and questions.

1 – No dramatic changes of the overall structure has taken place, the two lobes did not split nor appreciably move one with respect to the other. The number of pits, fractures, boulders has remained essentially the same. There are though noticeable exceptions in localized areas, as in Imothep, or the landslide in the region of Aswan.

2 – The evolution of surface properties attests the importance not only of the seasons, but also of the concavities of the irregular shape of the comet in determining its thermal status.

3 – The average loss of thickness is no more than 70 cm, with noticeable North – South differences. The mass loss at peak activity was 10^5 tons/day (10^{-6} of total mass). In total, the comet has lost no more than 0.2% of the mass it had at the beginning of such orbit.

4 – The average ratio between the mass of dust and the mass of gas is approximately 6 to 1, although it might be even much higher in localized areas and events, a very

dusty comet indeed. If instead of mass we consider the volume, the ratio is about 3 to 1. A consequence is that the greatest part of the mass must be composed by minerals present in the proto-solar nebula, and that 67P contains less water than say C1 chondrites. Probably, the dust is produced mostly by cliffs. However, not all the dust is lost to outer coma and tail, a fraction falls back on the comet, with a transfer effect from the southern to the northern hemisphere.

5 – A thin layer of dust acts as excellent thermal insulator. The presence of fractures and pits is needed to transfer some heat to the interior.

6 – The removal of dust reveals patches of H_2O and CO_2 ices, and a cyclic variation of colours of the surface.

7 – Given the paucity of gases, a still unanswered question is the mechanism of activity. How can the dusty jets remain so well collimated? is it because of the physical properties of the source regions or it is an effect of dust being trapped in gas shock waves?

8 – Reference [155] examines the general problem of geological processes in comets deriving from the six space missions that resolved the nuclei. There are many enigmatic features on cometary surfaces and significant unexplained diversity in landforms among cometary surfaces clearly exists. The exploration and understanding of geologic processes on comets is only beginning. These fascinating bodies will continue to provide a unique laboratory for examining common geologic processes under the uncommon conditions of very high porosity, very low strength, small particle sizes, and near-zero gravity.

In conclusion, the Rosetta mission has answered many questions left open by other cometary missions and ground and orbital telescopes, but as always in science, new questions appeared. Many papers are still in preparation, so that a full appreciation of the immense archive of unique data provided by the different scientific instruments on Rosetta must await some more time. Other space missions, great telescopes such as ALMA, E-ELT, JWST and so on are impatiently awaited the planetological community worldwide. Comet Halley, today reaching its aphelion, will come back in 2061. It is not too early to start thinking to a new ambitious mission to the mother of all comets.

* * *

GIOTTO and Rosetta have attested the enormous possibilities of European research and industries. The ESA personnel in ESAC, ESOC, ESTEC and ground stations have provided a support of outstanding quality. On the Italian side, the success of the two missions is due to the many researchers, post-docs, students, technicians in Universities, INAF Astronomical Observatories, CNR laboratories, in Firenze, Milano, Napoli, Padova, Roma, Trieste. Many National Industries have provided hardware and software of the greatest reliability and performances. The Italian Space Agency (and previously the CNR/Piano Spaziale Nazionale) have always supported financially and politically the Italian participation.

We cannot close this review without mentioning Angioletta Coradini, who contributed in a most effective way to many missions in the Solar System, and was responsible for VIRTIS until her untimely death in September 2011. Her name has been given to a gate on the landscape of comet 67P (fig. 35).

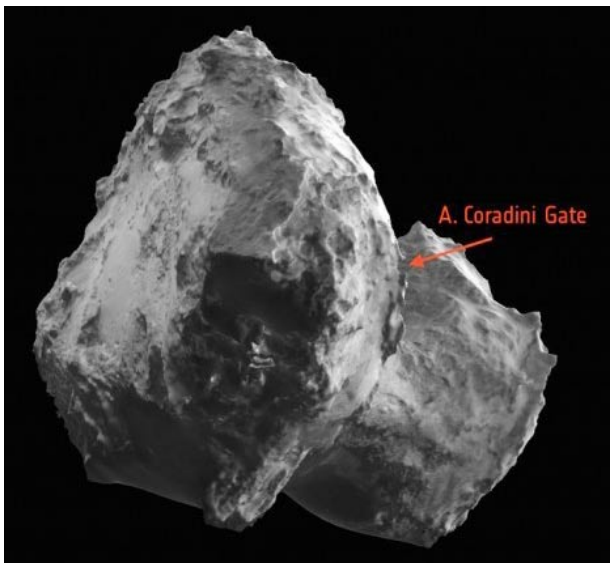

Fig. 35. – The gate A. Coradini on 67P identified on an OSIRIS image.

Credits

All OSIRIS images quoted on this review are *Credit ESA/Rosetta/MPS for OSIRIS Team MPS/UPD/LAM/IAA/SSO/INTA/UPM/DASP/IDA* or as specified in the text or caption to the relevant figure.

Appendix A.

GIOTTO *vs.* Rosetta, a comparison of two missions

GIOTTO was the first European interplanetary mission, directed to comet Halley/1P, with the primary scientific objectives to prove that comets have a nucleus and determine their characteristics. The spacecraft was launched from Kourou (French Guiana) on July 2, 1985 by an Ariane 1 rocket, with a total mass at launch of 950 kg. GIOTTO was accompanied by a veritable "armada" of five other spacecraft, two by Soviet Union, two by Japan and one (ICE) by USA. In those so difficult years, Halley's was the motivation of a large international collaboration. GIOTTO carried the Halley Multicolour Camera, with a Cassegrain telescope plus a flat metal mirror feeding it. Images were acquired by a CCD, one of the very first ever flown to space for scientific purposes [156]. Due to the fast spinning of the spacecraft, imaging was very difficult, and the HMC had more electronics than all the rest of the mission. Again, the FPGAs were among the first to be flown to space. GIOTTO passed near the nucleus at about 600 km minimum distance, acquiring many excellent images. Unfortunately, one minute after midnight of March, 13, 1986, a grain of cometary dust hit the exposed flat mirror and the camera did not operate any longer. Therefore, the HMC was able to image only one face of the comet.

Although deprived of its imaging system and of other scientific capabilities, GIOTTO went on to comet Grigg-Skiellerup (an old inactive comet with a period of about 5 years) for a so-called GEM, GIOTTO Extended Mission. After a 4-year long hibernation and an Earth swing-by, the spacecraft had to be hibernated for a second time. The G-S

comet was reached in July 1992, with a relative velocity of 14 km/s. After the encounter GIOTTO was again hibernated and directed to another Earth swing-by in 1999, this time at about 220000 km, but the spacecraft was not heard since.

Prompted by the great success of GIOTTO, in the XXI century the European Space Agency (ESA) undertook a new more ambitious mission named ROSETTA.

A drastic change of plans came right before the launch foreseen in spring 2003, because the uncertainties on the performances of the launcher Ariane-5 imposed a delay of one year. The originally planned comet 46P/Wirtanen had to be substituted, and the only reachable one was 67P/Churyumov-Gerasimenko, a small comet not visible to the naked eye, discovered in 1969 by the two (then) Soviet astronomers Klim Churyumov and Svetlana Gerasimenko. The change of comet entailed also the change of asteroids, so that finally:

Primary scientific objective: *comet 67P (C-G).*

Secondary scientific objectives: *two asteroids (Steins, Lutetia).*

Launch March 3, 2004 again from Kourou, with an Ariane-5 G+.

Mass of payload at launch: orbiter 2900 kg (inclusive of 1670 kg propellant and 165 kg scientific payload), equipped with a lander (Philae) of 100 kg.

Dimensions of the Orbiter: $2.8 \times 2.1 \times 2.0$ m, with 2 solar panels 14×2 m each.

Dimensions of Philae: $1 \times 1 \times 1$ m with 3 legs of 1 m.

Main differences between GIOTTO and Rosetta:

- GIOTTO: direct launch to the comet, duration less than 1 year, very fast "fly-by", small distance from Earth, spin stabilized.
- Rosetta: cruise mission of 12 years duration, need of "gravitational assist", three axis stabilized, high radiation dose.
- Relative kinetic energy: GIOTTO: $v \approx 70$ km/s, Rosetta: $v \approx 0.5$ km/s; GIOTTO *vs.* Rosetta ratio of energies of dust grain impacts ≈ 20000 (GIOTTO needed a shield, Rosetta did not).
- Very high duty of OSIRIS mechanisms: shutters more than 50000, and covers more than 10000 actuations each.

Rosetta distance to Sun, power and bit rate, time of flight for signals:

- The Sun-spacecraft distance varied between 180 and 600 million km.
- The light-time (one way) for communications was almost always > 8 min
- Signals transmitted and received in two bands: S- (2 GHz) and X- (8 GHz), received by three parabolic antennae of 35 m diameter, in Malargue (Argentina), New Norcia (Australia) and Cerebros (Spain). Support by NASA DSN (in particular the 70 m antenna at Goldstone, CA) needed in several phases of the mission.
- Power availability: 675 W at Jupiter, 1050 W at Mars
- Data downlink: 10 kbits/s at Jupiter, 75 kbits/s at Mars

Consequences:

- No real-time operation
- Occasional multi-instrument operation

– Compression algorithms needed for images, full frame images not possible in several phases, in particular during the comet landing final phases
– Long delay between data acquisition and data examination
– 3D image reconstruction severely hampered

Scientific Instrumentation on Rosetta are listed in tables VIII and IX.

TABLE VIII. – *The eleven instruments on the Orbiter.*

ALICE Ultraviolet Imaging Spectrometer (NASA)
CONSERT Comet Nucleus Sounding
COSIMA Cometary Secondary Ion Mass Analyser
GIADA Grain Impact Analyser and Dust Accumulator
MIDAS Micro-Imaging Analysis System
MIRO Microwave Instrument for the Rosetta Orbiter (NASA)
OSIRIS Rosetta Orbiter Imaging System
ROSINA Rosetta Orbiter Spectrometer for Ion and Neutral Analysis
RPC Rosetta Plasma Consortium
RSI Radio Science Investigation
VIRTIS Visible and Infrared Mapping Spectrometer

TABLE IX. – *The ten instruments on Philae.*

APXS Alpha Proton X-ray Spectrometer
ÇIVA/ROLIS Rosetta Lander Imaging System
CONSERT Comet Nucleus Sounding
COSAC Cometary Sampling and Composition experiment
MODULUS PTOLEMY Evolved Gas Analyser
MUPUS Multi-Purpose Sensor for Surface and Subsurface Science
ROMAP RoLand Magnetometer and Plasma Monitor
SD2 Sample and Distribution Device
SESAME Surface Electrical Sounding and Acoustic Monitoring Experiment

Several parameters of the 67P nucleus were known before freezing the characteristics of the spacecraft and its instrumentation, in particular of the landing module Philae. See table X.

The high inclination of the rotation axis to the orbital plane has the consequence that the Northern Hemisphere of the comet is illuminated by the Sun for the greater part of the orbit but never at small distances from the Sun, whilst the southern hemisphere only for few months around the perihelion, a short but intense summer.

An unfortunate event was the failure of Philae to stick to the surface. After a flawless descent to the surface of the comet in the foreseen place, the anchoring system failed, and Philae made a long flight which ended in the Abydos region (fig. 36). The lander was seen again by OSIRIS starting in May, 2016, with a definite confirmation in early September (fig. 37).

TABLE X. – *Properties of 67P nucleus known before the launch of Rosetta.*

Direct orbit	
Inclination to the ecliptic plane of about 7°,	
Eccentricity around 0.64,	
Semi-major axis of 3.36 AU (aphelion is just outside the orbit of Jupiter,	
perihelion just outside the orbit of the Earth).	
Period of 6.5 years.	
Radii of best fitting ellipsoid: $2.2 \times 1.3 \times 1.04$ km	
Surface: 47 km^2	
Volume: 19 km^3	
Mass 10^{13}–10^{14} kg	
Rotational period of nucleus: 12.40 h	
Obliquity of the rotation axis to the orbital plane: 55°	
Summer solstice	29.7.2013
Autumn equinox	10.5.2015
Date of Perihelion	13.8.2015
Winter solstice	04.9.2015
Spring equinox	18.3.2016

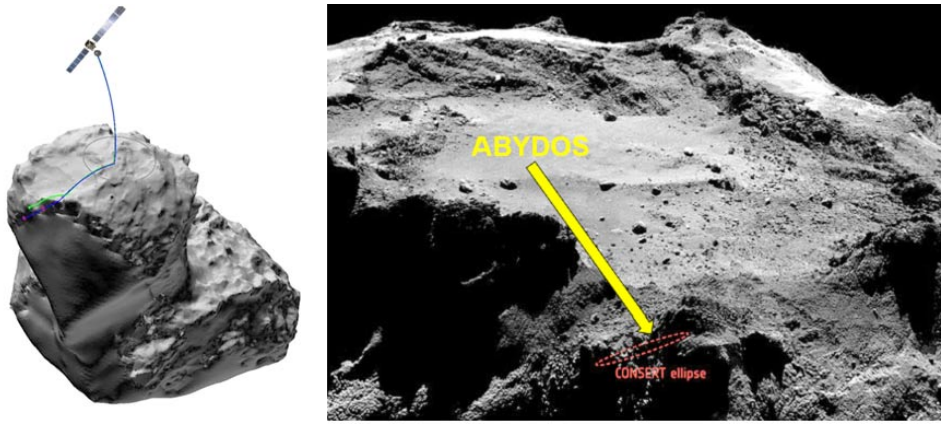

Fig. 36. – Left: a reconstruction of the three jumps made by Philae before final resting. Right: image of the region (Abydos) where Philae landed. The red oval delimitates the area where CONSERT indicated the rest position. (Adapted from: Ellipse: ESA/Rosetta/Philae/CONSERT; Image: ESA/Rosetta/MPS for OSIRIS Team MPS/UPD/LAM/IAA/SSO/INTA/UPM/DASP/IDA.)

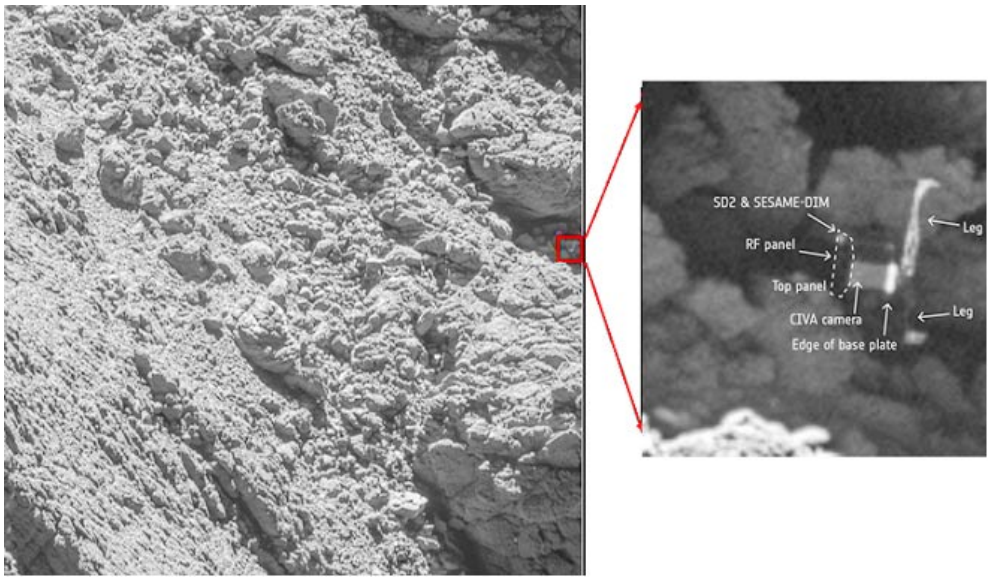

Fig. 37. – The lander Philae imaged by OSIRIS/NAC on Sept. 2, 2016.

Rosetta Journey milestones

1st Earth gravity assist:	4 March 2005
Mars gravity assist	25 February 2007 (loss of energy)
2nd Earth gravity assist:	13 November 2007
Asteroid Steins fly-by:	5 September 2008
3rd Earth gravity assist:	13 November 2009
Asteroid Lutetia fly-by:	10 July 2010
Enter deep space hibernation:	8 June 2011
Exit deep space hibernation:	20 January 2014
Comet rendezvous manoeuvres:	May–August 2014 (loss of energy)
Arrival at comet:	6 August 2014
Philae lander delivery:	12 November 2014
Crossing of Mars orbit:	early June 2015
Closest approach to Sun:	13 August 2015
Mission end:	30 September 2016

Appendix B.

The VEGA missions to comet Halley

For a full description of the Venus-Comet Halley Soviet missions VEGA-1 and VEGA-2 see R. Sagdeev in the book by Grewing *et al.* ref. [157], which contains several papers about the results by the VEGAs and by GIOTTO. VEGA-1 was launched on December 15, 1984, and VEGA-2 followed on December 21 on Proton rockets. VEGA-1 arrived at Venus on June 11, 1985, releasing the 750 kg descent vehicle. A series of supersonic

and subsonic parachutes reduced the speed further, and after a ten-minute descent in the clouds, the main parachute was detached and the lander fell freely, slowed only by aerodynamic braking. Surface contact was made after an hour long descent, and transmitted data from the surface for about 20 minutes, in conditions of 95 atm pressure and 467 °C.

VEGA-2 arrived on June 15, following a similar plan. It landed at a slightly higher elevation, the pressure at this site was 91 atm, with a temperature of 461 °C. The vehicles landed about 1300 km apart, near the equatorial plateau of Aphrodite Terra.

After their missions to Venus, the VEGA spacecraft reached Halley's comet. VEGA-1 passed within 8890 km of the comet nucleus on March 6, and VEGA-2 came within 8030 km on March 9. A steerable platform carried a system of cameras and spectrometers. The narrow angle camera (a Ritchey-Chretien telescope of 1200 mm focal length) could image visible, red, near and far infrared, and employed automatic aiming mechanisms to track the comet's nucleus. The camera had $15 \times 20\,\mu$rad FoV per pixel (3.5 arcsec). A wide angle camera had a focal length of 150 mm (28 arcsec resolution). A cryogenically cooled far-infrared spectrometer analysed the range of 2500–12000 nm, while a three channel spectrometer looked at the near infrared (950–1900 nm), visible/UV (275–715 nm) and far ultraviolet (120–290 nm).

See also several papers in Soviet Astronomy Letters of 1986 and in ref. [158].

VEGA-1 and -2 flew directly through the tail of the comet, with aluminium shields installed on one side to protect it from the cometary dust impacts. Both spacecraft survived, although damage reduced solar-panel power by 50%. After circling the Sun, the spacecraft passed through the tail of Halley's comet a second time in early 1987, and returned additional scientific information.

REFERENCES

[1] Maffei P., *La Cometa di Halley* (Mondadori Biblioteca EST) 1984 (in Italian).

[2] Tamman G. A. and Véron P., *Halleys Komet* (Birkhauser Verlag Basel) 1985 (in German).

[3] Yeomans D. K., *Comets* (John Wiley and Sons, Inc) 1991.

[4] Brand J. C. and Chapman R. D., *Introduction to Comets* (Cambridge University Press) 1981 second edition 2004.

[5] Kronk's Cometography: `http://cometography.com`.

[6] Swings P., "Cometary Spectra", *Quart. J. R. Astron. Soc.*, **6** (1965) 28.

[7] `http://history.nasa.gov/SP-404/ch4.htm`.

[8] Crovisier J., Bockelée-Morvan D., Colom P. and Biver N., "Comets at radio wavelengths", *C. R. Phys.*, **17** (2016) 985; DOI: 10.1016/j.crhy.2016.07.020.

[9] Drake J. F., Jenkins E. B., Bertaux J. L., Festou M. and Keller H. U., "Lyman-alpha observations of Comet Kohoutek 1973 XII with Copernicus", *Astrophys. J.*, **209** (1976) 302.

[10] Cosmovici C. B., Montebugnoli S., Orfei A., Pogrebenko S. and Colom P., "First evidence of planetary water maser emission induced by the comet/Jupiter Catastrophic event", *Planet. Space Sci.*, **44** (1996) 735.

[11] de Pater I., Forster J. R., Wright M., Butler B. J., Palmer P., Veal J. M., A'Hearn M. F. and Snyder L. E., "BIMA and VLA Observations of Comet Hale-Bopp at 22–115 GHz", *Astron. J.*, **116** (1998) 987.

[12] Harmon J. K., Nolan M. C., Howell E. S., Giorgini J. D. and Taylor P. A., "Radar Observations of Comet 103P/Hartley 2", *Astrophys. J. Lett.*, **734** (2011) 4.

[13] Kamoun P., Lamy P. L., Toth I. and Herique A., "Constraints on the subsurface structure and density of the nucleus of Comet 67P/Churyumov-Gerasimenko from Arecibo radar observations", *Astron. Astrophys.*, **568** (2014) 8.

[14] Dennerl K., Englhauser J. and Trümper J., "X-ray emissions from comets detected in the Röntgen X-ray satellite all-sky survey", *Science*, **277** (1997) 1625.
[15] Owens A., Oosterbroek T., Orr A., Parmar A. N., Schulz R., Antonelli L. A., Fiore F., Tozzi G. P., Maccarone M. C. and Piro L., "BeppoSAX LECS detection of comet C/1995 O1(Hale-Bopp)", *Nucl. Phys. B Proc. Suppl.*, **69** (1997) 735.
[16] Lisse C. M., Dennerl K., Englhauser J., Harden M., Marshall F. E., Mumma M. J., Petre R., Pye J. P., Ricketts M. J., Schmitt J. *et al.*, "Discovery of X-ray and Extreme Ultraviolet Emission from Comet C/Hyakutake 1996 B2", *Science*, **274** (1996) 205.
[17] Wegmann R., Schmidt H. U., Lisse C. M., Dennerl K. and Englhauser J., "X-rays from comets generated by energetic solar wind particles", *Planet. Space Sci.*, **46** (1998) 603.
[18] Bhardwaj A., Elsner R. F., Randall Gladstone G., Cravens T. E., Lisse C. M., Dennerl K., Branduardi-Raymont G., Wargelin B. J., Hunter Waite J., Robertson I. *et al.*, "X-rays from solar system objects", *Planet. Space Sci.*, **55** (2007) 1135.
[19] Festou M. C., Rickman H. and West R. M., "Comets I - Concepts and Observations", *Astron. Astrophys. Rev.*, **4** (1993) 363; DOI: 10.1007/BF00872944.
[20] Weaver H. A., Feldman P. D., Festou M. C., A'Hearn M. F. and Keller H. U., "IUE Observations of Faint Comets", *Icarus*, **47** (1981) 449.
[21] Festou M. C., *IUE-ULDA Access Guide No. 2 – Comets*, ESA SP 1134 (1990).
[22] *Comets, Asteroids and Zodiacal Light as Seen by ISO*, by Thomas G. Müller and Péter Ábrahám, Jacques Crovisier in *ISO Science Legacy: A Compact Review of ISO Major Achievements*, edited by Cesarsky C. and Salama A. (Springer Netherland) 2005, chapter 10.
[23] Snios B., Kharchenko V., Lisse C. M., Wolk S. J., Dennerl K. and Combi M. R., "Chandra Observations of Comets C/2012 S1 (ISON) and C/2011 L4 (PanSTARRS)", *Astrophys. J.*, **818** (2016) 10.
[24] McKay A. J., Kelley M. S. P., Cochran A. L., Bodewits D., DiSanti M. A., Dello Russo N. and Lisse C. M., "The CO2 abundance in Comets C/2012 K1 (PanSTARRS), C/2012 K5 (LINEAR), and 290P/Jäger as measured with Spitzer", *Icarus*, **266** (2016) 249.
[25] Chandra and comets, *Comets ISON & PanSTARRS: Comets in the "X"-Treme*, `http://chandra.harvard.edu/photo/2016/comets/` and *A Tour of Comets ISON & PanSTARRS*, `http://chandra.harvard.edu/resources/podcasts/ts/ts210416.html`.
[26] Rosetta, `http://blogs.esa.int/rosetta/`.
[27] Larson S. M. and Sekanina Z., "Coma morphology and dust-emission pattern of periodic Comet Halley. I - High-resolution images taken at Mount Wilson in 1910", *Astron. J.*, **89** (1984) 571; DOI: 10.1086/113551.
[28] Keller H. U., Barbieri C., Lamy P., Rickman H., Rodrigo R., Wenzel K.-P., Sierks H., A'Hearn M. F., Angrilli F. and the OSIRIS team, "OSIRIS- The Scientific Camera System Onboard Rosetta", *Space Sci. Rev.*, **128** (2007) 433.
[29] Rosetta VIRTIS, `http://www.ifsi-roma.inaf.it/virtis/index.php?categoryid=16`.
[30] Mottola S., Lowry S., Snodgrass C., Lamy P. L., Toth I., Rozek A., Sierks H., A'Hearn M. F., Angrilli F., Barbieri C. *et al.*, "The rotation state of 67P/Churyumov-Gerasimenko from approach observations with the OSIRIS cameras on Rosetta", *Astron. Astrophys.*, **569** (2014) 5.
[31] Coradini A., Capaccioni F., Drossart P., Semery A., Arnold G. and Schade U., "VIRTIS: The Imaging Spectrometer of the Rosetta Mission", *Adv. Space Res*, **24** (1999) 1105.
[32] Coradini A., Capaccioni F., Drossart P., Arnold G., Ammannito E., Angrilli F., Barucci A., Bellucci G., Benkhoff J., Bianchini G. *et al.*, "VIRTIS: An Imaging Spectrometer for the Rosetta Mission", *Space Sci. Rev.*, **128** (2007) 529; DOI: 101007/s11214-006-9127-5.

[33] Snodgrass C., Opitom C., de Val-Borro M., Jehin E., Manfroid J., Lister T., Marchant J., Jones G. H., Fitzsimmons A., Steele I. A. *et al.*, "The perihelion activity of comet 67P/Churyumov-Gerasimenko as seen by robotic telescopes", *Mon. Not. R. Astron. Soc.*, **462** (2016) S138; DOI: 10.1093/mnras/stw2300.

[34] Hapke B., "Bidirectional Reflectance Spectroscopy. 5. The Coherent Backscatter Opposition Effect and Anisotropic Scattering", *Icarus*, **157** (2002) 523; DOI: 10.1006/icar.2002.6853.

[35] Fornasier S., Hasselmann P. H., Barucci M. A., Feller C., Besse S., Leyrat C., Lara L., Gutierrez P. J., Oklay N., Tubiana C. *et al.*, "Spectrophotometric properties of the nucleus of comet 67P/Churyumov-Gerasimenko from the OSIRIS instrument onboard the ROSETTA spacecraft", *Astron. Astrophys.*, **583** (2015) 18.

[36] Fornasier S., Mottola S., Keller H. H., Barucci M. A., Davidsson B., Feller C., Deshapriya J. D. P., Sierks H., Barbieri C. and the OSIRIS Team, "Rosetta's comet 67P/Churyumov-Gerasimenko sheds its dusty mantle to reveal its icy nature", *Science*, **354** (2016) 1566; DOI: 10.1126/science.aag2671.

[37] Jorda L., Gaskell R., Capanna C., Hviid S., Lamy P., Ďurech J., Faury G., Groussin O., Gutiérrez P., Jackman C. *et al.*, "The global shape, density and rotation of Comet 67P/Churyumov-Gerasimenko from preperihelion Rosetta/OSIRIS observations", *Icarus*, **277** (2016) 257; DOI: 10.1016/j.icarus.2016.05.002.

[38] Filacchione G., Raponi A., Capaccioni F., Ciarniello M., Tosi F., Capria M. T., De Sanctis M. C., Migliorini A., Piccioni G., Cerroni P. *et al.*, "Seasonal exposure of carbon dioxide ice on the nucleus of comet 67P/Churyumov-Gerasimenko", *Science*, **354** (2016) 1563.

[39] Schrijver C. J., Brown J. C., Battams K., Saint-Hilaire P., Liu W., Hudson H. and Pesnell W. D., "Destruction of Sun-Grazing Comet C/2011 N3 (SOHO) Within the Low Solar Corona", *Science*, **335** (2013) 324; DOI: 10.1126/science.1211688.

[40] Schrijver C. J., Lisse C. M. and Downs C., "Comets as solar probes", *Phys. Today*, **66** (2013) 27; DOI: 10.1063/PT.3.2146.

[41] Sekanina Z. and Kracht R., *Disintegration of Comet C/2012 S1 (ISON) Shortly Before Perihelion: Evidence from Independent Data Sets*, arXiv:1404.5968 (2014).

[42] Keane J. V., Milam S. N., Coulson I. M., Kleyna J. T., Sekanina Z., Kracht R., Riesen T.-E., Meech K. J. and Charnley S. B., "Catastrophic Disruption of Comet ISON", *Astrophys. J.*, **831** (2016) 7; DOI: 10.3847/0004-637X/831/2/207.

[43] McCandliss S. R., Feldman P. D., Weaver H., Fleming B., Redwine K., Li M. J., Kutyrev A. and Moseley S. H., "Far-ultraviolet Observations of Comet C/2012 S1 (ISON) from FORTIS", *Astron. J.*, **152** (2016) 10; DOI: 10.3847/0004-6256/152/3/65.

[44] Fulle M., Leblanc F., Harrison R. A., Davis C. J., Eyles C. J., Halain J. P., Howard R. A., Bockeleé-Morvan D., Cremonese G. and Scarmato T., "Discovery of the atomic iron tail of comet McNaught using the heliospheric imager on STEREO", *Astrophys. J.*, **661** (2007) L93.

[45] Cavalié T., Feuchtgruber H., Lellouch E., de Val-Borro M., Jarchow C., Moreno R., Hartogh P., Orton G., Greathouse T. K., Billebaud F. *et al.*, "Spatial distribution of water in the stratosphere of Jupiter from Herschel HIFI and PACS observations", *Astron. Astrophys.*, **553** (2013) 16.

[46] Fernández Y. R., Kelley M. S., Lamy P. L., Toth I., Groussin O., Lisse C. M., A'Hearn M. F., Bauer J. M., Campins H., Fitzsimmons A. *et al.*, "Thermal properties, sizes, and size distribution of Jupiter-family cometary nuclei", *Icarus*, **226** (2013) 1138.

[47] Guzzo M. and Lega E., "A study of the past dynamics of comet 67P/C-G with Fast LyapunovIndicators", *Astron. Astrophys.*, **579** (2015) 7.

[48] Rickman H. *et al.*, "Secular Orbital Evolution of Jupiter family comets", *Astron. Astrophys.*, **598** (2017) A110.

[49] Schneider N. M., Deighan J. I., Stewart A. I. F., McClintock W. E., Jain S. K., Chaffin M. S., Stiepen A., Crismani M., Plane J. M. C., Carrillo-Sánchez J. D., Evans J. S., Stevens M. H., Yelle R. V., Clarke J. T., Holsclaw G. M., Montmessin F. and Jakosky B. M., "MAVEN IUVS observations of the aftermath of the Comet Siding Spring meteor shower on Mars", *Geophys. Res. Lett.*, **42** (2015) 4755.

[50] Pham L. B. S. and Karatekin Ö., "Scenarios of atmospheric mass evolution on Mars influenced by asteroid and comet impacts since the late Noachian", *Planet. Space Sci.*, **125** (2016) 1; DOI: 10.1016/j.pss.2015.09.022.

[51] `http://m.esa.int/Our_Activities/Space_Science/Mars_Express/Water_ice_in_crater_at_Martian_north_pole`.

[52] Cosmovici C. B. and Ortolani S., "Detection of new molecules in the visible spectrum of Comet IRAS-Araki-Alcock (1983 d)", *Nature*, **310** (1984) 122.

[53] Lamy P. L., Toth I., Weaver H. A., A'Hearn M. F. and Jorda L., "Properties of the nuclei and comae of 10 ecliptic comets from Hubble Space Telescope multi-orbit observations", *Mon. Not. R. Astron. Soc.*, **412** (2011) 1573.

[54] Cowen R., *History of Life* (Blackwell Science, Boston, Mass.) 2000.

[55] Jakosky B. M., *Science, Society, and the Search for Life in the Universe* (University of Arizona Press) 2006.

[56] Farinella P., Foschini L., Froeschlé Ch., Gonczi R., Jopek T. J., Longo G. and Michel P., "Probable asteroidal origin of the Tunguska Cosmic Body", *Astron. Astrophys.*, **377** (2001) 1081.

[57] Bertini I., "Main Belt Comets: a new class of small bodies in the Solar System", *Planet. Space Sci.*, **59** (2011) 365; DOI: 10.1016/j.pss.2011.01.014.

[58] Snodgrass C., Tubiana C., Vincent J. B., Sierks H., Hviid S., Moissl R., Boehnhardt H., Barbieri C. *et al.*, "Recent asteroid collision P/2010 A2 confirmed and dated by Rosetta/OSIRIS observation", *Nature*, **467** (2010) 814.

[59] `https://sites.google.com/site/castaliathemission/`.

[60] Altwegg K., Balsiger H., Bar-Nun A., Berthelier J. J., Bieler A., Bochsler P., Briois C., Calmonte U., Combi M., De Keyser J. *et al.*, "67P/Churyumov-Gerasimenko, a Jupiter family comet with a high D/H ratio", *Science*, **347** (2015) 1261952.

[61] Tsiganis K., Gomes R., Morbidelli A. and Levison H. F., "Origin of the orbital architecture of the giant planets of the Solar System", *Nature*, **435** (2005) 459.

[62] Rickman H. *et al.*, "Cometary Impact Rates on the Moon and Planets during the LHB", *Astron. Astrophys.*, **598** (2017) A67.

[63] Marty B., Avice G., Sano Y., Altwegg K., Balsiger H., Hässig M., Morbidelli A., Mousis O. and Rubin M., "Origins of volatile elements (H, C, N, noble gases) on Earth and Mars in light of recent results from the ROSETTA cometary mission", *Earth Planet. Sci. Lett.*, **441** (2016) 91.

[64] Robinson K. L. and Taylor G. J., "Heterogeneous distribution of water in the Moon", *Nat. Geosci.*, **7** (2014) 401.

[65] Sekanina Z. and Kracht R., "Strong Erosion-Driven Nongravitational Effects in Orbital Motions of the Kreutz Sungrazing System's Dwarf Comets", *Astrophys. J.*, **801** (2015) 19; DOI: 10.1088/0004-637X/801/2/135.

[66] Meech K. J., Pittichová J., Bar-Nun A., Notesco G., Laufer D., Hainaut O. R., Lowry S. C., Yeomans D. K. and Pitts M., "Activity of comets at large heliocentric distances pre-perihelion", *Icarus*, **201** (2009) 719.

[67] Snodgrass C., Jehin E., Manfroid J., Opitom C., Fitzsimmons A., Tozzi G. P., Faggi S., Yang B., K. Matthew M., Conn B. C. *et al.*, "Distant activity of 67P/Churyumov-Gerasimenko in 2014: Ground-based results during the Rosetta pre-landing phase", *Astron. Astrophys.*, **588** (2016) 12; DOI: 10.1051/0004-6361/201527834.

[68] Moreno F., Snodgrass C., Hainaut O., Tubiana C., Sierks H., Barbieri C., Lamy P. L., Rodrigo R., Koschny D., Rickman H. *et al.*, "The dust environment of comet 67P/Churyumov-Gerasimenko from Rosetta OSIRIS and VLT observations in the 4.5 to 2.9 AU heliocentric distance range inbound", *Astron. Astrophys.*, **587** (2016) 12.

[69] Bertini I., Thomas N. and Barbieri C., "Modeling of light scattering properties of cometary dust", *Astron. Astrophys.*, **461** (2007) 351.

[70] Lin Z. Y. *et al.*, "Morphology and dynamics of the jets of comet 67P/Churyumov-Gerasimenko: Early-phase development", *Astron. Astrophys.*, **583** (2015) A11; DOI: 10.1051/0004-6361/201525961.

[71] Lin Z.-Y., Lai I.-L., Su C.-C., Ip W.-H., Lee J.-C., Wu J.-S., Vincent J.-B., La Forgia F., Sierks H., Barbieri C. *et al.*, "Observations and analysis of a curved jet in the coma of comet 67P/Churyumov-Gerasimenko", *Astron. Astrophys.*, **588** (2016) 5; DOI:10.1051/0004-6361/201527784.

[72] Hines D. C. and Levasseur-Regourd A.-C., "Polarimetry observations of comets: Status, questions, future pathways", *Planet. Space Sci.*, **123** (2016) 41; DOI: 10.1016/j.pss.2015.11.016.

[73] Agarwal J., A'Hearn M. F., Vincent J.-B., Güttler C., Höfner S., Sierks H., Tubiana C., Barbieri C., Lamy P. L., Rodrigo R. *et al.*, "Acceleration of individual, decimetre-sized aggregates in the lower coma of comet 67P/Churyumov-Gerasimenko", *Mon. Not. R. Astron. Soc.*, **462** (2016) S78; DOI: 10.1093/mnras/stw2179.

[74] Fulle M., Ivanovski S. L., Bertini I., Gutierrez P., Lara L., Sierks H., Zakharov V., Della Corte V., Rotundi A., Barbieri C. *et al.*, "Rotating dust particles in the coma of comet 67P/Churyumov-Gerasimenko", *Astron. Astrophys.*, **583** (2015) 8.

[75] Ivanovski S. L., Zakharov V. V., Della Corte V., Crifo J.-F., Rotundi A. and Fulle M., "Dynamics of aspherical dust grains in a cometary atmosphere: I. axially symmetric grains in a spherically symmetric atmosphere", *Icarus*, **282** (2017) 333.

[76] A'Hearn M. F., Schleicher D. G., Millis R. L., Feldman P. D. and Thompson D. T., "Comet Bowell 1980b", *Astron. J.*, **89** (1984) 579.

[77] Fink U. and Rubin M., "The calculation of Afρ and mass loss rate for comets", *Icarus*, **221** (2012) 721.

[78] Merouane S., Zaprudin B., Stenzel O., Langevin Y., Altobelli N., Della Corte V., Fischer H., Fulle M., Hornung K., Silén J. *et al.*, "Dust particle flux and size distribution in the coma of 67P/Churyumov-Gerasimenko measured in situ by the COSIMA instrument on board Rosetta", *Astron. Astrophys.*, **596** (2016) 12.

[79] Della Corte V., Accolla M., Ferrari M., Ivanovski S., Lucarelli F., Mazzotta Epifani E., Rietmeijer F. J. M., Sordini R. and Rotundi A., *GIADA (Grain Impact Analyser and Dust Accumulator) prepares for the comet 67P/Churyumov-Gerasimenko encounter*, in *European Planetary Science Congress 2012, 23-28 September, 2012 Madrid, Spain* (2012) article ID: EPSC2012-684.

[80] Fulle M., Marzari F., Della Corte V., Fornasier S., Sierks H., Rotundi A., Barbieri C., Lamy P. L., Rodrigo R., Koschny D. *et al.*, "Evolution of the Dust Size Distribution of Comet 67P/Churyumov-Gerasimenko from 2.2 AU to Perihelion", *Astrophys. J.*, **821** (2016) 14.

[81] Benvenuti P., *Spectroscopic observations of comet Kohoutek (1973f), 2*, in *The Study of Comets, Part 1* (NASA, Goddard Space Flight Center) 1976, pp. 185–198.

[82] Szegö K., Glassmeier K.-H., Bingham R., Bogdanov A., Fischer C., Haerendel G,. Brinca A., Cravens T., Dubinin E., Sauer K., *et al.*, "Physics of Mass Loaded Plasmas", *Space Sci. Rev.*, **94** (2000) 429.

[83] Mandt K. E., Eriksson A., Edberg N. J. T., Koenders C., Broiles T., Fuselier S. A., Henri P., Nemeth Z., Alho M., Biver N. *et al.*, "RPC observation of the development and evolution of plasma interaction boundaries at 67P/Churyumov-Gerasimenko", *Mon. Not. R. Astron. Soc.*, **462** (2016) S9.

[84] Goetz C., Koenders C., Richter I., Altwegg K., Burch J., Carr C., Cupido E., Eriksson A., Güttler C., Henri P *et al.*, "First detection of a diamagnetic cavity at comet 67P/Churyumov-Gerasimenko", *Astron. Astrophys.*, **588** (2016) 6.

[85] Huebner W. F., *Physics and Chemistry of Comets*, (Springer-Verlag, Berlin, New York) 1990, p. 391.

[86] Mumma M. J. and Charnley S. B., "The Chemical Composition of Comets—Emerging Taxonomies and Natal Heritage", *Annu. Rev. Astron. Astrophys.*, **49** (2011) 471.

[87] Cochran Anita L., Levasseur-Regourd Anny-Chantal, Cordiner Martin, Hadamcik Edith, Lasue Jérémie, Gicquel Adeline, Schleicher David G., Charnley Steven B., Mumma Michael J., Paganini Lucas *et al.*, "The Composition of Comets", *Space Sci. Rev.*, **197** (2015) 9; DOI: 10.1007/s11214-015-0183-6.

[88] Cremonese G., Capria M. T. and De Sanctis C., "Catalog of the emission lines in the visible spectrum of comet 153P/Ikeya-Zhang", *Astron. Astrophys.*, **461** (2007) 789.

[89] Arpigny C. *et al.*, *Atlas of Cometary Spectra*, in preparation, private communication, 2017.

[90] Cremonese G., Boehnhardt H., Crovisier J., Rauer H., Fitzsimmons A., Fulle M., Licandro J., Pollacco D., Tozzi G. P. and West R. M., "Neutral Sodium from Comet Hale-Bopp: A Third Type of Tail", *Astrophys. J.*, **490** (1997) L199.

[91] Dello Russo N., Vervack R. J., Kawakita H., Cochran A., McKay A. J., Harris W. M., Weaver H. A., Lisse C. M., DiSanti M. A., Kobayashi H. *et al.*, "The compositional evolution of C/2012 S1 (ISON) from ground-based high-resolution infrared spectroscopy as part of a worldwide observing campaign", *Icarus*, **266** (2016) 152; DOI: 10.1016/j.icarus.2015.11.030.

[92] Bodewits D., Lara L. M., A'Hearn M. F., La Forgia F., Gicquel A., Kovacs G., Knollenberg J., Lazzarin M., Lin Z.-Y., Shi X. *et al.*, "Changes in the Physical Environment of the Inner Coma of 67P/Churyumov–Gerasimenko with Decreasing Heliocentric Distance", *Astron. J.*, **152** (2016) 15; DOI: 10.3847/0004-6256/152/5/130.

[93] Le Roy L., Altwegg K., Balsiger H., Berthelier J.-J., Bieler A., Briois C., Calmonte U., Combi M. R., De Keyser J., Dhooghe F. *et al.*, "Inventory of the volatiles on comet 67P/Churyumov-Gerasimenko from Rosetta/ROSINA", *Astron. Astrophys.*, **583** (2015) 12.

[94] Altwegg K., Balsiger H., Bar-Nun A., Berthelier J.-J., Bieler A., Bochsler P., Briois C., Calmonte U., Combi M. R., Cottin H. *et al.*, "Prebiotic chemicals–amino acid and phosphorus–in the coma of comet 67P/Churyumov-Gerasimenko", *Sci. Adv.*, **2** (2016) e1600285.

[95] Rubin M., Altwegg K., van Dishoeck E. F. and Schwehm G., "Molecular Oxygen in Oort Cloud Comet 1P/Halley", *Astrophys. J. Lett.*, **815** (2016) L11.

[96] Balsiger H., Altwegg K., Bar-Nun A., Berthelier J.-J., Bieler A., Bochsler P., Briois C., Calmonte U., Combi M., De Keyser J. *et al.*, "Detection of argon in the coma of comet 67P/Churyumov-Gerasimenko", *Sci. Adv.*, **1** (2015) e1500377.

[97] Feldman P. D., A'Hearn M. F., Bertaux J.-L., Feaga L. M., Parker J. Wm, Schindhelm E., Steffl A. J., Stern S. A., Weaver H. A., Sierks H. and Vincent J.-B., "Measurements of the near-nucleus coma of comet 67P/Churyumov-Gerasimenko with the Alice far-ultraviolet spectrograph on Rosetta", *Astron. Astrophys.*, **583** (2015) 8.

[98] Feldman P. D., A'Hearn M. F., Feaga L. M., Bertaux J.-L., Noonan J., Parker J. Wm, Schindhelm E., Steffl A. J., Stern S. A. and Weaver H. A., "The Nature and Frequency of the Gas Outbursts in Comet 67P/Churyumov-Gerasimenko Observed by the Alice Far-ultraviolet Spectrograph on Rosetta", *Astrophys. J. Lett.*, **825** (2016) 5.

[99] Migliorini A., Piccioni G., Capaccioni F., Filacchione G., Bockelée-Morvan D., Erard S., Leyrat C., Combi M. R., Fougere N., Crovisier J. *et al.*, "Water and carbon dioxide distribution in the 67P/Churyumov-Gerasimenko coma from VIRTIS-M infrared observations", *Astron. Astrophys.*, **589** (2016) 12.

[100] De Sanctis M. C., Capaccioni F., Ciarniello M., Filacchione G., Formisano M., Mottola S., Raponi A., Tosi F., Bockelée-Morvan D., Erard S. *et al.*, "The diurnal cycle of water ice on comet 67P/Churyumov-Gerasimenko", *Nature*, **525** (2015) 500; DOI: 10.1038/nature14869.

[101] Lee S., von Allmen P., Allen M., Beaudin G., Biver N., Bockelée-Morvan D., Choukroun M., Crovisier J., Encrenaz P., Frerking M. *et al.*, "Spatial and diurnal variation of water outgassing on comet 67P/Churyumov-Gerasimenko observed from Rosetta/MIRO in August 2014", *Astron. Astrophys.*, **583** (2015) 10.

[102] Keller H. U., Arpigny C., Barbieri C., Bonnet R. M., Cazes S., Coradini M., Cosmovici C. B., Delamere W. A., Huebner W. F., Hughes D. *et al.*, "First Halley multicolour camera imaging results from GIOTTO", *Nature*, **321** (1986) 320.

[103] `https://www.nasa.gov/missions`.

[104] Keller H. U., Küppers M., Fornasier S., Gutiérrez P. J., Hviid S. F., Jorda L., Knollenberg J., Lowry S. C., Rengel M., Bertini I., Cremonese G. *et al.*, "Observations of Comet 9P/Tempel 1 around the Deep Impact event by the OSIRIS cameras onboard Rosetta", *Icarus*, **187** (2007) 87 (re-published in the special issue of *Icarus*, **191**, Issue 2 (2007) 241.

[105] Sierks H., Barbieri C., Lamy P. L., Rodrigo R., Koschny D., Rickman H., Keller H. U., Agarwal J., A'Hearn M. F., Angrilli F. *et al.*, "On the nucleus structure and activity of comet 67P/Churyumov-Gerasimenko", *Science*, **347** (2015) aaa1044.

[106] Stooke P.J. and Abergel A., "Morphology of the nucleus of Comet P/Halley", *Astron. Astrophys.*, **248** (1991) 656.

[107] Preusker F., Scholten F., Matz K.-D., Roatsch T., Willner K., Hviid S. F., Knollenberg J., Jorda L., Gutiérrez P. J., Kührt E. *et al.*, "Shape model reference system definition and cartographic mapping standards for comet 67P/Churyumov-Gerasimenko - Stereo-photogrammetric analysis of Rosetta/OSIRIS image data", *Astron. Astrophys.*, **583** (2015) 19.

[108] El-Maarry M. R., Thomas N., Gracia-Berná A., Pajola M., Lee J.-C., Massironi M., Davidsson B., Marchi S., Keller H. U., Hviid S. F. *et al.*, "Regional surface morphology of comet 67P/Churyumov-Gerasimenko from Rosetta/OSIRIS images: The southern hemisphere", *Astron. Astrophys.*, **593** (2016) 20; DOI: 10.1051/0004-6361/201628634.

[109] Sekanina Z., Larson S. M., Hainaut O., Smette A. and West R. M., "Major outburst of periodic Comet Halley at a heliocentric distance of 14 AU", *Astron. Astrophys.*, **263** (1992) 367.

[110] Szabó G. M., Kiss L. L., Pál A., Kiss C., Sárneczky K., Juhász A., Hogerheijde M. R., "Evidence for Fresh Frost Layer on the Bare Nucleus of Comet Hale-Bopp at 32 AU Distance", *Astrophys. J.*, **761** (2012) 7.

[111] A'Hearn M. F., "Comets as building blocks", *Annu. Rev. Astron. Astrophys.*, **49** (2011) 281.

[112] Groussin O., Jorda L., Auger A.-T., Kührt E., Gaskell R., Capanna C., Scholten F., Preusker F., Lamy P., Hviid S. *et al.*, "Gravitational slopes, geomorphology, and material strengths of the nucleus of comet 67P/Churyumov-Gerasimenko from OSIRIS observations", *Astron. Astrophys.*, **583** (2015) 12.

[113] Mousis O., Guilbert-Lepoutre A., Brugger B., Jorda L., Kargel J. S., Bouquet A., Auger A.-T., Lamy P., Vernazza P., Thomas N. and Sierks H., "Pits Formation from Volatile Outgassing on 67P/Churyumov-Gerasimenko", *Astrophys. J. Lett.*, **814** (2015) 5.

[114] Weissman P., "Planetary science: Sink holes and dust jets on comet 67P", *Nature*, **523** (2015) 42.

[115] Giacomini L., Massironi M., El-Maarry M. R., Penasa L., Pajola M., Thomas N., Lowry S. C., Barbieri C., Cremonese G., Ferri F. *et al.*, "Geologic mapping of the Comet 67P/Churyumov-Gerasimenko's Northern hemisphere", *Mon. Not. R. Astron. Soc.*, **462** (2016) S352.

[116] Massironi M., Simioni E., Marzari F., Cremonese G., Giacomini L., Pajola M., Jorda L., Naletto G., Lowry S., El Maarry M. R. *et al.*, "Two independent and primitive envelopes of the bilobate nucleus of comet 67P", *Nature*, **526** (2015) 402.

[117] Kofman W., Herique A., Barbin Y., Barriot J.-P., Ciarletti V., Clifford S., Edenhofer P., Elachi C., Eyraud C., Goutail J.-P. *et al.*, "Properties of the 67P/Churyumov-Gerasimenko interior revealed by CONSERT radar", *Science*, **349** (2015) aab0639.

[118] Pätzold M., Andert T., Hahn M., Asmar S. W., Barriot J.-P., Bird M. K., Häusler B., Peter K., Tellmann S., Grün E., Weissman P. R., Sierks H., Jorda L., Gaskell R., Preusker F. and Scholten F., "A homogeneous nucleus for comet 67P/Churyumov-Gerasimenko from its gravity field", *Nature*, **530** (2016) 63.

[119] Keller H. U., Mottola S., Davidsson B., Schröder S. E., Skorov Y., Kührt E., Groussin O., Pajola M., Hviid S. F., Preusker F. *et al.*, "Insolation, erosion, and morphology of comet 67P/Churyumov-Gerasimenko", *Astron. Astrophys.*, **583** (2015) 16.

[120] Thomas N., Davidsson B., El-Maarry M. R., Fornasier S., Giacomini L., Gracia-Berná A. G., Hviid S. F., Ip W.-H., Jorda L., Keller H. U. *et al.*, "Redistribution of particles across the nucleus of comet 67P/Churyumov-Gerasimenko", *Astron. Astrophys.*, **583** (2015) 18.

[121] Samarasinha N. H. and Mueller B. E. A., "Component periods of non-principal-axis rotation and their manifestations in the lightcurves of asteroids and bare cometary nuclei", *Icarus*, **248** (2015) 347.

[122] Belton M. J. S., Julian W. H., Anderson A. J. and Mueller B. E. A., "The spin state and homogeneity of Comet Halley's nucleus", *Icarus*, **93** (1991) 183.

[123] Gutiérrez P. J., Jorda L., Gaskell R. W., Davidsson B. J. R., Capanna C., Hviid S. F., Keller H. U., Maquet L., Mottola S., Preusker F. *et al.*, "Possible interpretation of the precession of comet 67P/Churyumov-Gerasimenko", *Astron. Astrophys.*, **590** (2016) 15.

[124] Toth I. and Lisse C. M., "On the rotational breakup of cometary nuclei and centaurs", *Icarus*, **181** (2006) 162.

[125] Vincent J.-B., A'Hearn M. F., Lin Z.-Y., El-Maarry M. R., Pajola M., Sierks H., Barbieri C., Lamy P. L., Rodrigo R., Koschny D. *et al.*, "Summer fireworks on comet 67P", *Mon. Not. R. Astron. Soc.*, **462** (2015) S184.

[126] Vincent J.-B., Oklay N., Pajola M., Höfner S., Sierks H., Hu X., Barbieri C., Lamy P. L., Rodrigo R., Koschny D. *et al.*, "Are fractured cliffs the source of cometary dust jets? Insights from OSIRIS/Rosetta at 67P/Churyumov-Gerasimenko", *Astron. Astrophys.*, **587** (2016) 15.

[127] Gicquel A., Vincent J.-B., Agarwal J., A'Hearn M. F., Bertini I., Bodewits D., Sierks H., Lin Z.-Y., Barbieri C., Lamy P. L. *et al.*, "Sublimation of icy aggregates in the coma of comet 67P/Churyumov-Gerasimenko detected with the OSIRIS cameras on board Rosetta", *Mon. Not. R. Astron. Soc.*, **462** (2016) S57; DOI: 10.1093/mnras/stw2117.

[128] Cremonese G., Simioni E., Ragazzoni R., Bertini I., La Forgia F., Pajola M., Oklay N., Fornasier S., Lazzarin M., Lucchetti A. *et al.*, "Photometry of dust grains of comet 67P and connection with nucleus regions", *Astron. Astrophys.*, **588** (2016) 8; DOI: 10.1051/0004-6361/201527307.

[129] Della Corte V., Rotundi A., Fulle M., Ivanovski S., Green S. F., Rietmeijer F. J. M., Colangeli L., Palumbo P., Sordini R., Ferrari M. *et al.*, "67P/C-G inner coma dust properties from 2.2 au inbound to 2.0 au outbound to the Sun", *Mon. Not. R. Astron. Soc.*, **462** (2016) S210; DOI: 10.1093/mnras/stw2529.

[130] Knollenberg J., Lin Z. Y., Hviid S. F., Oklay N., Vincent J.-B., Bodewits D., Mottola S., Pajola M., Sierks H., Barbieri C. *et al.*, "A mini outburst from the nightside of comet 67P/Churyumov-Gerasimenko observed by the OSIRIS camera on Rosetta", *Astron. Astrophys.*, **596** (2016) 10.

[131] Groussin O., Sierks H., Barbieri C., Lamy P., Rodrigo R., Koschny D., Rickman H., Keller H. U., A'Hearn M. F., Auger A.-T. *et al.*, "Temporal morphological changes in the Imhotep region of comet 67P/Churyumov-Gerasimenko", *Astron. Astrophys.*, **583** (2015) 4; DOI: 10.1051/0004-6361/201527020.

[132] Ip W.-H., Lai I.-L., Lee J.-C., Cheng Y.-C., Li Y., Lin Z.-Y., Vincent J.-B., Besse S., Sierks H., Barbieri C. *et al.*, "Physical properties and dynamical relation of the circular depressions on comet 67P/Churyumov-Gerasimenko", *Astron. Astrophys.*, **591** (2016) 10; DOI: 10.1051/0004-6361/201628156.

[133] Grün E., Agarwal J., Altobelli N., Altwegg K., Bentley M. S., Biver N., Della Corte V., Edberg N., Feldman P. D., Galand M. *et al.* "The 19 Feb. 2016 Outburst of Comet 67P/CG: An ESA Rosetta Multi-Instrument Study", *Mon. Not. R. Astron. Soc.*, **457** (2016) 4454; DOI: 10.1093/mnras/stw2088.

[134] Keller H. U., Mottola S., Skorov Y. and Jorda L., "The changing rotation period of comet 67P/Churyumov-Gerasimenko controlled by its activity", *Astron. Astrophys.*, **579** (2015) L5.

[135] Gulkis S., Allen M., von Allmen P., Beaudin G., Biver N., Bockelée-Morvan D., Choukroun M., Crovisier J., Davidsson B. J. R., Encrenaz P. *et al.*, "Subsurface properties and early activity of comet 67P/Churyumov-Gerasimenko", *Science*, **347** (2015) aaa0709.

[136] Schloerb F. P., Keihm S., von Allmen P., Choukroun M., Lellouch E., Leyrat C., Beaudin G., Biver N., Bockelée-Morvan D., Crovisier J. *et al.*, "MIRO observations of subsurface temperatures of the nucleus of 67P/Churyumov-Gerasimenko", *Astron. Astrophys.*, **583** (2015) 11.

[137] Choukroun M., Keihm S., Schloerb F. P., Gulkis S., Lellouch E., Leyrat C., von Allmen P., Biver N., Bockelée-Morvan D., Crovisier J. *et al.*, "Dark side of comet 67P/Churyumov-Gerasimenko in Aug.-Oct. 2014. MIRO/Rosetta continuum observations of polar night in the southern regions", *Astron. Astrophys.*, **583** (2015) 10.

[138] Thomas N., Sierks H., Barbieri C., Lamy P. L., Rodrigo R., Rickman H., Koschny D., Keller H. U., Agarwal J., A'Hearn M. F. *et al.*, "The morphological diversity of comet 67P/Churyumov-Gerasimenko", *Science*, **347** (2015) aaa0440.

[139] Pajola M., Vincent J.-B., Güttler C., Lee J.-C., Bertini I., Massironi M., Simioni E., Marzari F., Giacomini L., Lucchetti A. *et al.*, "Size-frequency distribution of boulders $\geq$7 m on comet 67P/Churyumov-Gerasimenko", *Astron. Astrophys.*, **583** (2015) 17.

[140] Pajola M., Lucchetti A., Vincent J.-B., Oklay N., El-Maarry M. R., Bertini I., Naletto G., Lazzarin M., Massironi M., Sierks H. *et al.*, "The southern hemisphere of 67P/Churyumov-Gerasimenko: Analysis of the preperihelion size-frequency distribution of boulders $\geq$ 7 m", *Astron. Astrophys.*, **592** (2016) 5 DOI: 10.1051/0004-6361/201628887.

[141] Barucci M. A., Filacchione G., Fornasier S., Raponi A., Deshapriya J. D. P., Tosi F., Feller C., Ciarniello M., Sierks H., Capaccioni F. *et al.*, "Detection of exposed H2O ice on the nucleus of comet 67P/Churyumov-Gerasimenko as observed by Rosetta OSIRIS and VIRTIS instruments", *Astron. Astrophys.*, **595** (2016) 13 DOI: 10.1051/0004-6361/201628764.

[142] Poulet F., Lucchetti A., Bibring J.-P., Carter J., Gondet B., Jorda L., Langevin Y., Pilorget C., Capanna C. and Cremonese G., "Origin of the local structures at the Philae landing site and possible implications on the formation and evolution of 67P/Churyumov-Gerasimenko", *Mon. Not. R. Astron. Soc.*, **462** (2016) S23.

[143] Lucchetti A., Cremonese G., Jorda L., Poulet F., Bibring J.-P., Pajola M., La Forgia F., Massironi M., El-Maarry M. R., Oklay N. *et al.*, "Characterization of the Abydos region through OSIRIS high-resolution images in support of CIVA measurements", *Astron. Astrophys.*, **585** (2016) 5.

[144] La Forgia F., Giacomini L., Lazzarin M., Massironi M., Oklay N., Scholten F., Pajola M., Bertini I., Cremonese G., Barbieri C. *et al.*, "Geomorphology and spectrophotometry of Philae's landing site on comet 67P/Churyumov-Gerasimenko", *Astron. Astrophys.*, **583** (2015) 18.
[145] Luu J., Marsden B. G. and Jewitt D. *et al.*, "A new dynamical class of object in the outer Solar System", *Nature*, **387** (1997) 573.
[146] Levison H. F., Morbidelli A., Tsiganis K., Nesvorný D. and Gomes R., "Late Orbital Instabilities in the Outer Planets Induced by Interaction with a Self-gravitating Planetesimal Disk", *Astron. J.*, **142** (2011) 11.
[147] Morbidelli A. and Rickman H., "Comets as collisional fragments of a primordial planetesimal disk", *Astron. Astrophys.*, **583** (2015) A43.
[148] Davidsson B. J. R. *et al.*, "'The primordial Nucleus of comet 67P/Churiumov Gerasimenko", *Astron. Astrophys.*, **592** (2016) A63.
[149] Hirabayashi M., Scheeres D. J., Chesley S. R., Marchi S., McMahon J. W., Steckloff J., Mottola S., Naidu S. P. and Bowling T., "Fission and reconfiguration of bilobate comets as revealed by 67P/Churyumov–Gerasimenko", *Nature*, **534** (2016) 352.
[150] Jutzi M. and Benz W., "Formation of bi-lobed shapes by sub-catastrophic collisions. A late origin of comet 67P's structure", *Astron. Astrophys.*, **597** (2017) 10.
[151] Jutzi M., Benz W., Toliou A., Morbidelli A. and Brasser R., "How primordial is the structure of comet 67P? Combined collisional and dynamical models suggest a late formation", *Astron. Astrophys.*, **597** (2017) 13.
[152] Luspay-Kuti A., Mousis O., Hässig M., Fuselier S. A., Lunine J. I., Marty B., Mandt K. E., Wurz P. and Rubin M., "The presence of clathrates in comet 67P/Churyumov-Gerasimenko", *Sci. Adv.*, **2** (2016) 1501781.
[153] Mousis O., Ozgurel O., Lunine J. I., Luspay-Kuti A., Ronnet T., Pauzat F., Markovits A. and Ellinger Y., "Stability of Sulphur Dimers (S_2) in Cometary Ices", *Astrophys. J.*, **835** (2017) 5; DOI: 10.3847/1538-4357/aa5279.
[154] Fulle M., Altobelli N., Buratti B., Choukroun M., Fulchignoni M., Grün E., Taylor M. G. G. T. and Weissman P., "Unexpected and significant findings in comet 67P/Churyumov-Gerasimenko: an interdisciplinary view", *Mon. Not. R. Astron. Soc.*, **462** (2016) S2; DOI: 10.1093/mnras/stw1663.
[155] Sunshine J. M., Thomas N., El-Maarry M. R. and Farnham T. L., "Evidence for geologic processes on comets", *J. Geophys. Res. Planets*, **121** (2016) 2194; DOI: 10.1002/2016JE005119.
[156] Schmidt W. K. H., Keller H. U., Wilhelm K., Arpigny C., Barbieri C., Biermann L., Bonnet R. M., Cazes S., Cosmovici C. B., Delamere W. A. *et al.*, "The GIOTTO Halley Multicolour Camera", *ESA Spec. Publ., ESA SP-1077*, (1986) 149.
[157] Grewing M., Praderie F. and Reinhard R. (Editors), *Exploration of Halley's Comet* (Springer-Verlag) 1988, p. 984.
[158] Sagdeev R. Z., Szabo F., Avanesov G. A., Cruvellier P., Szabo L., Szego K., Abergel A., Balazs A., Barinov I. V., Bertaux J.-L. *et al.*, "Television observations of comet Halley from VEGA spacecraft", *Nature*, **321** (1986) 262.